Journal of Radiological Protection

Official journal of the Society for Radiological Protection

PAPER • OPEN ACCESS

Surface-clearance levels for the normal reuse of objects for 413 radionuclides

To cite this article: Teun van Dillen *et al* 2022 *J. Radiol. Prot.* **42** 041507

IOP Publishing J. Radiol. Prot. 42 (2022) 041507 https://doi.org/10.1088/1361-6498/ac89f7

Journal of Radiological Protection

PAPER

Surface-clearance levels for the normal reuse of objects for 413 radionuclides

Teun van Dillen[1,*], **Federica Russo**[2,3] **and Chantal Mommaert**[2]

[1] Centre for Environmental Safety and Security, National Institute for Public Health and the Environment (RIVM), PO Box 1, NL-3720 BA Bilthoven, The Netherlands
[2] Bel V, Walcourtstraat 148, B-1070 Brussels, Belgium
[3] Currently employed elsewhere.
[*] Author to whom any correspondence should be addressed.

E-mail: Teun.van.Dillen@rivm.nl

Keywords: surface contamination, clearance levels, reuse, probabilistic, SUDOQU

OPEN ACCESS

RECEIVED
26 April 2022

REVISED
8 July 2022

ACCEPTED FOR PUBLICATION
16 August 2022

PUBLISHED
5 December 2022

Abstract

This paper provides surface-clearance levels for 413 radionuclides for the normal reuse of objects leaving the controlled area of a nuclear facility. Four sets of surface-specific clearance levels are derived based on choices of dose coefficients (DCs) in probabilistic dose assessments using the SUrface DOse QUantification model (SUDOQU; van Dillen and van Dijk 2018 *J. Radiol. Prot.* **38** 1147–203). The general dose criteria for clearance, extended with a suitable dose constraint for the concept of the representative person, are applied in the derivations. These clearance levels apply to the total of fixed and removable radioactive contamination on the surface of objects. The results are discussed in the context of conservatism of the exposure scenarios (parameters, DCs), and guidance is given on the selection and application of the values.

1. Introduction

1.1. Motivation and scope

For decades there have been many discussions on what values to use when performing clearance based on surface-specific measurements. Levels of 0.04 Bq cm^{-2} for radiotoxic alpha emitters and 0.4 Bq cm^{-2} for beta/gamma and low-toxicity alpha emitters are widely used. These levels are based on the definition of contamination in the Transport Regulations by the International Atomic Energy Agency (IAEA 2018) and an old study by Fairbairn (1961). However, they are also often contested and challenged, especially when used for purposes other than the safe transport of radioactive materials. Only a thorough study on the derivation of nuclide-specific surface-clearance levels (SCLs) can provide a founded answer to the raised issue. An example of such a study is presented in 'Radiation Protection 101', commissioned by the European Commission (EC 1999), deriving clearance levels for recycling or reuse. The current paper presents the results of a new comprehensive study on surface contamination geared towards the normal reuse of objects or items cleared from the controlled area of a nuclear facility.

In the aftermath of the accident with the Fukushima Daiichi nuclear power plant (Japan, 2011), the Dutch National Institute for Public Health and the Environment (RIVM) developed a new methodology for deriving criteria for screening potentially surface-contaminated items (van Dillen 2015, van Dillen and van Dijk 2018), e.g. (non-food) consumer goods and conveyances. This methodology, entitled SUrface DOse QUantification (SUDOQU), calculates the annual effective dose for consumers and non-radiological workers for a set of well-defined deterministic scenarios. Given the similarity of the situation with objects leaving the controlled area of a nuclear facility and the corresponding need for well-founded criteria for surface-specific clearance, a joint project between Bel V (a subsidiary of the Federal Agency for Nuclear Control, Belgium) and RIVM was set up to evaluate the suitability of the SUDOQU methodology for this case. Based on a preliminary, deterministic study by Russo *et al* (2018a, 2018b), the collaboration was extended to develop *probabilistic* scenarios for the derivation of surface-specific clearance levels for over 400 radionuclides. The main advantage of a probabilistic approach is that it considers a (broad) range of potential exposure scenarios, resulting in a spread in dose that one may expect to occur in the population exposed to such items.

The original SUDOQU methodology has been adapted and extended to include a probabilistic approach to the derivation of scenario-based SCLs. A new method is presented to establish clearance levels from evaluated dose distributions of exposed individuals, respecting both the concept of high- and low-probability scenarios for clearance (with corresponding dose criteria) and the concept of the representative person (ICRP 2006). The scenarios considered in this study are representative of a clearance situation, to be distinguished from exemption situations as originally foreseen in the RIVM study (van Dillen 2015). The materials considered are objects leaving a radiologically controlled area of a nuclear facility, to be reused in a non-radiological environment, typically an office or a dwelling. Reuse scenarios involve the *normal* reuse of a contaminated item (i.e. no material processing) by non-radiological workers or adult members of the public (MOP). The exposure of children is not considered in this study. Only immediate reuse is regarded, which means that radioactive decay and other surface-removal processes due to a potential delay or waiting time are *not* taken into account. The contamination is modelled to have a fixed and a removable component. The nuclide-specific surface-clearance levels derived in this work thus relate to the *total* level of surface contamination, i.e. the sum of fixed and removable components. Practical aspects related to the measurement of surface contamination and to the implementation of these clearance levels in regulations are outside the scope of this paper.

1.2. Organisation of the paper

This paper is organised in four main sections. Section 2 describes the materials and methods used for the dose calculations: the evolution from deterministic to probabilistic calculations with the SUDOQU model, the description and choice of fixed and distributed input parameters as well as the selected dose coefficients (DCs). It also describes the treatment of radioactive progeny in dose evaluations. Section 3 presents the new methodology used for the derivation of the clearance levels. This includes imposing suitable dose criteria for clearance, defining a method for establishing clearance levels from probabilistic calculations, and sampling statistics and convergence of these probabilistic calculations. In section 4, results of five probabilistic calculations, each one resulting in a nuclide-specific set of surface clearance values (in Bq cm^{-2}), are analysed and discussed. In section 5, some guidance is given on the selection and application of the derived clearance levels and issues of conservatism are discussed. Conclusions and potential future developments close this paper. Theoretical details on the SUDOQU methodology as used for dose calculations in this paper and the values of the derived SCLs for 413 radionuclides can be found in the appendices.

2. Materials and methods for dose calculations

2.1. From deterministic to probabilistic calculations with the SUDOQU model

The SUDOQU model (van Dillen 2015, van Dillen and van Dijk 2018) assumes surface- and air-contamination levels, the time dependence of which is governed by a system of coupled differential equations. These equations describe the mass (activity) balance imposed by the involved removal and deposition mechanisms. The surface-activity concentration (Bq cm^{-2}) is considered to decrease by radioactive decay, resuspension and wipe-off (transfer of removable activity to the hands). Resuspended activity contributes to the (increase in) air-activity concentration (Bq m^{-3}) and, in turn, partly re-deposits onto the object's surface (and on surrounding surfaces). The air-activity concentration is further affected by radioactive decay and ventilation. Different exposure pathways are considered: external exposure to gamma (and neutron) radiation, internal exposure due to inhalation or indirect ingestion of removable activity, and exposure of the skin by wipe-off/transfer of contamination and by direct contact with the object's surface. The effective dose can be calculated as the sum of the contributions of these pathways. Based on these intrinsic properties, the SUDOQU methodology is suitable for clearance and exemption calculations, especially when considering public reuse scenarios, because they often involve the prolonged use of the same object. A brief description and summary of the equations used for calculations in this paper can be found in appendix B.

The applicability of the SUDOQU methodology for clearance calculations was investigated in a pilot project, which also allowed better understanding of the interplay among the involved mechanisms and its effect on the effective dose. This was achieved by performing several *deterministic* calculations of the annual effective dose resulting from exposure to typical office items, e.g. a bookcase or an office desk, considering different scenarios of use and different radionuclides (Russo *et al* 2018a, 2018b).

Results of SUDOQU were benchmarked against those of a model reported in EC (1999) for the normal reuse scenario of a tool cabinet. Both models proved to be in good agreement (Russo *et al* 2018b) when using similar parameter values (with results from SUDOQU somewhat more conservative). Another

Table 1. Overview of SUDOQU's input parameters determining the time-dependence of the surface- and air-contamination levels. Values of fixed parameters are listed in the third column. Probability-density functions for distributed input parameters (labelled as 'varied' in the third column) are described in table 3.

Parameter	Description	Value	Unit
$f_{\mathrm{rem},i}$	Removable fraction of nuclide i	Varied	—
A_{cont}	Contaminated surface of the object	Varied	cm^2
ΔT_{tot}	Total considered time of the scenario (1 year)	8760	h
f_{use}	Fraction of time for object use (duty factor)	Varied	—
$\bar{\xi}_{\mathrm{use},i}$	Time-averaged resuspension rate during object use	Varied	h^{-1}
$\bar{\phi}_{\mathrm{use}}$	Time-averaged wipe-off frequency during object use	Varied	h^{-1}
$\bar{f}_{\mathrm{oth},i}$	Time-averaged transfer efficiency (object-to-hand)	Varied	—
A_{floor}	Total floor area of room or office	30×10^4	cm^2
H	Height of room or office	250	cm
V	Volume of room or office ($A_{\mathrm{floor}}H$)	7.5×10^7	cm^3
λ_v	Air-exchange rate (room or office)	0.50	h^{-1}
κ_v	Volumetric ventilation/air-flow rate ($\lambda_v V$)	3.75×10^7	cm^3 h^{-1}
$v_{d,i}$	Indoor deposition velocity	Varied	cm h^{-1}
$\lambda_{d,i}$	Indoor deposition-loss-rate constant ($v_{d,i}/H$)	Varied	h^{-1}
A_{hands}	Contaminated skin area of the hands	Varied	cm^2
$m_{\mathrm{hands},i}$	Time multiplication factor for hand exposure	1.0	—
A_{face}	Contaminated skin area of the face	100	cm^2
$m_{\mathrm{face},i}$	Time multiplication factor for face exposure	2.0	—
$\bar{f}_{\mathrm{htf},i}$	Average transfer efficiency (hands-to-face)	0.10	—

benchmarking study, presented in Russo *et al* (2018a), also showed good agreement with results obtained by the RESRAD-BUILD model (Kamboj *et al* 2011) for a similar exposure scenario.

The gained insight into the interplay among the involved mechanisms also disclosed the importance and difficulty of a detailed sensitivity analysis, especially when considering various radionuclides with distinct differences in dominating exposure pathways. Therefore, the next step after this pilot study was to develop a SUDOQU model capable of performing *probabilistic* dose assessments. In contrast to a deterministic dose evaluation based on fixed input-parameter values, the probabilistic assessment results in a distribution of doses for each radionuclide separately, taking into account the sensitivity of the dose to distributed input parameters. By applying proper dose criteria for clearance, these dose distributions can then be used to derive nuclide-specific SCLs (in Bq cm^{-2}). Both the range and shape of this distribution influence the value of the clearance level.

2.2. Description and choice of the input parameters

The probabilistic study presented in this paper uses both distributed and fixed input parameters of the SUDOQU model. The choice to vary an input parameter in this probabilistic study is primarily based on whether its value is expected to change significantly with behaviour, i.e. the way the object is used or handled, and with the properties of the object and its contamination. The type of probability-density function (pdf) for the distributed parameters in the probabilistic calculations is based as much as possible on the available information about the parameter values. For the remaining parameters, fixed values were based on realistically conservative conditions from deterministic calculations (van Dillen and van Dijk 2018, Russo 2018a) to avoid underestimation of the dose. The size of the office or room is a typical example of such a fixed parameter. A short description of all input parameters of the SUDOQU model can be found in tables 1 and 2.

2.2.1. Fixed input parameters

Various parameters are set to fixed values, listed in tables 1 and 2. These values correspond to the default values in tables 1 and 2 of van Dillen and van Dijk (2018). Only the floor area of the room or office has been modified, from 50 m^2 to 30 m^2, which is assumed to be more appropriate for a small office and which is more conservative for dose assessments. Consequently, the volume V and the volumetric air-flow rate κ_v of the room also deviate from their earlier, default values.

In the current study, the choice was made to fix the air-exchange rate λ_v at 0.5 h^{-1}, a conservative value for dose evaluations representing poor ventilation. This value is reasonable considering the experimental studies on air-exchange rates in the United States, as summarised in Yu *et al* (2003, section J.2.6), and a more recent review on ventilation rates in European dwellings by Dimitroulopoulou (2012).

Skin contamination of hands and face by transfer (object-to-hand and hand-to-face) is a process determined by both the particular use of the object and the physical and chemical properties of the object

Table 2. Overview of input parameters for probabilistic dose-assessments. Values of fixed parameters are listed in the third column. Probability-density functions for distributed input parameters (labelled as 'varied' in the third column) are described in table 3.

Parameter	Description	Value	Unit
$f_{\mathrm{att},i}$	Attenuation factor from shielding	1.0	—
$f_{\mathrm{conv},i}$	Conversion factor from $H_p(10)_i$ to $E_{\mathrm{ext},i}$ (see appendix B.1)	1.0	—
R	Radius of (disk-shaped) object ($\sqrt{A_{\mathrm{cont}}/\pi}$)	Varied	cm
L	Distance to centre of (disk-shaped) object	Varied	cm
cor_g	Geometrical correction factor	1.0	—
$f_{\mathrm{resp},i}$	Respirable fraction	1.0	—
$\mathrm{cor}_{\mathrm{air},i}$	Correction factor for local air-contamination	1.0	—
I	Breathing rate	1.2	$\mathrm{m}^3\ \mathrm{h}^{-1}$
f_{ing}	Fraction of area of hands for ingestion	0.01	—
$F_{\mathrm{htm},i}$	Average transfer factor (hands-to-mouth)	1.0	—
Φ_{ing}	Secondary ingestion frequency	Varied	h^{-1}
w_{skin}	Tissue weighting factor of the skin	0.01	—
$A_{\mathrm{skin,total}}$	Total ultraviolet radiation-exposed skin area	3000	cm^2
f_{cont}	Fraction of objects contaminated (only for $\delta = 0$)	1.0	—
$A_{\mathrm{skin,contact}}$	Skin area in direct contact with the object during use	Varied	cm^2
$m_{\mathrm{skin,contact}}$	Time multiplication factor for direct contact with object	Varied	—

and contaminants. Key parameters defining the overall contamination-transfer process to the hands ($\bar{f}_{\mathrm{oth},i}$, $\bar{\phi}_{\mathrm{use}}$ and A_{hands}, table 1) are therefore modelled probabilistically and are sampled from corresponding pdfs. However, since details on the exact transfer process *during* a wipe-off event are generally unknown, the effective time-multiplication factor for skin contamination of the hands, $m_{\mathrm{hands},i}$, is fixed at a conservative value of 1.0. The effective duration of contamination of the hands is therefore assumed to be as long as the duration of object use. Furthermore, as skin contamination of the face only constitutes a minor exposure pathway in current dose evaluations, the associated parameters A_{face}, $m_{\mathrm{face},i}$ and $\bar{f}_{\mathrm{htf},i}$ are fixed at their default values as well (table 1).

The respiratory rate was set to a value of 1.2 $\mathrm{m}^3\ \mathrm{h}^{-1}$, which equals the average breathing rate of a reference worker as defined by ICRP (1994). Elevated breathing rates larger than this default value for the entire period of use in a poorly ventilated, small office were judged unrealistic and too conservative for the current dose evaluations.

The effective skin area from which contamination is completely ingested per secondary ingestion event can be written as $F_{\mathrm{htm},i} f_{\mathrm{ing}} A_{\mathrm{hands}}$ (van Dillen and van Dijk 2018). Since A_{hands} is modelled as a distributed parameter, so is this effective ingestion area. Per 100 cm^2 of contaminated skin of the hands, ingestion is (on average) modelled to occur from only 1 cm^2. The parameters $F_{\mathrm{htm},i}$ and f_{ing} are therefore fixed at their default values of 1.0 and 0.01, respectively. However, it is realistic to assume that the effective skin area for ingestion remains at 1 cm^2 for $A_{\mathrm{hands}} < 100\ \mathrm{cm}^2$. With $F_{\mathrm{htm},i} = 1.0$, parameter f_{ing} then attains a value of $1.0\ \mathrm{cm}^2/A_{\mathrm{hands}}$, having a maximum of 0.25 for the smallest value of $A_{\mathrm{hands}} = 4.0\ \mathrm{cm}^2$. Note that, for $A_{\mathrm{hands}} < 100\ \mathrm{cm}^2$, the value of f_{ing} is not fixed but varies with the (distributed) value of A_{hands}.

2.2.2. Distributed parameters

Distributed parameters are varied randomly and independently by sampling from pdfs and are chosen such that they typically have a large impact on one or more of the exposure pathways and thus on the dose results. Obviously, the actual impact of a (change in) parameter value depends on the type of radionuclide investigated, since its DCs determine which pathways are dominant. Distributed parameters, 12 in total, were selected based on results from an earlier study by Russo *et al* (2018a) and by additional sensitivity analyses in which the (change in) total annual effective dose was investigated as a function of separate input parameters. Their type of distribution and values of the underlying coefficients are listed in table 3; descriptions of parameters are found in tables 1 and 2.

The pdfs employed in this study are: uniform, normal, triangular and lognormal. The choice for a pdf is mainly based on information from the literature about these parameters, combined with the range of values that is found or judged most likely to occur. Details on these choices are given below per type of distribution.

2.2.2.1. Uniform distribution

If little or no information is available and/or all values within a certain range are assumed to be equally likely, then a uniform distribution is chosen. This type of distribution is chosen for four input parameters: the wipe-off frequency during object use ($\bar{\phi}_{\mathrm{use}}$), the secondary ingestion rate (Φ_{ing}), the time-multiplication factor for direct contact with the object ($m_{\mathrm{skin,contact}}$) and the contaminated surface area of the object (A_{cont}).

Table 3. Overview of the 12 distributed parameters for probabilistic modelling in SUDOQU. Shown are the type of distribution and the input parameters defining these distributions: minimum and maximum value, mode (most likely value), and, for (log) normal distributions, the values of μ (mean value, in absence of truncation) and σ (standard deviation). For lognormal distributions the values of μ and σ are those of the underlying normal distribution of the natural logarithm of the distributed parameter.

Parameter	Unit	Distribution	Min	Max	Mode	μ	σ
$f_{\mathrm{rem},i}$	—	Triangular	0	0.5	0.1	—	—
A_{cont}	cm^2	Uniform	0.01×10^4	10×10^4	—	—	—
f_{use}	—	Normal	0	1.0	0.228	0.228	0.07
$\bar{\xi}_{\mathrm{use},i}$	h^{-1}	Lognormal	0	—	1.0×10^{-6}	−12.18	1.28
$\bar{\phi}_{\mathrm{use}}$	h^{-1}	Uniform	0.1	2.0	—	—	—
$\bar{f}_{\mathrm{oth},i}$	—	Normal	0	—	0.10	0.10	0.025
$v_{d,i}$	cm h^{-1}	Lognormal	0	—	90	5.13	0.80
A_{hands}	cm^2	Triangular	4	800	400	—	—
L	cm	Normal	10	—	60	60	20
Φ_{ing}	h^{-1}	Uniform	0.1	2.0	—	—	—
$A_{\mathrm{skin,contact}}$	cm^2	Triangular	0	200	100	—	—
$m_{\mathrm{skin,contact}}$	—	Uniform	0	0.75	—	—	—

Parameters $\bar{\phi}_{\mathrm{use}}$ and Φ_{ing} are behavioural parameters about which little is known. Minimum and maximum values of both parameters are set at 0.1 h^{-1} and 2.0 h^{-1}, respectively, covering both realistic and conservative situations that we judge appropriate for the current study.

Parameter $m_{\mathrm{skin,contact}}$ ($\leqslant 1$) defines the fraction of time-of-use in which the skin is in direct contact with the object. This parameter strongly depends on the type of object considered and therefore no specific region of values is preferred. The minimum value is 0 (negligible contact) and the maximum value is 0.75, with large(r) values expected for objects like tables and chairs.

The object's contaminated area A_{cont} is a key input parameter of the SUDOQU model. The derived SCL will depend on the value of A_{cont} as it determines the total amount of activity one is exposed to. Rather than determining the dependence of the dose and clearance level as a function of A_{cont}, A_{cont} is considered probabilistically as well. The advantage and practicality of such a treatment of A_{cont} is that the *overall* clearance level becomes independent of the size of the contaminated object—of course within the range of considered surface areas. In this study, A_{cont} is uniformly varied from 100 cm^2 to 100 000 cm^2 (0.01–10 m^2). This was chosen as a typical size range of objects possibly cleared from a nuclear facility, without any preferred size.

2.2.2.2. Normal distribution

Normal distribution is used for parameters whose values have a preferred region around a mean value μ. This mean value is also the most likely value in the pdf (the mode). The standard deviation σ defines the spread around the mean value. The resulting distributions have their majority of values (95%) between $\mu \pm 2\sigma$. Theoretically, the normal distribution is not bounded by minimum and maximum values. In the current study, however, truncation of the pdf was applied by imposing either a minimum or maximum value (or both) to exclude unrealistic situations. Note that truncation may cause the mean of the resulting pdf to deviate slightly from its mode. The (truncated) normal distribution is chosen for the following three input parameters: the distance of the receptor to the object (L), the fraction of time for object use (duty factor, f_{use}) and the transfer efficiency (object-to-hand: $\bar{f}_{\mathrm{oth},i}$). Default parameter values from van Dillen and van Dijk (2018) are taken as the mean value (mode) of the pdf, whereas standard deviations were chosen such that the corresponding parameter range covers both realistic and sufficiently conservative situations. For the object-receptor distance L, the minimum value was set to 10 cm since values smaller than this are considered unrealistic and too conservative for dose calculations. The duty factor was truncated between values of 0 and 1.0 (the upper truncation here has no effect on the drawn values). For transfer efficiency, only a minimum value of 0 was imposed.

2.2.2.3. Triangular distribution

Like the normal distribution, triangular distribution is chosen for parameters whose values have a preferred region around some most likely value (mode). The difference is that the triangular distribution has (user-defined) minimum and maximum values and may be asymmetric around the mode, and the range is limited by realistic (physical) values for the parameter. The mean value may therefore be significantly different from the mode. Triangular distribution is employed for the following three input parameters: the initial removable fraction of contamination ($f_{\mathrm{rem},i}$), the contaminated skin area of the hands (A_{hands}) and the skin area in direct contact with the object during its use ($A_{\mathrm{skin,contact}}$).

In the current study, we assume that at least 50% of the surface-contamination level is fixed, since objects are usually cleaned before they exit the nuclear facility. Therefore the value of the removable fraction varies between 0 (fixed contamination only) and 0.50. The most likely value is set at 0.10, taken from EC (1999) and Yu *et al* (2003). As a result of this asymmetric pdf, the mean value of $f_{\mathrm{rem},i}$ is 0.20.

The contaminated area of the hands, A_{hands}, is assumed to vary between 4 cm^2 and 800 cm^2. The minimum value represents the area of a few fingertips while the maximum value represents the area of two hands contaminated on both sides including part of the wrists. The mode is set to the default value of 400 cm^2 presented in van Dillen and van Dijk (2018) and IAEA (2005a), which is roughly equal to the average value of the pdf (401 cm^2).

For direct skin contact with the object, the area $A_{\mathrm{skin,contact}}$ is varied between 0 cm^2 (virtually no contact) and 200 cm^2 (one side of the hand including part of the wrist). The mode is set at a value of 100 cm^2, which equals the mean value of this pdf.

2.2.2.4. Lognormal distribution

Lognormal distribution is used for parameters that vary over several orders of magnitude. The mean value μ and standard deviation σ are of those of the underlying normal distribution of the natural logarithm of the parameter or quantity considered. Here, those parameters are the resuspension rate $\bar{\xi}_{\mathrm{use},i}$ and the deposition velocity $v_{d,i}$; both parameters are strongly influenced by the aerosol size distribution. Based on available experimental data for $\bar{\xi}_{\mathrm{use},i}$ and $v_{d,i}$ (see e.g. Yu *et al* (2003) for an overview of the data), the mode and 99-percentile of the distributions were selected, from which the values for μ and σ could be derived numerically. The final distributions cover the range of experimental data well, with preferred values around the modes. For the deposition velocity, the mode was set at 90 cm h^{-1} (2.5×10^{-4} m s^{-1} = 0.25 mm s^{-1}) and the 99-percentile at 1080 cm h^{-1} (3.0×10^{-3} m s^{-1} = 3.0 mm s^{-1}), leading to the distribution's coefficients of $v_{d,i}$ as defined in table 3.

For the resuspension rate, the default value of 10^{-4} h^{-1} (2.8×10^{-8} s^{-1}) in van Dillen and van Dijk (2018) and IAEA (2005a) is considered to be a conservative value, especially considering the fact that *protracted* resuspension is regarded for the (regular) use of the same object throughout the year. Therefore, the time-averaged resuspension rate is assumed to be several orders (at least two) of magnitude smaller than this conservative default value. The mode was assumed to be 10^{-6} h^{-1} (2.8×10^{-10} s^{-1}), while the 99-percentile was set to 10^{-4} h^{-1}, leading to the distribution's coefficients of $\bar{\xi}_{\mathrm{use},i}$ as defined in table 3.

2.2.3. Correlation of parameters and consistency checks

In the current probabilistic evaluations, distributed parameters are drawn randomly and *independently* from the 12 distribution functions defined in table 3. We acknowledge the fact that correlations between these parameters may exist. Also, correlations between fixed and distributed parameters may exist. As details on most of these (possible) correlations are unknown, especially when considering the protracted use of the same object throughout the year, it was not feasible to take them into account. This means that, for some drawings (i.e. sets of parameter values), the resulting scenario and dose evaluation may be less realistic. However, the current study probes all various combinations of exposure pathways, which we consider a proper approach for determining limiting values for surface contamination.

As explained by van Dillen and van Dijk (2018), there are several conditions to combinations of parameters. If these conditions are not met, the resulting exposure scenario is impossible. Therefore, consistency checks were performed for several combinations of input parameters and small adjustments were made when necessary. For example, in case the skin area in direct contact with the object exceeds its contaminated area, the skin-contact area is set equal to the area of contamination. Adjustments only occur in less than 0.03% of all samplings.

2.3. DCs

The total exposure considered for the derivation of surface-specific clearance levels consists of external gamma (and neutron) exposure, internal exposure by inhalation and ingestion of activity and skin exposure by transfer of contamination, and by direct contact with the object. For each of these exposure pathways, an appropriate DC has to be used for each radionuclide. The choice of the DCs used for the calculations in this paper as well as the specific choices made for the reference calculation are described below (see also section 4).

2.3.1. External dose-rate coefficients

Based on updated nuclear decay data for 1252 radionuclides, published by ICRP (2008), Otto (2016) calculated conversion coefficients to personal dose equivalents for point-like sources at depths of 0.07, 3 and 10 mm. These coefficients are calculated taking into account the contribution of various particles emitted under a variety of decay modes: photons, electrons/positrons and neutrons. Furthermore, a distinction is made between two boundary cases, labelled as 'shielded' and 'unshielded'. The shielded personal dose equivalent assumes shielding of directly ionising particles through self-absorption in the source, while photons and neutrons are unaffected by this assumption. Gamma photons (511 keV) from annihilation of positrons from $\beta+$ decay with electrons are included in these 'shielded' coefficients as well.

Since the personal dose equivalent at 10 mm depth, $h_p(10)_i$, is the recommended proxy for the protection quantity 'effective dose' for external exposure to gamma rays and neutrons, but not for external exposure to electrons and positrons, calculations in the current study use the radionuclide-specific, 'shielded' DCs. Therefore, it is judged an appropriate and conservative quantity for external radiation dosimetry in all exposure geometries.

2.3.2. Inhalation DCs

Inhalation dose coefficients ($DC_{inh,i}$) are taken from ICRP Publication 119 (ICRP 2012) and from the Japan Atomic Energy Research Institute (JAERI 2002) for additional radionuclides, since not all DCs as part of the 'Occupational Intakes of Radionuclides' series (ICRP 2015) were updated at the time this study was conducted.

Inhalation dose coefficients depend on the size distribution of airborne aerosols with attached radioactivity, which is characterised by the 'activity median aerodynamic diameter' (AMAD). For workers, inhalation DCs are available for an AMAD of 1 μm and 5 μm, where the latter value represents the default, reference size distribution for occupational (workplace) exposures. This is recommended in case no information about the physical characteristics of the aerosols is available (ICRP 1994). In this paper, 'worker' does not refer to a radiological worker, but to individuals who may use the objects daily in their occupation (EC 2000). Inhalation DCs for MOP, published in ICRP (1995), are only available for an AMAD of 1 μm. This is the recommended default value for indoor and outdoor exposure of MOP in the general environment.

The reference calculation in this study (section 4.1) uses inhalation DCs for workers based on the default AMAD of 5 μm, selecting for each radionuclide the maximum value among the available lung-absorption types (fast(F)/medium(M)/slow(S)). This conservative approach is similar to what was done in EC (1999) and is believed to be an adequate approach for (committed) dose evaluations aimed at the derivation of clearance values. Calculations with maximum DCs based on an AMAD of 1 μm (workers, adult MOP) have also been performed to investigate the impact of the aerosols' size distribution and exposed individuals. Note that other clearance studies (e.g. IAEA 2005b) may have used different DCs based on different assumptions.

2.3.3. Ingestion DCs

Similar to the inhalation dose conversion coefficients, the ingestion exposure pathway is modelled using DCs for both workers and adult MOP, taken from ICRP (2012) and JAERI (2002). The most conservative value among those available for each radionuclide is chosen (largest value depending on the f_1 value), independent of the choice made for the inhalation DC. As mentioned in section 2.3.2, this conservative approach is believed to be appropriate for the derivation of radionuclide-specific clearance values. The reference calculation in this paper uses the ingestion DCs for workers (section 4.1).

2.3.4. Skin dose-rate coefficients

This study uses a comprehensive set of dose-rate coefficients for the local skin-equivalent dose published by the German Commission on Radiological Protection, SSK (2017). Dose values are averaged over an area of 1 cm^2 and over a skin depth of 50–100 μm of the epidermis containing the basal layer of target stem cells that are believed to be responsible for the induction of non-melanoma skin cancer. This definition of local skin dose (coefficient) is similar to that in ICRP (2010). Note that the use of these dose-rate coefficients ignores that, in reality, the basal layer at particular sites on the body, e.g. the finger tips or palm of the hands, may be located at skin depths larger than 150 μm (NRPB 1997). These coefficients include contributions of alpha particles (for energies >6 MeV), beta particles and photons. For the photon contribution to these coefficients, the assumption is made that a large part of the skin is contaminated with the considered radionuclide.

Since there is no conclusive experimental or epidemiological evidence of the harmful effects of high-energy, alpha-particle exposure of the skin (Eatough 1997, Charles 2007), the reference calculation (section 4.1) in the current study ignores the skin-dose contribution caused by alpha-particles, as in many similar studies (EC 1993, 1999, 2000, IAEA 2005a, 2005b). However, we will also illustrate the possible effect of alpha-particle exposure to skin dose and to derived SCLs by including its contribution to the local skin-equivalent dose and the effective dose.

2.4. Treatment of radioactive progeny

Even though the current study assumes that, initially (at $t = 0$, time of clearance), the object is contaminated *only* with parent radionuclide P, the delayed ingrowth of radioactive progeny (daughter nuclides D) after clearance is taken into account in the dose evaluations. A method similar to that described in EC (2000) and IAEA (2005b) is employed in which DCs of the parent radionuclides are modified to include a weighted contribution of their corresponding daughter nuclides. Recently, this method has been worked out and adapted by van Dillen *et al* (2020). The dose contribution related to the *ex-vivo* ingrowth of progeny is indirectly taken into account by adding the DCs of the daughter nuclides ($\mathrm{DC_D}$) to those of the parent, head-of-chain radionuclides ($\mathrm{DC_P}$) using proper weighting factors w_D:

$$\mathrm{DC}_{\mathrm{tot,P}} = \mathrm{DC_P} + \sum_{\text{progeny D}} w_\mathrm{D}\mathrm{DC_D}, \tag{1}$$

where the sum extends over all progeny of parent nuclide P. These nuclide-specific weighting factors, with values between 0 and 1, are generic in the sense that they can be used for the DCs of all exposure pathways: external radiation exposure, skin-contamination exposure and internal exposure by inhalation or ingestion. The weighting-factor values w_D were taken from the new, conservative model presented in section 2.3 of van Dillen *et al* (2020) using a scenario-integration time of one year, i.e. $\tilde{w}_D\,(\tau = 1\ \mathrm{y})$. The two main advantages of this method using conservative weighting factors are:

- the resulting dose evaluation itself remains relatively simple and only regards the head-of-chain, parent radionuclide P; and
- compliance with the (annual) dose criteria immediately after clearance ensures future compliance with these criteria as well, at least within a time frame of one century. This is because these weighting factors consider the progeny's maximum contribution to the dose in this time frame, and attribute it to the first year after clearance.

Even though these dose assessments may overestimate the contribution related to the ingrowth of radioactive progeny, this approach is acceptable for the derivation of (surface-)clearance values. See more in section 5.2.

If the activity of a progeny radionuclide is already present at $t = 0$, its dose contribution should generally be evaluated separately and added to that of the corresponding parent (head-of-chain) radionuclide. This is because the dose related to the parent radionuclide only includes the contribution of its progeny ingrowth starting at time of clearance, in the absence of any progeny at $t = 0$. This can be translated to the formal, regulatory decision process of clearance based on limiting values as follows. For a surface-contaminated item comprising a mixture of radionuclides of artificial origin, the following condition should be met to comply with the annual dose criteria (known as the sum-of-fractions or weighted-sum rule):

$$\sum_i \frac{C_i}{\mathrm{SCL}_i} \leqslant 1, \tag{2}$$

with C_i the surface-contamination level (Bq cm^{-2}) of the ith radionuclide and SCL_i its derived surface-clearance level (Bq cm^{-2}). The sum in principle extends over all radionuclides present on the surface of the item, *even if they occur in the same decay chain*, i.e. it is a sum over all parent and daughter radionuclides.

However, there are situations for which the presence of an *initial* surface contamination of a daughter radionuclide at time of clearance results in a dose that is relatively small compared to the dose from the ingrowth of that daughter nuclide from its parent nuclide. The SCL of a parent nuclide, $\mathrm{SCL_{Parent}}$, then takes sufficient account of the (initial) presence of its daughter nuclide through the weighted dose conversion coefficients and there is no need to consider (and measure) this daughter nuclide separately. Consequently, the term $C_\mathrm{Daughter}/\mathrm{SCL_{Daughter}}$ of that specific nuclide can be disregarded from the aforementioned sum of fractions. In this case, the parent nuclide is labelled as P+ (see table A.1), indicating that its derived clearance level *fully* includes one (or more) daughter nuclides that can be excluded from the sum rule. This occurs, for example, for parent nuclides that decay into short-lived daughter nuclides, such as Cs-137/Ba-137m (indicated as Cs-137+). IAEA (2005b, section 3.1.2) and EC (2000, section 2.2) describe the criteria for determining if and which daughter nuclides are fully covered by the clearance level of their parent.

For daughter nuclides at which several branched decay chains merge together, we considered the main branch (with the highest compound yield) to determine whether these criteria are met for this daughter nuclide. In table A.2 of appendix A, the resulting P+ list of parent-progeny radionuclides is presented. If a parent radionuclide from this table is present, its listed daughter radionuclides need not be considered separately for clearance *if their presence is only due to ingrowth by radioactive decay*. Table A2 deviates slightly from those in IAEA (2005b) and EC (2000).

3. Methodology for derivation of clearance levels

Clearance levels are derived through a stepwise process. First, the dose incurred by an individual is assessed, as a result of exposure to a hypothetical unit radioactive contamination level (e.g. 1 Bq cm^{-2}) in a given scenario. Subsequently, the resulting dose is compared to the applicable dose criterion. In order not to exceed the dose criterion, the postulated radioactive contamination level is scaled by the ratio of the dose criterion to the resulting dose. The newly calculated contamination level is the corresponding clearance level for that scenario, respecting the dose criterion. This process is described in section 3.2 and visualised in section 4.2 (figure 1).

3.1. General dose criteria for clearance

In IAEA (2005b), the clearance levels were derived as the minimum of the activity-concentration values obtained from various deterministic scenarios using:

- realistic parameter values in combination with an effective dose criterion of 10 μSv yr^{-1}; and
- low-probability parameter values in combination with an effective dose criterion of 1 mSv yr^{-1} and a (local) skin-equivalent dose limit of 50 mSv yr^{-1}.

These activity-concentration values, published in IAEA (2004), are embedded in the European Council Directive (EC 2014) and in the International Basic Safety Standards from the IAEA (2018). Hence, since clearance values in current international regulations and standards are based on these dose criteria, they were also used as the basis for the derivation of SCLs in this paper.

3.2. Derivation of clearance levels based on a probabilistic approach

In a *deterministic* assessment, the annual dose resulting from an exposure calculation using fixed values for the input parameters of the scenario is a single value. As described in IAEA (2005b), two separate evaluations can be performed, one for realistic scenarios (normal use) and one for conservative, low-probability scenarios (potential exposures e.g. incidents), each with distinct dose criteria. The *minimum* value of the calculated contamination levels, based on scaling of the dose value with the corresponding dose criterion, could then be regarded as the clearance level for the radionuclide under consideration.

In a *probabilistic* study, such as the one presented in this paper, one or more input parameters of the dosimetric model are varied by random sampling from pdfs (section 2.2.2). Consequently, the result of such an assessment is not a single value of the dose, but a distribution of doses calculated for a postulated, unit contamination level (here 1 Bq cm^{-2}). The advantage is that both realistic and low-probability exposures are captured by this distribution and one can get a sense of the relative conservatism of a specific scenario when compared with the dose distribution. The derivation of clearance levels based on a probabilistic dose assessment proceeds in a similar manner as that described for a deterministic assessment, but scaling of the contamination level is performed by equating certain percentiles of the (annual effective or skin-equivalent) dose distribution with corresponding dose criteria. In addition, it offers the flexibility and advantage of introducing additional dose constraints such as the one related to the concept of the 'representative person' as defined by ICRP (2006). In this context, and considering the principles of clearance and exemption, an annual effective dose of 100 μSv yr^{-1} was suggested previously by Hattori (2008) as a suitable (minimum) dose constraint for the optimization of radiological protection of the public. Ogino and Hattori (2009) successfully applied this dose constraint in their probabilistic verification study on exemption levels for surface contamination. Hence, our study employs this effective dose constraint in conjunction with the dosimetric translation of 'representative person' in probabilistic assessments.

The probabilistic approach of the dose assessment consists of 10^5 evaluations of the annual effective dose and the local skin-equivalent dose, each evaluation with input parameters randomly drawn from the pdfs defined in table 3 and with an initial surface-contamination level of 1 Bq cm^{-2}. The SCLs are then derived from the resulting dose distribution, for each radionuclide separately.

More specifically, certain percentiles of the dose distribution are scaled to the criteria described earlier. The $p = 50$th percentile (median value) is compared with, and scaled to, the annual effective dose criterion of 10 μSv yr^{-1} for realistic scenarios. This percentile is judged appropriate, since it is equally likely to draw an individual dose from the distribution lower or higher than the median dose. The $p = 99$th percentile is scaled to the annual effective dose criterion of 1 mSv yr^{-1} for conservative, low-probability scenarios. Similarly, the 99th percentile of the local skin-equivalent dose distribution is benchmarked against its corresponding criterion of 50 mSv yr^{-1}. The use of the 99th dose percentile for conservative, low-probability scenarios is inspired by the risk model presented in EC (1993, appendix C).

Additionally, the concept of the representative person—as defined in ICRP (2006)—is integrated in a similar manner. The representative person is an (hypothetical) individual who 'receives a dose that is representative of the more highly exposed people in the population'. For probabilistic dose assessments, the representative person is related to the 95th percentile of the dose distribution. More specifically, the probability of a person, randomly drawn from the population, receiving a dose greater than that of the representative person should be smaller than about 5% (ICRP 2006, section 3.5). To incorporate this concept in the current methodology, the 95th percentile of the effective dose distribution is required not to exceed the dose constraint of 100 μSv yr^{-1}.

In section 4.2, this methodology of deriving the limiting SCL using these four dose-percentile scalings is visualised for two radionuclides: Co-60 and Ac-227.

3.3. Rounding procedure

A rounding procedure could be applied to the derived SCLs similar to what has been done for the mass-specific clearance levels, as described in IAEA (2005b) and EC (2000), where logarithmic rounding is applied to powers of ten. This means that a derived value between 3×10^x and $3 \times 10^{x+1}$ is rounded to a value of 10^{x+1}.

This rounding procedure is typically applied when performing deterministic calculations to derive exemption or clearance levels. It reflects and expresses the absence of accuracy related to the dosimetric modelling especially since a spread around chosen fixed parameter values is to be expected. The situation is somewhat different in the case of probabilistic assessments, where such variations in parameter values are accounted for in parameter distributions. However, uncertainties related to the choice of pdfs and their input coefficients, additional variations in the fixed parameters and assumptions (simplifications) made in the dosimetric model may still justify the use of a rounding procedure. Rounding of clearance levels is not performed in this paper and is left to the reader.

3.4. Sampling statistics and convergence

All probabilistic calculations in this paper were performed using 10^5 scenario-based dose evaluations with input parameters randomly and independently drawn from their corresponding distribution functions (section 2.2.2). The question arises as to whether 10^5 evaluations are sufficient for the percentiles of the two dose distributions to have converged to their 'true' values, and with that the corresponding clearance levels. Therefore, in a preliminary assessment, a convergence study among all 413 nuclides was performed to investigate the values of the dose distributions' percentiles as a function of the number of independent dose evaluations, NMC. Several calculations using NMC $= 10$, 10^2, 10^3, 10^4 and 10^5 parameter-value drawings (selections) and subsequent dose evaluations were performed. This assessment indicated that of the order of 10^4 dose evaluations would already be sufficient for converged SCL values based on the 50th percentile of the annual effective dose distribution or on the 99th percentile of the annual, local skin-equivalent dose distribution. Among the 413 nuclides, the 99th skin-dose percentile actually exhibited the smallest variation between calculations with 10^4 and 10^5 dose evaluations, despite the fact that the tail of a dose distribution typically suffers from poor(er) statistics. The small variation can be explained by the fact that the skin-dose distribution is sensitive to only a limited number of distributed parameters: some do not influence the local skin-equivalent dose at all (such as the distance L), while several others merely affect it indirectly (such as the resuspension rate). Larger variations between calculations with 10^4 and 10^5 dose evaluations were obtained for the 95th and 99th percentiles of the annual effective dose and, hence, NMC was set to 10^5.

Next, 95% confidence intervals (95% CI) for the dose-distributions' percentiles can be determined to investigate the remaining uncertainties or variations from the sampling statistics using NMC $= 10^5$. We use the non-parametric bootstrap method to determine these 95% CIs. To this end, the originally obtained (empirical) dose distributions (for effective dose E_{tot} and local skin-equivalent dose $H_{\mathrm{skin,tot}}$) are resampled *with replacement*, for each radionuclide separately. In total, 2000 resamples (bootstrap samples) are taken, each one of size 10^5, equal to that of the original distributions. For each bootstrap sample the relevant percentiles are determined. From the 2000 resulting values of the pth dose percentile ($p = 50$, 95 or 99 for the effective dose and $p = 99$ for the local skin-equivalent dose), the bootstrap's standard deviation σ_p can be determined, i.e. the standard error of the pth dose percentile. Assuming these dose percentiles to be 'normally' distributed, the 95% CI of the pth percentile is then evaluated as $D_p \pm 1.96\sigma_p$ where D_p (either E_{tot} or $H_{\mathrm{skin,tot}}$) is the dose percentile of the original distribution (not the mean value of this percentile obtained from the resampling). The relative 95% CI, given by $1.96\sigma_p/D_p$ (expressed in %), is a measure of the relative spread or uncertainty in the pth dose percentile resulting from Monte-Carlo sampling and is calculated for each percentile and for all radionuclides. Results of this analysis are presented in section 4.8.

Table 4. Overview of the five calculations, indicating the exposed individual, the AMAD considered for inhalation, the skin-dosimetry model (with/without contribution of alpha-particle radiation), and the model configuration ($\delta = 1$ for the SUDOQU model set within the mass-balance framework; $\delta = 0$ for the model in the absence of mass-balance and physical decay). The final column indicates the section in which the results are presented and discussed. Calculation 1 is the reference calculation (ref) of this study.

Calc. nr.	Exposed individual	AMAD for inhalation DC	Skin dosimetry (with/without α)	Model switch δ	Section
1 (ref)	Worker	5 μm	Without	1	4.3
2	Worker	5 μm	With	1	4.4
3	Worker	1 μm	Without	1	4.5
4	Adult member of public	1 μm	Without	1	4.6
5	Worker	5 μm	Without	0	4.7

4. Results and discussion

4.1. Description of the calculations

This section describes the results of five sets of calculations of surface-specific clearance levels: one reference calculation and four variations. They all use the SUDOQU model with ingredients as described in section 2 and applying the methodology from section 3. In the first calculation, the maximum inhalation and ingestion DCs for workers are used, with inhalation DCs based on an AMAD of 5 μm, similar to the calculations in EC (1999). Therefore, this calculation is the *reference* calculation in this study. The local skin-equivalent DCs consider contributions of beta-particle and gamma-photon radiation only. The calculation is performed using the RIVM-SUDOQU model based on mass/activity-balance equations which best describe the normal reuse scenarios after clearance, and thus with model switch δ set to 1 (van Dillen and van Dijk 2018).

The other four calculations are similar to the reference calculation, but with variations in the applied DCs (calculations 2 through 4) or model configuration (calculation 5). Calculation 2 includes the contribution of (high-energy) alpha-particle radiation to the skin dosimetry, calculation 3 uses an AMAD value for workers of 1 μm, calculation 4 applies the maximum inhalation and ingestion DCs for adult MOP with a default AMAD of 1 μm for inhalation. Calculation 5 uses the same DCs as those in the reference computation, but was performed in the absence of the mass/activity-balance framework (and ignoring physical decay), with δ set to 0. A brief summary of the different computations is presented in table 4. Each calculation results in a set of radionuclide-specific values of the SCL (Bq cm^{-2}), with those from calculations 1 through 4 listed in table A.1 of appendix A.

In section 4.2, we first visualise the methodology for deriving the SCL (section 3.2) by means of examples for Co-60 and Ac-227. Results of the reference calculation are presented in section 4.3. Sections 4.4 through 4.7 report the results of the other four calculations, each with a comparison to the reference calculation. Finally, section 4.8 deals with issues related to uncertainties from sampling statistics (relative 95% confidence intervals).

4.2. Derivation of clearance level from dose distribution: examples for Co-60 and Ac-227

A probabilistic dose computation evaluated at a total, initial surface-contamination level of $C_0 = 1.0$ Bq cm^{-2} for a given radionuclide results in a set of 10^5 values (section 3.4) for both the total annual effective dose E_{tot} and the annual local, skin-equivalent dose $H_{\mathrm{skin,tot}}$. The spectrum or distribution of these doses can be visualised by the probability density (yr μSv^{-1}) of the annual dose quantity (μSv yr^{-1}). Such spectra are useful to illustrate the methodology of deriving the limiting SCL. This methodology is shown below for two radionuclides: Co-60 and Ac-227.

The probability-density spectra for Co-60 at $C_0 = 1.0$ Bq cm^{-2} resulting from the reference computation (table 4; section 4.3) are shown in figure 1(a) for E_{tot} and figure 1(b) for $H_{\mathrm{skin,tot}}$. The dose percentiles $E_{\text{50-perc.}}$, $E_{\text{95-perc.}}$, $E_{\text{99-perc.}}$ and $H_{\text{skin,99-perc.}}$ are indicated by the arrows and vertical dash-dotted lines, with their numerical values listed in table 5. Within the plotted dose range, the percentile-related dose criteria from sections 3.1 and 3.2 are plotted as grey, dotted vertical lines, e.g. $E_{\mathrm{50,crit}}$ and $E_{\mathrm{95,crit}}$ in figure 1(a).

At an initial surface-contamination level of 1.0 Bq cm^{-2}, the 50th percentile of the calculated effective dose distribution, $E_{\text{50-perc.}}$ (30 μSv yr^{-1}), exceeds the corresponding dose criterion of $E_{\mathrm{50,crit}} = 10$ μSv yr^{-1}, whereas the other percentiles are well below their corresponding criteria. Scaling of the distribution is thus necessary to fulfil all dose criteria. If the initial surface-contamination level is scaled (multiplied) by the ratio $E_{\mathrm{50,crit}}/E_{\text{50-perc.}}$, we obtain SCL_{50} with a value of 0.33 Bq cm^{-2}. As seen from the scaled dose distribution in figure 1(c), the criteria for all dose percentiles are now met. This also follows from the (scaled) dose-percentile data in table 5. Similar scaling of the distributions with respect to the other relevant dose percentiles, shown in figures 1(d)–(f), results in at least one criterion that is exceeded, as seen from the

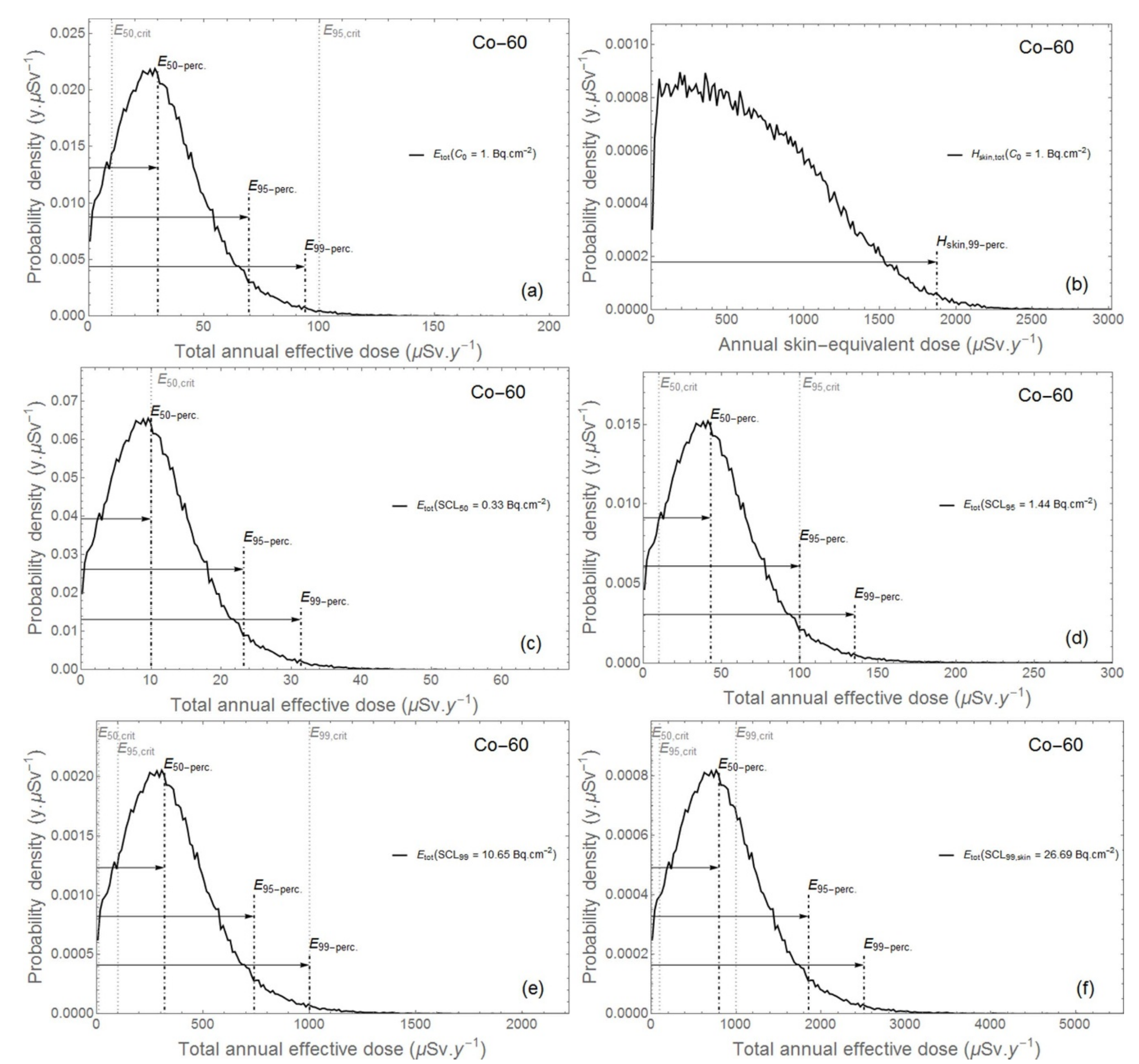

Figure 1. Probability-density functions of the annual effective dose E_{tot} (a) and the annual local, skin-equivalent dose $H_{\mathrm{skin,tot}}$ (b), calculated for Co-60 using an initial, total surface contamination level of 1.0 Bq cm^{-2}. Their dose percentiles are indicated by the arrows and dash-dotted vertical lines ($E_{\text{50-perc.}}$, $E_{\text{95-perc.}}$ and $E_{\text{99-perc.}}$ for the effective dose and $H_{\text{skin,99-perc.}}$ for the local skin-equivalent dose) and the percentile-related dose criteria are shown by the vertical, grey-dotted lines. The effective-dose spectra in figures (c) through (f) are similar to that in (a), but scaled such that a certain dose percentile equals its corresponding criterion. These spectra thus show the effective-dose distributions for initial contamination levels of SCL_{50}, SCL_{95}, SCL_{99} and $\mathrm{SCL}_{99,\mathrm{skin}}$, respectively. Scaled distributions of $H_{\mathrm{skin,tot}}$ are not shown.

Table 5. Percentiles of dose distributions for Co-60: the 50th, 95th and 99th percentiles of the annual effective dose ($E_{\text{50-perc.}}$, $E_{\text{95-perc.}}$ and $E_{\text{99-perc.}}$, respectively) and the 99th percentile of the annual local, skin-equivalent dose ($H_{\text{skin,99-perc.}}$) for initial contamination levels of C_0, SCL_{50}, SCL_{95}, SCL_{99}, and $\mathrm{SCL}_{99,\mathrm{skin}}$.

Initial surface contamination (Bq cm^{-2})		$E_{\text{50-perc.}}$ (μSv yr^{-1})	$E_{\text{95-perc.}}$ (μSv yr^{-1})	$E_{\text{99-perc.}}$ (μSv yr^{-1})	$H_{\text{skin,99-perc.}}$ (μSv yr^{-1})
C_0	1.00	**29.95**	69.48	93.91	1873.42
SCL_{50}	0.33	*10.00*	23.20	31.35	625.47
SCL_{95}	1.44	**43.11**	*100.00*	135.17	2696.36
SCL_{99}	10.65	**318.93**	**739.82**	*1000.00*	19 948.30
$\mathrm{SCL}_{99,\mathrm{skin}}$	26.69	**799.40**	**1854.35**	**2506.48**	*50 000.00*

Values equal to their corresponding dose criteria are given in *italics*, and in **boldface** if they exceed them. Raw computational data are shown with the fractional part of each value displayed in two digits. The total number of digits may thus exceed the actual significance of 2–3 digits.

boldface values in table 5. For example, at $\mathrm{SCL}_{99} = 10.65$ Bq cm^{-2} for which $E_{\text{99-perc.}} = E_{99,\mathrm{crit}}$, the scaled 50th and 95th effective dose percentiles exceed their corresponding criteria of 10 μSv yr^{-1} and 100 μSv yr^{-1}, respectively. Hence, the surface-specific clearance level for Co-60, SCL, at which all four dose criteria are met, is equal to SCL_{50}. This is the *minimum* of the four percentile-related clearance levels, i.e. the *most restrictive*

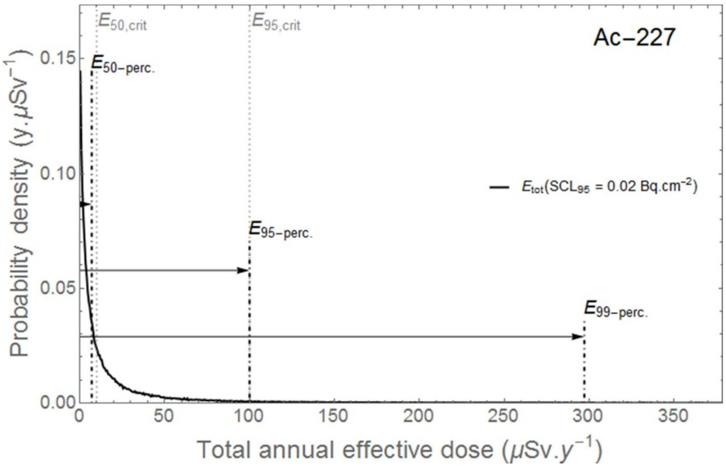

Figure 2. Probability density as a function of the annual effective dose for Ac-227 scaled to an initial surface-contamination level of $SCL_{95} = 0.02$ Bq cm^{-2}. Similar to figure 1(d) for Co-60, with the difference that for Ac-227 the dose criterion of the 95th percentile is limiting (most restrictive).

Table 6. Percentiles of dose distributions for Ac-227. Similar to table 5 for Co-60.

Initial surface contamination (Bq cm^{-2})		$E_{50\text{-perc.}}$ (μSv yr^{-1})	$E_{95\text{-perc.}}$ (μSv yr^{-1})	$E_{99\text{-perc.}}$ (μSv yr^{-1})	$H_{\text{skin,99-perc.}}$ (μSv yr^{-1})
C_0	1.00	**351.63**	**4978.17**	**14 789.94**	7308.21
SCL_{50}	0.03	*10.00*	**141.58**	420.61	207.84
SCL_{95}	0.02	7.06	*100.00*	297.10	146.81
SCL_{99}	0.07	**23.77**	**336.59**	*1000.00*	494.14
$SCL_{99,skin}$	6.84	**2405.70**	**34 058.76**	**101 187.13**	*50 000.00*

value. Obviously, any contamination level smaller than this SCL will also comply with the four imposed criteria. For this calculation, the value of SCL = 0.33 Bq cm^{-2} is therefore also the *maximum* value at which all four criteria are satisfied. Any value larger than that leads to the exceedance of at least one dose criterion.

Not all radionuclides have an effective dose distribution as the one displayed in figure 1(a) for Co-60. Some nuclides may have a dose-probability density with its mode located at a small value and with a tail that extends to (very) large values. An example of such a distribution is displayed in figure 2 for radionuclide Ac-227, which has already been scaled to its most restrictive SCL of $SCL_{95} = 0.02$ Bq cm^{-2}. At this minimum level, agreement with all imposed dose criteria is obtained, as also follows from the (scaled) dose-percentile data in table 6. The fact that another dose criterion (i.e. $E_{95,\text{crit}}$ instead of $E_{50,\text{crit}}$ for Co-60) determines the SCL is therefore directly related to the different shape of the dose distribution, which was the motive for developing the method described in section 3.2.

Using this probabilistic technique, nuclide-specific SCLs are derived for the five calculations described in table 4. To indicate which dose percentile is limiting for the SCL, a label is added: E50, E95, E99 or Hskin99. For Co-60, the label is E50 (effective dose, 50th percentile scaled to its criterion, i.e. SCL_{50}) and for Ac-227 it is E95, both for the reference calculation (section 4.3). These labels are included in table A.1 of appendix A. Table 7 provides an overview of how many of the 413 radionuclides have their SCL limited by a certain dose criterion in the five calculations. For the majority of radionuclides (86%–94%), the limiting value of the derived SCL is based on the 50th percentile of the effective dose distribution. The 99th percentile of the effective dose distribution is never limiting, which indicates that, at the limiting SCL, the effective dose exceeds the criterion of 1 mSv yr^{-1} in much less than 1% of all probabilistic dose evaluations for all radionuclides considered. At the derived clearance levels, it is thus very unlikely that the effective dose limit of 1 mSv yr^{-1} is exceeded.

4.3. Clearance levels for reference calculation (worker, AMAD = 5 μm, no alpha skin dose)

Choices made for the DCs in the reference calculation were similar to those in EC (1999), although updated, corrected and extended datasets have been used for calculations in this article (section 2.3). A scatter plot of these clearance levels (versus nuclide number) is shown in figure 3 for radionuclides with a half-life <1 day

Table 7. For the five calculations in table 4, the number of nuclides are listed for which the surface-clearance level is limited by a certain dose percentile: E50 E95, E99 and Hskin99 (definitions in text).

	Calculation				
Limiting criterion	1	2	3	4	5
E50	385	365	371	357	389
E95	5	2	20	34	9
E99	0	0	0	0	0
Hskin99	23	46	22	22	15

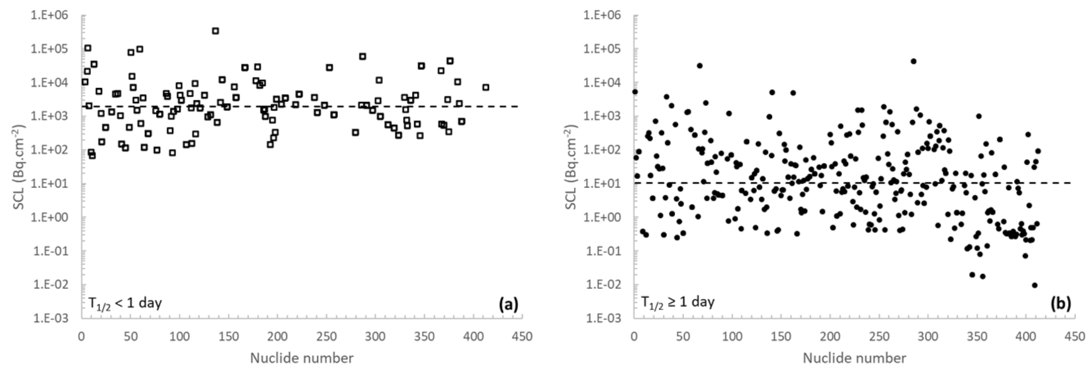

Figure 3. Derived surface-clearance level SCL (Bq cm^{-2}) for 413 radionuclides in the reference calculation are shown. Nuclide numbers and numerical values of SCL can be found in table A.1 of appendix A. Data are plotted for radionuclides with a half-life <1 day in (a) and ⩾1 day in (b). Median SCL values are indicated by the dashed, horizontal lines: 1.93 × 10^{3} Bq cm^{-2} for nuclides with $T_{1/2} < 1$ day and 1.04 × 10^{1} Bq cm^{-2} for nuclides with $T_{1/2} \geqslant 1$ day.

(a) and ⩾1 day (b). Median values for the data plotted in both graphs are indicated by the dashed, horizontal lines.

The scatter plot in figure 3(a) shows that radionuclides with half-lives smaller than one day have large SCLs, inasmuch as contamination (fixed and removable) vanishes within at most several days by radioactive decay. Hence, annual doses remain small and corresponding values of SCL are large as they are inversely proportional to the dose. The median value of the data in figure 3(a) is 1.93 × 10^{3} Bq cm^{-2} but values can exceed 10^{5} Bq cm^{-2}. Rh-103m holds the largest value of 3.36 × 10^{5} Bq cm^{-2} (nuclide 137; $T_{1/2} = 0.94$ h).

Nuclides with half-lives larger than one day typically have a much smaller clearance level, which can already be seen from the median value of 1.04 × 10^{1} Bq cm^{-2} in figure 3(b). This is not only related to the longer half-life of these radionuclides, but also to the values of their DCs, which may, in turn, also depend on half-life. The dependence of DCs on half-life will, however, be less pronounced, since some of them are expressed as dose rates (external, skin), and since DCs in this study include weighted contributions of radioactive progeny. Small clearance levels with values well below 1 Bq cm^{-2} mostly occur among heavy radionuclides with a mass number above 200, which are often high-toxicity alpha emitters and/or nuclides with high-toxicity alpha-emitting progeny. This can usually be attributed to large values of DCs for inhalation and ingestion. Many of the long-lived, high-toxicity alpha emitters have a clearance level between 0.1 Bq cm^{-2} and 0.4 Bq cm^{-2}, e.g. Ra-226, Th-229, U-232, Pu-239 and Am-241 (with radioactive progeny included). The three nuclides with the smallest clearance levels in the dataset are Ac-227 (nuclide 345, $T_{1/2} = 21.8$ years, β^-/α-emission), its parent Pa-231 (nuclide 356, $T_{1/2} = 3.28 \times 10^4$ years, α-emission) and Cf-254 (nuclide 409, $T_{1/2} = 0.17$ years, spontaneous fission) with values of 0.020 Bq cm^{-2}, 0.018 Bq cm^{-2} and 0.010 Bq cm^{-2}, respectively. The fact that Cf-254 has the smallest surface-clearance value despite the relatively short half-life is caused by the large contribution of external radiation. The point-source constant for the personal dose equivalent $h_p(10)$ is about 131 times larger than that of Co-60 (Otto 2016), with a 95% contribution from high-energy neutrons emitted during spontaneous fission of Cf-254. Hence, radionuclides that decay with a significant fraction by spontaneous fission are even more radiotoxic than high-toxicity alpha emitters.

The strong dependence of the clearance level on the radionuclides' half-lives can best be seen in figure 4 showing SCL as a function of $T_{1/2}$(s). For $T_{1/2} < 1$ year, the band of clearance levels is inversely proportional to the half-life, as seen by the dashed guide-to-the-eye. In this half-life dominated region, the band of clearance levels extends over two orders of magnitude caused by the spread in DCs. For instance, at $T_{1/2} = 1$ day, values range between 40 Bq cm^{-2} and 4000 Bq cm^{-2}. The inverse proportionality can be

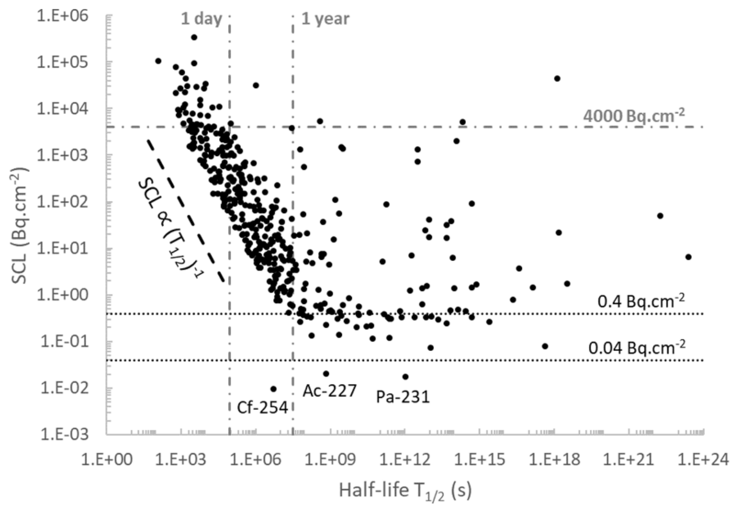

Figure 4. Derived surface-clearance level SCL (Bq cm^{-2}) for 413 radionuclides in the reference calculation as a function of their half-life $T_{1/2}$ (s). The thick dashed line is a guide-to-the-eye showing inverse proportionality to the half-life. The dotted, horizontal lines indicate the levels defined as contamination in the IAEA transport regulations (IAEA 2018, para 214). The dash-dotted horizontal line at 4000 Bq cm^{-2} indicates the upper range of the clearance values at one day. Nuclides with a derived SCL < 0.04 Bq cm^{-2} are labelled by name.

understood well from the model equations (appendix B). With the physical decay constant λ_r much larger than other surface-removal constants, annual doses are proportional to $\Psi(\lambda_r \Delta T_{\text{tot}})$, with function Ψ defined in appendix B and $\Delta T_{\text{tot}} = 1$ year. For large λ_r, $\Psi \propto (\lambda_r)^{-1}$ and thus doses are proportional to $T_{1/2}$. With SCL inversely proportional to the dose, we thus obtain SCL $\propto \left(T_{1/2}\right)^{-1}$, as seen in figure 4.

Next, the band of SCL values starts to level off at $T_{1/2} = 1$ year since this equals the scenario-integration time for annual dose evaluations. For $T_{1/2} > 1$ year, the majority of values seem to concentrate around 0.4 Bq cm^{-2}, the activity level above which contamination is defined for beta and gamma emitters and low-toxicity alpha emitters in the Transport Regulations by the IAEA (2018). Again, there is a large spread in values, with higher values, for e.g. parent radionuclides that decay mainly by electron capture or low-energy beta emission, both without the presence of any radiotoxic progeny. Values much smaller than 0.4 Bq cm^{-2} are also possible, as discussed earlier; the smallest values (Ac-227, Pa-231 and Cf-254) are even below 0.04 Bq cm^{-2}, the activity level defining contamination for 'other alpha emitters' in IAEA (2018). In section 5.3, we compare these SCLs with those from (EC 1999, table 7.5).

As seen from table 7 (calculation 1), over 93% of all derived clearance levels are limited by the 50th percentile of the annual effective dose distribution. Almost 6% of the values is limited by the 99th percentile of the annual, local skin-equivalent dose distribution. A little over 1% of the clearance levels is based on the 95th percentile of the annual effective dose distribution (Gd-148, Ac-227, Pa-231, Cm-242, Cf-248). No clearance levels are limited by the 99th percentile of the annual effective dose distribution.

4.4. Clearance levels for calculation 2 with alpha contribution to skin dose

The second calculation is almost identical to the reference calculation, i.e. with maximum DCs for workers, for inhalation based on an AMAD of 5 μm and performed using the RIVM-SUDOQU model ($\delta = 1$), but it includes the contribution of high-energy alpha emission to the skin dose. In effect, only nuclides emitting alpha particles of energy >6 MeV will contribute to the skin dose as they have sufficient energy to reach the sensitive layer containing the basal cells (SSK 2017). Starting from nuclide Pb-212, total skin-DCs deviate from those used in the reference calculation. Below, we will therefore only focus on the changes among these 90 heavy nuclides (number 324 through 413).

Values of limiting SCL can be found in table A.1 in appendix A and are shown in figure 5(a) as a function of the nuclide number. As a comparison, the values from the reference calculation are shown in figure 5(b). The minimum and maximum values among these 90 nuclides have not changed by including the alpha contribution to the skin dosimetry, with the minimum value still at 0.01 Bq cm^{-2} for Cf-254. However, more radionuclides have shifted into the region of 0.02–0.04 Bq cm^{-2} as a result of this contribution (the region between nuclides 340 and 360). For example, Ra-226 (nuclide 340) decreases from 0.12 Bq cm^{-2} to 0.03 Bq cm^{-2} and Th-229 (nuclide 350) from 0.12 Bq cm^{-2} to 0.02 Bq cm^{-2}. The overall decrease in clearance levels can be seen from the decrease in median value for these 90 radionuclides, decreasing from 5.40 Bq cm^{-2} to 1.40 Bq cm^{-2} (dashed lines in figure 5).

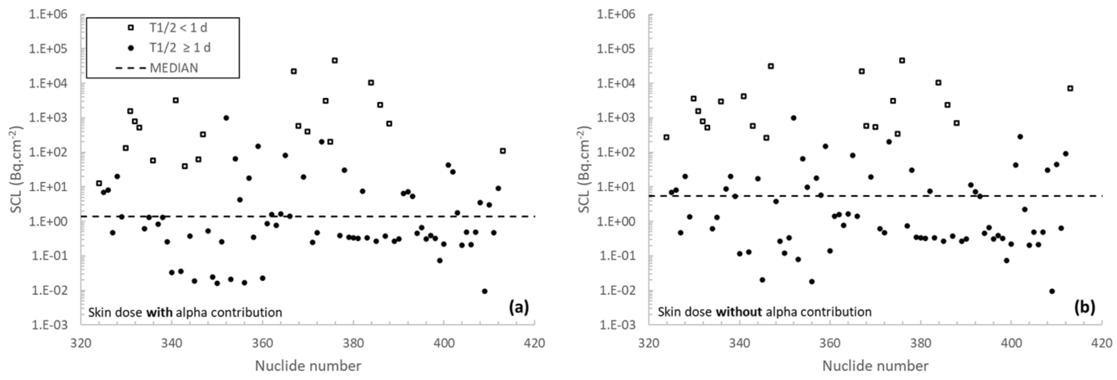

Figure 5. Derived surface-clearance level SCL (Bq cm^{-2}) for 90 heavy radionuclides (Pb-212 through Fm-254) in calculation 2 including the contribution of alpha emission to the skin dose (a). As a comparison, data from the reference calculation, without this contribution, are shown in (b). Median values: 1.40 Bq cm^{-2} in (a) and 5.40 Bq cm^{-2} in (b).

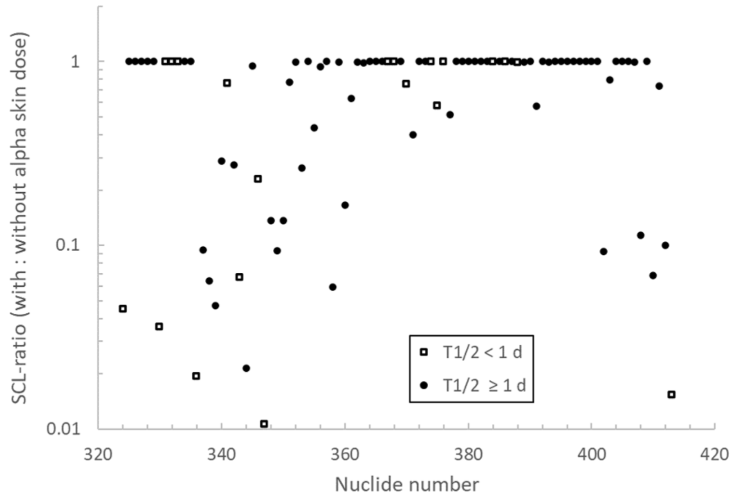

Figure 6. Ratio of surface-clearance values with an alpha contribution to the skin dose (calculation 2) to those without alpha contribution (calculation 1) for 90 heavy radionuclides: Pb-212 through Fm-254.

To clearly visualise the change in SCL, the ratio of clearance levels (with alpha: without alpha) is shown in figure 6. For 25 nuclides, the SCL decreases by more than a factor of two (ratio < 0.5), of which 15 by a factor of larger than ten (ratio < 0.1). The largest decrease is observed for Th-226 (number 347): its SCL drops by two orders of magnitude from 3.05×10^4 Bq cm^{-2} to 3.24×10^2 Bq cm^{-2} (ratio of 0.01). This is mainly caused by daughter radionuclide Ra-222: its large contribution results from alpha emission at an energy of 6.6 MeV. Since alpha-particle energy increases with decreasing half-life (Geiger and Nuttal 1911), the largest alpha skin-DCs are found for (very) short-lived radionuclides, such as Po-211 through Po-216 (SSK 2017). These high-energy alpha emitters appear as progeny in several decay chains headed by a parent radionuclide listed in table A.1 and are thus the main cause for the drop in SCL as observed in figures 5 and 6. Due to the increased skin dose, the SCL for 23 additional nuclides is limited by the local skin-equivalent dose (Hskin99) instead of the effective dose (E50 or E95), as seen in table 7.

4.5. Clearance levels for calculation 3 with AMAD = 1 μm

For the third calculation, the reference settings of calculation 1 are adopted, but with maximum, occupational inhalation DCs based on an AMAD of 1 μm instead of 5 μm (table 4). The ratio of inhalation DCs (AMAD = 1 μm: AMAD = 5 μm) varies between 0.48 and 1.93, i.e. either about a factor of two smaller or larger. Of the 413 radionuclides, 203 have a smaller DC, while 199 show a larger DC for an AMAD of 1 μm. However, for heavy radionuclides (mass number > 210), the inhalation DC is mostly larger for an AMAD of 1 μm.

Figure 7 shows the ratio of the derived clearance levels (AMAD = 1 μm: AMAD = 5 μm). As suggested by the ratio of DCs, clearance levels for an AMAD of 1 μm can either be larger or smaller, with ratios varying between 0.75 for Cm-244 (nuclide 395) and Cf-248 (nuclide 403), and 1.19 for Gd-148 (nuclide 246).

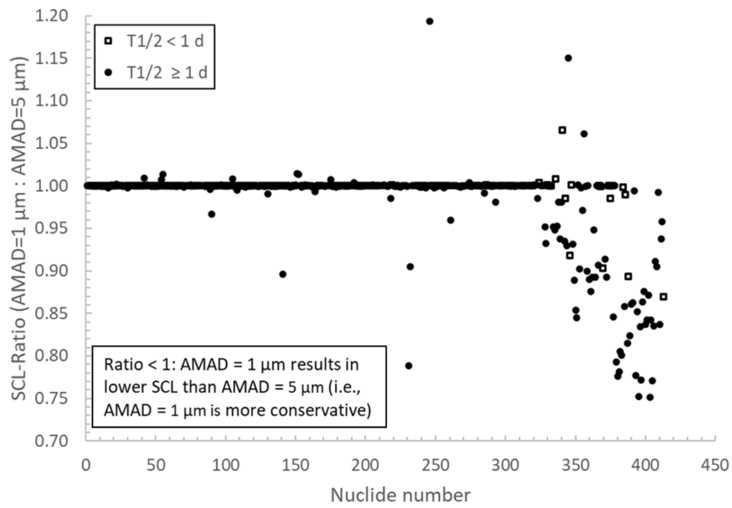

Figure 7. Ratio of surface-clearance values obtained with occupational inhalation dose coefficients based on an AMAD of 1 μm (calculation 3) to those based on an AMAD of 5 μm (calculation 1) for the 413 radionuclides in this study.

The derived clearance levels for nuclides with a mass number larger than 210 (nuclide number > 323) are affected most by the change in AMAD, but the effect remains relatively modest, with deviations of at most 33% for a ratio of 0.75. The lowest values of SCL hardly change and remain those of Ac-227, Pa-231 and Cf-254, with values of 0.023 Bq cm^{-2}, 0.019 Bq cm^{-2} and 0.010 Bq cm^{-2}, respectively.

Compared to the reference calculation, more radionuclides have their SCL limited by the 95th percentile of the effective dose distribution, as seen from table 7. This mostly occurs for heavy nuclides for which the inhalation pathway becomes even stronger due to increased inhalation DCs. This pathway strongly depends on the distribution of the resuspension rate, which is characterised by a long tail of the lognormal distribution. The effective dose distribution is therefore also characterised by an extended tail causing the limiting criterion to shift from the 50th to the 95th percentile.

4.6. Clearance levels for calculation 4 with DCs for adult MOP

In calculation 4, public DCs instead of occupational DCs are used for inhalation and ingestion. The reference settings from calculation 1 are adopted but with maximum values of DCs for adult MOP. For inhalation, DCs are based on an AMAD of 1 μm. The ratio of these coefficients to those used in the reference calculation varies between 0.5 (Rb-81) and 11.3 (Tc-97) and is mostly larger than 1 for heavy nuclides with mass numbers above 210. Not only inhalation DCs can change, but also the maximum coefficients related to the ingestion pathway. Most ingestion DCs for adult MOP are equal or close to those for workers, but for 25 radionuclides the deviation is more than 10%, their values being either smaller or larger. Nuclides Bi-210, Po-209 and Po-210 have maximum ingestion DCs that are five times larger for adult MOP.

For the majority of radionuclides, derived clearance levels are close to those in the reference calculation (see table A.1 in appendix A). The minimum levels are again those of Ac-227, Pa-231 and Cf-254 with values of 0.023 Bq cm^{-2}, 0.018 Bq cm^{-2} and 0.010 Bq cm^{-2}, respectively.

Changes can best be observed by considering the ratio of clearance levels (MOP: Worker) as shown in figure 8. Ratios significantly smaller than 1 occur mostly for heavy nuclides. The largest reduction in clearance level, by a factor of almost five (ratio between 0.21 and 0.23), is observed for Bi-210, Po-209 and Po-210, all three limited by the 50th percentile of the annual effective dose (E50) in both calculations. In principle their factor-five-reduction in SCL is related to the combined effect of larger DCs for inhalation (factor 2–4) and for ingestion (factor 5 as mentioned above). From this it is likely that the ingestion pathway is dominant for scenarios around the 50th percentile of the effective dose distribution.

As in calculation 3—also employing inhalation DCs with AMAD = 1 μm (for workers)—more clearance levels are limited by the 95th percentile of the effective dose distribution (E95) compared to those in the reference calculation (table 7). As explained in section 4.5, this is related to an extended tail of the effective dose distributions brought about by the inhalation pathway with increased DCs.

4.7. Clearance levels for calculation 5 in the absence of mass/activity balance and radioactive decay

Calculation 5 uses DCs identical to those in reference calculation 1 for all exposure pathways, but is performed without the mass-balance formulation and radioactive decay. In SUDOQU this is achieved by setting model switch δ to 0, thereby ignoring removal, decay and deposition processes. This leads to a

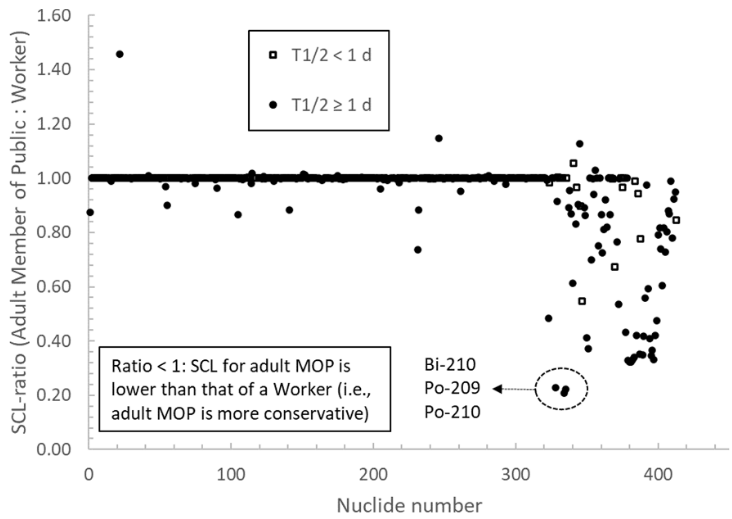

Figure 8. Ratio of surface-clearance values obtained with public ingestion and inhalation dose coefficients for adults (calculation 4) to those obtained with occupational dose coefficients (reference calculation) for the 413 radionuclides in this study.

constant surface-contamination level throughout the year, as can be seen from the equations in appendix B. As explained by van Dillen and van Dijk (2018), this type of model, which resembles the basic model from IAEA (2005a), is adequate for scenarios in which individuals may be exposed to a continuous flow of freshly contaminated items. For the reuse scenarios considered in the current study, this type of model is less adequate, but results are presented merely to demonstrate the effect of mass/activity-balance and decay processes. Data of the corresponding clearance levels are therefore not listed in table A.1 in appendix A but only shown in figure 9(a) for the 413 radionuclides in this study. Results of the reference calculation (section 4.3) with $\delta = 1$ are shown in figure 9(b) as a comparison. The absence of removal and decay mechanisms leads to a band of clearance levels scattered around a median value of 0.91 Bq cm^{-2}, which is much smaller than its reference counterpart of 41.4 Bq cm^{-2}. The smallest levels in this study can again be assigned to Ac-227, Pa-231 and Cf-254 with values of 5.1×10^{-3} Bq cm^{-2}, 4.6×10^{-3} Bq cm^{-2} and 2.1×10^{-3} Bq cm^{-2}, respectively, a factor of about four smaller than those in the reference calculation. Exposure to constant surface- and air-contamination levels not only leads to more restrictive clearance levels, but also to a smaller spread in these levels (i.e. a narrower band), as is visible from figures 9(a) and (b).

Figure 9(c) shows the SCL from figure 9(a) as a function of the half-life. Unlike the reference calculation (figure 4), no dependence on half-life is observed, since radioactive decay is ignored. More derived clearance levels attain values between 0.04 Bq cm^{-2} and 0.4 Bq cm^{-2} (IAEA 2018). Despite the fact that the calculation without removal and decay processes is more conservative, values significantly smaller than 0.04 Bq cm^{-2} are not observed, with the exception of the aforementioned three nuclides.

Figure 9(d) shows the ratio of clearance levels in calculation 5 to those in the reference calculation, as a function of half-life. For $T_{1/2} < 1$ year, there is a clear proportionality with half-life, as seen by the dashed guide-to-the-eye. As explained in section 4.3, this is the region dominated by radioactive decay within a scenario-integration period of one year. Since $\mathrm{SCL}_{\delta=0}$ is independent of $T_{1/2}$ and $\mathrm{SCL}_{\delta=1} \propto \left(T_{1/2}\right)^{-1}$, the ratio is proportional to $T_{1/2}$. For some short-lived radionuclides, however, the observed ratio is up to a factor three smaller than the ratio estimated using the half-life proportionality relation. These nuclides are—besides radioactive decay—greatly affected by activity-removal processes such as wipe-off and resuspension, and they are typically characterised by large DCs for inhalation, e.g. Ra-223, Ac-225, Am-242 and Es-253.

For $T_{1/2} > 1$ year, the effect of radioactive decay becomes smaller and the ratio levels off and saturates at values between 0.25 and 0.90. This can be clearly seen from the inset of figure 9(d). For these long-lived radionuclides, the effect of the removal and deposition mechanisms in the SUDOQU model becomes clearly visible. Clearance levels in the conservative model with constant contamination levels ($\mathrm{SCL}_{\delta=0}$) can thus be up to four times smaller (more restrictive) than those in the model including these mechanisms ($\mathrm{SCL}_{\delta=1}$). Note that this is similar to the observation for some of the short-lived nuclides, as previously mentioned. The fact that the impact of pure mass-/activity balance is limited to a factor of at most four can for instance be attributed to the limited contribution of removable surface contamination ($f_{\mathrm{rem},i}$, table 3), being smaller than 50% of the total surface contamination in each scenario of the probabilistic computation.

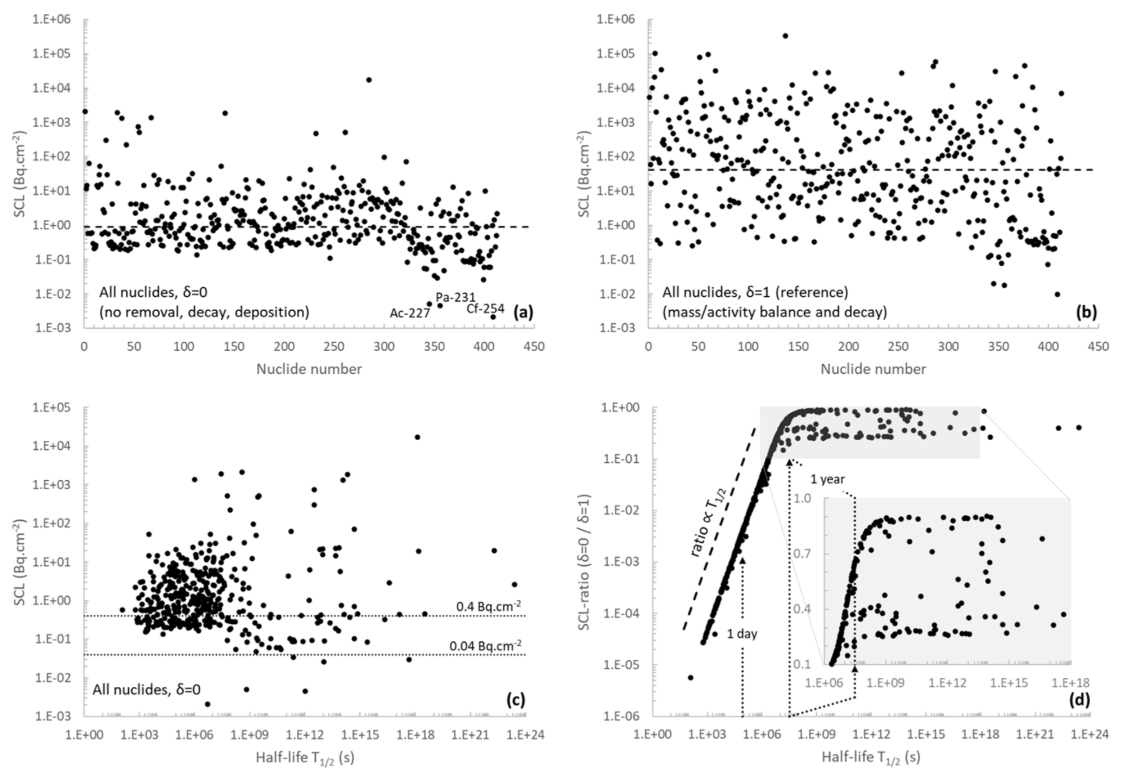

Figure 9. Derived surface-clearance levels, SCL (Bq cm^{-2}), for 413 radionuclides in calculation 5 in the absence of removal, decay and deposition mechanisms, $\delta = 0$ (a). As a comparison, data from the reference calculation, which includes these mechanisms, are plotted in (b). Median values: 0.91 Bq cm^{-2} in (a) and 41.4 Bq cm^{-2} in (b). Clearance levels from (a) are plotted again as a function of half-life $T_{1/2}$ (s) in (c). The dotted, horizontal lines indicate the levels defined as contamination in the transport regulations (IAEA 2018). The ratio of clearance levels from calculation 5 with $\delta = 0$ to those from reference calculation 1 with $\delta = 1$ (ratio of data in (c) to those in figure 4) as a function of half-life (s) is shown in (d). The thick dashed line is a guide-to-the-eye showing proportionality to half-life. The grey shaded area is magnified in the inset of (d), but with the vertical axis on a linear scale.

Table 8. The relative 95% confidence interval of dose percentiles in the reference calculation (section 3.4). Minimum, maximum, median and mean values among 413 radionuclides in this study are presented for the 50th, 95th and 99th percentiles of the annual effective dose distribution (E50, E95 and E99, respectively) and for the 99th percentile of the annual, local skin-equivalent dose distribution (Hskin99).

Values in %	E50	E95	E99	Hskin99
Minimum	0.36	0.48	0.74	0.51
Maximum	1.28	2.28	4.25	0.68
Median	0.49	0.65	0.96	0.57
Mean	0.55	0.83	1.32	0.58

4.8. Uncertainties from sampling statistics

Uncertainties from sampling statistics can be determined by calculating the relative 95% confidence intervals. These intervals were derived using the bootstrap method described in section 3.4. For the reference calculation, table 8 shows the minimum, maximum, median and mean values of the relative 95% confidence intervals among 413 radionuclides for the four dose percentiles labelled E50, E95, E99 and Hskin99. They remain relatively small for all percentiles and for all nuclides, on average between 0.5% and 1.3%, in worst cases not exceeding 4.3%. The observed relative spread or uncertainty in dose approximately equals the relative uncertainty in the corresponding clearance levels. Remembering that the limiting SCL is never based on the 99th percentile of the effective dose distribution (table 7), the relative uncertainties—*resulting from sampling statistics only*—are judged acceptable for the current study. They are likely to be much smaller than other variations and uncertainties related to the assumptions in the methodology, such as theoretical model assumptions, the choice of pdfs for distributed parameters and the choice of fixed-parameter values.

Limiting SCLs in table A.1 in appendix A are presented without any uncertainties, but based on the results in table 8 a typical relative sampling uncertainty of the order of 1% should be taken into account.

5. Selection and application of values

5.1. Selection of clearance levels

The development of different sets of clearance levels in this probabilistic study was based on the following considerations:

- Should the end-user of the cleared object be considered as a 'worker' or as an 'adult member of the public' in terms of inhalation and ingestion DCs by the ICRP?
- In the case of a 'worker', what size of AMAD should be used: 1 μm or 5 μm?
- Should the contribution of high-energy alpha radiation be included in the assessment of the skin-dose?
- What is the benefit of taking into account mass-balance in removal mechanisms as well as radioactive decay in the exposure and dose assessment, i.e. using the SUDOQU methodology?

Since five sets of nuclide-specific SCLs have been derived (table 4), the selection of the set judged best appropriate for final use will depend on the existing radiation-protection (regulatory) framework.

The choice of DCs influences the values of the governing clearance levels mediated by changes in the underlying dose distributions. Choices with respect to DCs used in the first calculation (section 4.3) show the largest resemblance with those in EC (1999), which is the reason for regarding the corresponding SCLs as the reference set. Other sets, resulting from calculations with alternative DCs (sections 4.4 through 4.6), are generally more restrictive, especially for heavy radionuclides (mass number above 210). We emphasise that this does not imply that the reference set is not sufficiently conservative. In fact, section 5.2 shows that a sufficient level of conservatism is considered in each calculation.

Clearance levels resulting from the calculation in the absence of radioactive decay and mass/activity balance (calculation 5, section 4.7) were merely evaluated with the aim to demonstrate the effect of these removal mechanisms and the benefit of applying a more realistic model. We believe that these derived levels are too restrictive when considering the prolonged reuse of single items cleared from a nuclear facility and therefore they are not listed in table A.1.

Note that a set of clearance levels should be considered as an entity and selection from different sets to compose a 'customised' one is not in line with the derivation methodology and therefore not recommended. As the clearance values in table A.1 were derived with a sufficient level of conservatism (section 5.2), additionally imposed conservatism either with respect to the practical aspects of verification of compliance or resulting from the formal integration of these levels in (existing) regulations is not recommended.

5.2. Issues of conservatism

As mentioned in section 5.1, there is an implicit level of conservatism embedded in the derivation of surface-clearance values based on the SUDOQU methodology, which applies to each calculation presented in this paper. These aspects are discussed below.

5.2.1. Time-related issues

Activity-concentration values derived in IAEA (2005b) consider a certain waiting or decay time between the moment of clearance and the start of the exposure scenario. Such a waiting time was not considered in the current SUDOQU study, in correspondence with the surface-contamination model presented in EC (1999). This finds its origin in the consideration of *immediate reuse* of the object after exiting the controlled area of a nuclear facility, which is a conservative, but not unrealistic, approach.

In SUDOQU, as in most models, use of and exposure to the contaminated object is assumed to be spread out over the entire duration of the scenario (one year). Use and exposure within a much shorter time interval, say $\leqslant$1 day, can significantly deviate from this 'average' behaviour. This may be of particular importance for short-lived radionuclides with half-lives of the order of a day or less. In addition, it can be shown that SUDOQU's air-quality model loses its validity for such short-lived radionuclides. Both effects imply that the uncertainty in derived clearance levels increases with decreasing half-life. With this in mind, a pragmatic and conservative approach could be to set an upper limit to the SCLs for short-lived radionuclides with half-lives $\leqslant$1 day, restricting them to a maximum value of e.g. 4000 Bq cm^{-2}. This upper limit is suggested based on the values presented in figure 4 for the reference calculation (see dash-dotted, horizontal line). To clarify further, application of this *optional* truncation would mean that, for short-lived radionuclides with $T_{1/2} \leqslant 1$ day, the final clearance level would be the minimum of the derived level (value from table A.1) and the suggested upper limit of 4000 Bq cm^{-2}. Of course, a different upper limit may be judged more appropriate if another time-scale is regarded for characterising 'short-lived' (e.g. one hour or one week).

5.2.2. DCs for intake of radionuclides

Committed DCs for the occupational or public intake of radionuclides were taken as the *maximum* of the available values over lung-absorption type (F, M, S; inhalation) and over f_1-values (fractional absorption in the gastrointestinal tract; ingestion) for each radionuclide. Moreover, inhalation and ingestion are treated independently when considering their maximum values. In addition, when considering the contribution from the *ex-vivo* ingrowth of radioactive progeny (section 2.4), maximum DCs of these progeny radionuclides are used in the weighted sum of equation (1). Note that the use of maximum DCs may introduce incompatibilities in the internal dosimetry, brought about by possible differences in chemical or physical properties of inhaled or ingested material. However, such a conservative approach is judged appropriate when deriving limiting values, ensuring a proper level of protection.

5.2.3. Treatment of radioactive progeny

Dose contributions related to the *ex-vivo* ingrowth of radioactive progeny are taken into account by a weighted sum of DCs, as expressed by equation (1) in section 2.4. The progeny DC weighting factors employed in this study are the 'conservative' values $\tilde{w}_D\,(\tau = 1$ year) from van Dillen *et al* (2020, section 2.3). They take into account the fact that ingrowth may be delayed over many years and regard the progeny's maximum contribution to the dose within a future time frame of one century. For each daughter radionuclide separately, the (delayed) maximum contribution is assumed to occur already in the first year of exposure for which the dose is calculated. A similar approach was applied in EC (2000) and IAEA (2005b), although using somewhat different (conservative) weighting factors as described in van Dillen *et al* (2020).

To find out how these conservative weighting factors affect the SCLs in table A.1, we performed an additional calculation similar to the reference calculation but with 'realistic' weighting factors $w_{\mathrm{D}}\,(\tau = 1$ year) from van Dillen *et al* (2020, section 2.2). Despite the fact that these factors may estimate the first-year dose more realistically, they are not recommended for deriving clearance values, since the annual dose sometime in the future (within 100 years) may exceed the actual first-year dose due to delayed ingrowth. These results are therefore not presented in this paper. Suffice it to mention that the majority of clearance levels derived from the additional assessment based on (more) 'realistic' first-year dose distributions do not deviate considerably from those based on 'conservative' first-year dose distributions (section 4.3). More specifically, only six radionuclides in the considered set would change their clearance level by a factor of more than two, of course with smaller (more restrictive) values based on the assessment with 'conservative' weighting factors. The impact of the imposed conservatism thus remains limited.

Finally, one may argue that, for the non-fixed component of contamination, removal of parent-nuclide activity from the surface by wipe-off and resuspension would inhibit the ingrowth of radioactive progeny and thus that the use of these conservative weighting factors could (in certain cases) lead to an overconservative estimate of the dose. It is not unlikely, however, that part of the fixed contamination (parent and progeny) eventually becomes removable with time, and the use of these weighting factors would then partly compensate the dosimetry for this 'sweating' mechanism, which is not explicitly modelled by SUDOQU.

5.2.4. Surface area of contamination

SCLs depend on the dimensions of the contaminated surface. To deal with this issue, the surface area of contamination residing on the object, A_{cont}, is treated as a distributed parameter with values *uniformly* varying between 0.01 m^2 and 10 m^2. In this way, clearance levels derived from the probabilistic assessments (table A.1) take into account the fact that objects vary in size, and for areas not exceeding 10 m^2, they can be used for a decision on clearance. This range covers most common situations and objects. With an average size of about 5 m^2, the derived levels are conservative for small objects (<1 m^2) and more realistic for larger objects (of several m^2).

5.2.5. Fixed input parameters

Several input parameters of the SUDOQU model are set to fixed numerical values (see tables 1 and 2) selected such that they have a conservative impact on a certain dose contribution. For example, the size of the room (30 m^2) or the air-exchange rate (0.5 h^{-1}) are relatively small values, both leading to a conservative estimate of the committed effective dose from inhalation of airborne activity. Though conservative, they are not unrealistic either and therefore judged appropriate for the current study.

5.2.6. Skin dosimetry

In this paper, the skin dose is evaluated conservatively. This is done as follows: first, the effective duration of skin contamination (and exposure) is set to the full duration of object use ($m_{\mathrm{hands},i} = 1.0$). Second, local skin-equivalent dose rate coefficients from SSK (2017) are conservative in the sense that, for the contribution of gamma-photon exposure, a large surface area of the skin is inherently assumed to be contaminated.

Furthermore, dose contributions from transfer of contamination and from skin contact are added independently as seen from equation (B.22) in appendix B.

In the calculation of the contribution of the local skin-equivalent dose to the effective dose, the contaminated skin area exposed to ionising radiation is assumed to be located on the area that is also regularly exposed to ultraviolet radiation (UVR). NRPB (1997) and ICRP (1992) show that this UVR-primed skin has a much (1000-fold) higher radiosensitivity of developing non-melanoma skin cancer than UVR-shielded skin. By adopting this finding, the effective dose contribution from this UVR-primed part of the skin (face, neck and outer aspects of hands and arms: $A_{\mathrm{skin,total}} = 3000\ \mathrm{cm}^2$) is six times larger than what we would have found if we had used a uniform radiosensitivity (whole-body skin: $A_{\mathrm{skin,total}} = 18\,000\ \mathrm{cm}^2$). This choice is judged to be the proper dosimetric approach for the current study, with some conservatism in the fact that the palm-side of the hands is assumed to be UVR-exposed. Similar dosimetric assumptions were made in IAEA (2005a).

The inclusion of alpha-particle exposure to the skin dosimetry introduces an aspect that is not considered in other dosimetric studies. One should bear in mind that any shielding, for instance from a thin layer of moisture on the exposed skin, may already lead to a significant reduction of the alpha contribution to the local skin-equivalent dose. Apart from such shielding, whether or not to regard this contribution as being conservative remains a topic of debate, as the associated, harmful effects remain uncertain (section 2.3.4). Also note that this contribution only affects the clearance level of some radionuclides in the set corresponding to calculation 2 (radionuclides with alpha emission >6 MeV, or radionuclides with such high-energy alpha-emitting progeny).

5.2.7. Overconservative?

The embedded conservatism in dosimetric calculations, as outlined above, ensures that derived clearance levels provide a sufficient level of radiological protection. At the same time, however, the combined effect may lead to the risk of overprotection by clearance levels that are too restrictive, which may in turn lead to practical and economic problems. Therefore, special attention should be paid to the issue of overconservatism.

The fact that removal mechanisms other than radioactive decay were taken into account leads to more realistic modelling and thus to less conservatism, as clearly demonstrated in section 4.7.

Furthermore, realistic ranges of distributed parameters were chosen. Even though the tails of these parameter distributions extend to values which can be considered conservative, the probability of encountering multiple parameters with a conservative dosimetric impact is small. Such evaluations determine the right tail of the dose distribution, which in the current methodology is also benchmarked against proper dose criteria (section 3). As seen from table 7, the limiting clearance level for the majority of radionuclides is based on the 50th percentile of the effective dose distribution which is governed by (combinations of) realistic values of the 12 distributed parameters. We therefore believe that sufficient care was taken to prevent overconservatism.

5.3. Comparison with radiation protection 101 for reuse

In 'Radiation Protection 101' (RP101) published by the EC (1999), surface-specific clearance levels have also been derived for the recycling or reuse of metals arising from the dismantling of nuclear installations. Besides differences in input-parameter values, the main differences between this European study and the SUDOQU study described in this paper are as follows.

- Scenarios in EC (1999) also consider recycling and processing of scrap metals.
- For the reuse scenarios, EC (1999) also takes into account that the objects are refurbished. These scenarios also consider cleaning and sanding of equipment released from the facility.
- Clearance levels in EC (1999, tables 7.4 and 7.5) follow from deterministic dose evaluations.

Despite these differences, it is interesting to compare the results from both studies for the reuse scenarios. The results are presented in figure 10, showing the ratio of clearance levels (SUDOQU : RP101). For all radionuclides up to the actinides, clearance levels from the SUDOQU study are more restrictive (smaller) than those from RP101. For most of these radionuclides, the dominant scenario in RP101 is related to the direct, normal reuse of the item. However, for some nuclides in the actinide group, RP101 obtains more conservative clearance levels (ratio larger than 1). In this case, the governing pathway is inhalation due to cleaning or sanding of the item, neither of these activities being considered by SUDOQU. The ratio of clearance levels typically ranges between 1 and 1.3 and does not exceed 2.4 for the radionuclides considered in RP101. Even though clearance levels from both studies cannot be compared directly, the results are of the same order of magnitude when considering the differences between and uncertainties in both studies.

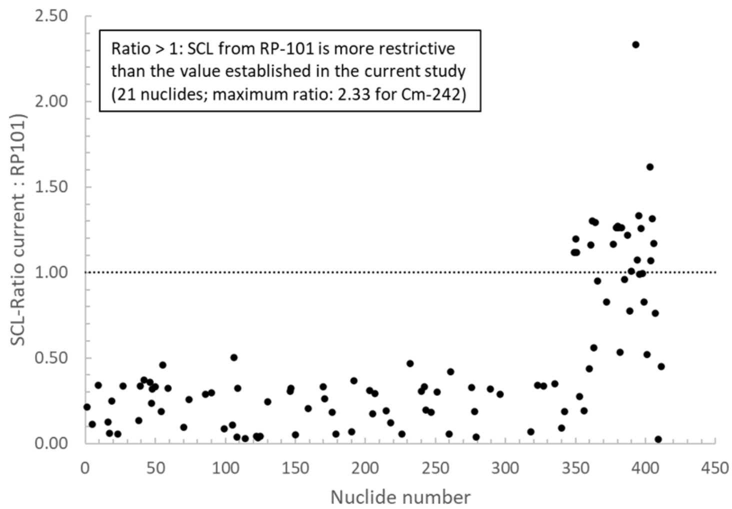

Figure 10. Ratio of surface-clearance values obtained for the normal reuse scenarios in the current study (reference calculation 1, table A.1) and those from RP101 (EC 1999, table 7.5). The latter clearance values also consider cleaning and sanding of items or equipment.

Extension of the SUDOQU methodology to include scenarios such as refurbishment is part of future work, as suggested in section 6.

5.4. Application of values and verification of compliance

The scope of the SCLs provided in this probabilistic study (table A.1) is limited to the *immediate and prolonged, normal reuse of single items* leaving the controlled area of a nuclear facility. They apply to non-radiological workers and adult MOP. The values can in principle not be used for other purposes (e.g. clearance for other purposes such as recycling, exemption) or for children unless a safety assessment proves otherwise.

Unlike the study by the EC (1999), refurbishing or processing (e.g. cutting, scrapping, sanding) the item is not considered by the exposure scenarios in our work. As follows from section 5.3, a comparison of clearance levels with those from EC (1999, table 7.5 for reuse) shows that the values presented in this paper are generally more restrictive. For some isotopes in the actinide group, they can be less restrictive, which is associated with refurbishment scenarios. However, their relative difference is generally less than 30% (figure 10).

Once an appropriate set of clearance levels is selected from table A.1 for use or implementation in regulation, the following additional conditions apply to the use of these values:

(a) the derived levels apply to solid objects with contamination only at their surface;
(b) the values apply to the *total* level of surface contamination, i.e. the sum of the fixed and removable components;
(c) the values apply to objects with contaminated surface areas up to 10 m^2; and
(d) in the case of a mixture of radionuclides, verification of compliance with the clearance levels should proceed using the sum-of-fractions as expressed by equation (2). Some radionuclides may perhaps be ignored from this sum if their presence is solely due to the radioactive ingrowth from a parent radionuclide. For such cases, table A.2 indicates which progeny radionuclides can be ignored in the presence of a certain parent radionuclide. More details can be found in section 2.4.

Technical details regarding measurements, sampling and statistics which are important aspects in the verification of compliance, are outside the scope of this paper. Such details can be found elsewhere, e.g. in IAEA (2012).

6. Summary, conclusions and outlook

6.1. Summary

In this paper, we have derived the SCL for 413 radionuclides for the normal reuse of objects leaving the controlled area of a licensed nuclear facility. This was done using probabilistic dose assessments using the SUDOQU model (van Dillen and van Dijk 2018) and applying appropriate dose criteria respecting the concepts of clearance and the representative person. This model takes into account radioactive decay and other removal processes in a mass/activity balance framework. Based on specific choices for DCs, four sets of surface-specific clearance values were derived (values in table A.1) and guidance on the selection and application of these values was provided. These clearance levels were benchmarked against results obtained from a conservative version of the SUDOQU model without removal processes.

6.2. Main conclusions

We have demonstrated the benefit of deriving SCLs using a realistic model based on mass/activity balance, which is appropriate when regarding the prolonged reuse of contaminated items as it avoids overconservatism. Interestingly, clearance levels for long-lived radionuclides appear to be of the same order of magnitude as the generic values defining 'contamination' in the IAEA Transport Regulations: 0.4 Bq cm^{-2} for beta and gamma emitters and low toxicity alpha emitters, or 0.04 Bq cm^{-2} for all other alpha emitters (IAEA 2018). These values find their origin in a study by Fairbairn (1961). A comparison with clearance levels from (EC 1999, table 7.5 for reuse) shows that the values derived in this paper are generally more restrictive, except for various isotopes in the actinide group. This is associated with refurbishment scenarios (e.g. cutting, scrapping, sanding), which are not considered in the current SUDOQU study. However, despite this limitation, their relative difference is generally less than 30%.

6.3. Suggestions for future work

In the current study, derived clearance levels apply to all objects with contaminated surface areas up to 10 m^2. In certain cases, however, it may be useful to have clearance levels for specific object size categories, e.g. 0.01–0.1 m^2 (small objects), 0.1–1.0 m^2 (medium-sized objects) and 1.0–10 m^2 (large objects). Such clearance levels can be derived by limiting the range of the contaminated area in the existing, probabilistic SUDOQU model. Calculations could also be performed for users other than adults. This would require the use of appropriate DCs as well as the adapted input parameters defining the exposure scenario. These calculations could also be performed using updated inhalation and ingestion DCs for workers (ICRP 2015) and MOP (under development). Finally, clearance levels could be calculated based on scenarios other than normal, immediate reuse, e.g. for recycling and processing such as described in EC (1999). This would require significant changes to the existing SUDOQU model.

Acknowledgments

The authors would like to thank Arjan van Dijk (RIVM) for discussions and contributions to the development of SUDOQU, which enabled the study presented in this paper, Laurens Bogaardt (Department of Statistics, Informatics and Modelling; RIVM) for his suggestions regarding statistical sampling uncertainties, and Astrid Kloosterman (RIVM) for her critical review of the original manuscript. This work was financially supported by Bel V.

Disclaimer

Great care was given to the correctness and the numerical accuracy in the calculations of the surface-specific clearance values listed in table A.1 of appendix A of this paper. In case inconsistencies or errors in model assumptions/equations or in these derived values are encountered, please contact the authors. RIVM and Bel V accept no liability or claims whatsoever for any direct or indirect damage, including financial or other loss, caused by any errors or incompleteness in the dataset or by misuse or misinterpretation of these surface-specific clearance levels.

Appendix A. Surface-specific clearance values for 413 radionuclides

Table A1. Derived surface-specific clearance levels (SCL). Column 1: Nuclide number. Column 2: Parent radionuclide. Column 3: Half-life of parent radionuclide. Column 4: SCL from reference calculation (Worker, AMAD = 5 μm, without alpha contribution to skin dose coefficients). Column 5: Dose percentile determining the value of SCL (E50, E95, E99, Hskin99) for reference calculation. The following columns are similar to those for the reference calculation: Column 6: SCL with alpha skin dose (calculation 2). Column 7: Dose percentile for calculation 2. Column 8: SCL for AMAD = 1 μm (calculation 3). Column 9: Dose percentile for calculation 3. Column 10: SCL using dose coefficients for adult member of the public (calculation 4). Column 11: Dose percentile for calculation 4. Parent radionuclides with a + indicates that one or more daughter radionuclides have been fully taken into account in the SCL of the parent radionuclide (see section 2.4). These progeny radionuclides are listed in table A.2.

Nr.	Nuclide	Half-life (s)	SCL Reference (Bq cm^{-2})	Percentile Reference	SCL With α-skin (Bq cm^{-2})	Percentile With α-skin	SCL AMAD = 1 μm (Bq cm^{-2})	Percentile AMAD = 1 μm	SCL Public (Bq cm^{-2})	Percentile Public
1	H-3	$3.89 \times 10^{+8}$	$5.36 \times 10^{+3}$	E50	$5.36 \times 10^{+3}$	E50	$5.36 \times 10^{+3}$	E50	$4.69 \times 10^{+3}$	E50
2	Be-7	$4.60 \times 10^{+6}$	$5.81 \times 10^{+1}$	E50	$5.81 \times 10^{+1}$	E50	$5.81 \times 10^{+1}$	E50	$5.81 \times 10^{+1}$	E50
3	Be-10	$4.77 \times 10^{+13}$	$1.65 \times 10^{+1}$	Hskin99	$1.65 \times 10^{+1}$	Hskin99	$1.65 \times 10^{+1}$	Hskin99	$1.65 \times 10^{+1}$	Hskin99
4	C-11	$1.22 \times 10^{+3}$	$1.04 \times 10^{+4}$	E50	$1.04 \times 10^{+4}$	E50	$1.04 \times 10^{+4}$	E50	$1.04 \times 10^{+4}$	E50
5	C-14	$1.80 \times 10^{+11}$	$8.80 \times 10^{+1}$	Hskin99	$8.80 \times 10^{+1}$	Hskin99	$8.80 \times 10^{+1}$	Hskin99	$8.80 \times 10^{+1}$	Hskin99
6	N-13	$5.98 \times 10^{+2}$	$2.12 \times 10^{+4}$	E50	$2.12 \times 10^{+4}$	E50	$2.12 \times 10^{+4}$	E50	$2.12 \times 10^{+4}$	E50
7	O-15	$1.22 \times 10^{+2}$	$1.04 \times 10^{+5}$	E50	$1.04 \times 10^{+5}$	E50	$1.04 \times 10^{+5}$	E50	$1.04 \times 10^{+5}$	E50
8	F-18	$6.59 \times 10^{+3}$	$1.99 \times 10^{+3}$	E50	$1.99 \times 10^{+3}$	E50	$1.99 \times 10^{+3}$	E50	$1.99 \times 10^{+3}$	E50
9	Na-22	$8.21 \times 10^{+7}$	3.76×10^{-1}	E50	3.76×10^{-1}	E50	3.76×10^{-1}	E50	3.76×10^{-1}	E50
10	Na-24	$5.39 \times 10^{+4}$	$8.43 \times 10^{+1}$	E50	$8.43 \times 10^{+1}$	E50	$8.43 \times 10^{+1}$	E50	$8.43 \times 10^{+1}$	E50
11	Mg-28+	$7.53 \times 10^{+4}$	$6.61 \times 10^{+1}$	E50	$6.61 \times 10^{+1}$	E50	$6.61 \times 10^{+1}$	E50	$6.61 \times 10^{+1}$	E50
12	Al-26	$2.26 \times 10^{+13}$	2.96×10^{-1}	E50	2.96×10^{-1}	E50	2.96×10^{-1}	E50	2.96×10^{-1}	E50
13	Si-31	$9.44 \times 10^{+3}$	$3.40 \times 10^{+4}$	Hskin99	$3.40 \times 10^{+4}$	Hskin99	$3.40 \times 10^{+4}$	Hskin99	$3.40 \times 10^{+4}$	Hskin99
14	P-32	$1.23 \times 10^{+6}$	$2.58 \times 10^{+2}$	E50	$2.58 \times 10^{+2}$	E50	$2.57 \times 10^{+2}$	E50	$2.57 \times 10^{+2}$	E50
15	P-33	$2.19 \times 10^{+6}$	$3.16 \times 10^{+2}$	Hskin99	$3.16 \times 10^{+2}$	Hskin99	$3.16 \times 10^{+2}$	Hskin99	$3.16 \times 10^{+2}$	Hskin99
16	S-35	$7.56 \times 10^{+6}$	$2.24 \times 10^{+2}$	E50	$2.24 \times 10^{+2}$	E50	$2.24 \times 10^{+2}$	E50	$2.22 \times 10^{+2}$	E50
17	Cl-36	$9.50 \times 10^{+12}$	$1.76 \times 10^{+1}$	Hskin99	$1.76 \times 10^{+1}$	Hskin99	$1.76 \times 10^{+1}$	Hskin99	$1.76 \times 10^{+1}$	Hskin99
18	Cl-38	$2.23 \times 10^{+3}$	$5.46 \times 10^{+3}$	E50	$5.46 \times 10^{+3}$	E50	$5.46 \times 10^{+3}$	E50	$5.46 \times 10^{+3}$	E50
19	K-40	$3.95 \times 10^{+16}$	$3.70 \times 10^{+0}$	E50	$3.70 \times 10^{+0}$	E50	$3.70 \times 10^{+0}$	E50	$3.70 \times 10^{+0}$	E50
20	K-42	$4.45 \times 10^{+4}$	$1.17 \times 10^{+3}$	E50	$1.17 \times 10^{+3}$	E50	$1.17 \times 10^{+3}$	E50	$1.17 \times 10^{+3}$	E50
21	K-43	$8.03 \times 10^{+4}$	$1.70 \times 10^{+2}$	E50	$1.70 \times 10^{+2}$	E50	$1.70 \times 10^{+2}$	E50	$1.70 \times 10^{+2}$	E50
22	Ca-41	$3.22 \times 10^{+12}$	$7.16 \times 10^{+2}$	E50	$7.16 \times 10^{+2}$	E50	$7.18 \times 10^{+2}$	E50	$1.04 \times 10^{+3}$	E50
23	Ca-45	$1.41 \times 10^{+7}$	$6.57 \times 10^{+1}$	Hskin99	$6.57 \times 10^{+1}$	Hskin99	$6.57 \times 10^{+1}$	Hskin99	$6.57 \times 10^{+1}$	Hskin99
24	Ca-47	$3.92 \times 10^{+5}$	$3.17 \times 10^{+1}$	E50	$3.17 \times 10^{+1}$	E50	$3.17 \times 10^{+1}$	E50	$3.17 \times 10^{+1}$	E50

(Continued.)

Table A1. (Continued.)

Nr.	Nuclide	Half-life (s)	SCL Reference (Bq cm^{-2})	Percentile Reference	SCL With α-skin (Bq cm^{-2})	Percentile With α-skin	SCL AMAD = 1 μm (Bq cm^{-2})	Percentile AMAD = 1 μm	SCL Public (Bq cm^{-2})	Percentile Public
25	Sc-44	$1.43 \times 10^{+4}$	$4.66 \times 10^{+2}$	E50	$4.66 \times 10^{+2}$	E50	$4.66 \times 10^{+2}$	E50	$4.66 \times 10^{+2}$	E50
26	Sc-44m+	$2.11 \times 10^{+5}$	$2.78 \times 10^{+1}$	E50	$2.78 \times 10^{+1}$	E50	$2.78 \times 10^{+1}$	E50	$2.78 \times 10^{+1}$	E50
27	Sc-46	$7.24 \times 10^{+6}$	$1.14 \times 10^{+0}$	E50	$1.14 \times 10^{+0}$	E50	$1.14 \times 10^{+0}$	E50	$1.14 \times 10^{+0}$	E50
28	Sc-47	$2.89 \times 10^{+5}$	$3.18 \times 10^{+2}$	E50	$3.18 \times 10^{+2}$	E50	$3.18 \times 10^{+2}$	E50	$3.18 \times 10^{+2}$	E50
29	Sc-48	$1.57 \times 10^{+5}$	$2.89 \times 10^{+1}$	E50	$2.89 \times 10^{+1}$	E50	$2.89 \times 10^{+1}$	E50	$2.89 \times 10^{+1}$	E50
30	Ti-44+	$1.89 \times 10^{+9}$	3.05×10^{-1}	E50	3.05×10^{-1}	E50	3.04×10^{-1}	E50	3.04×10^{-1}	E50
31	Ti-45	$1.11 \times 10^{+4}$	$1.35 \times 10^{+3}$	E50	$1.35 \times 10^{+3}$	E50	$1.35 \times 10^{+3}$	E50	$1.35 \times 10^{+3}$	E50
32	V-48	$1.38 \times 10^{+6}$	$3.80 \times 10^{+0}$	E50	$3.80 \times 10^{+0}$	E50	$3.80 \times 10^{+0}$	E50	$3.80 \times 10^{+0}$	E50
33	V-49	$2.85 \times 10^{+7}$	$3.79 \times 10^{+3}$	Hskin99	$3.79 \times 10^{+3}$	Hskin99	$3.79 \times 10^{+3}$	Hskin99	$3.79 \times 10^{+3}$	Hskin99
34	Cr-51	$2.39 \times 10^{+6}$	$1.61 \times 10^{+2}$	E50	$1.61 \times 10^{+2}$	E50	$1.61 \times 10^{+2}$	E50	$1.61 \times 10^{+2}$	E50
35	Mn-51	$2.77 \times 10^{+3}$	$4.53 \times 10^{+3}$	E50	$4.53 \times 10^{+3}$	E50	$4.53 \times 10^{+3}$	E50	$4.53 \times 10^{+3}$	E50
36	Mn-52	$4.83 \times 10^{+5}$	$9.06 \times 10^{+0}$	E50	$9.06 \times 10^{+0}$	E50	$9.06 \times 10^{+0}$	E50	$9.06 \times 10^{+0}$	E50
37	Mn-52m	$1.27 \times 10^{+3}$	$4.71 \times 10^{+3}$	E50	$4.71 \times 10^{+3}$	E50	$4.71 \times 10^{+3}$	E50	$4.71 \times 10^{+3}$	E50
38	Mn-53	$1.17 \times 10^{+14}$	$2.03 \times 10^{+3}$	Hskin99	$2.03 \times 10^{+3}$	Hskin99	$2.03 \times 10^{+3}$	Hskin99	$2.03 \times 10^{+3}$	Hskin99
39	Mn-54	$2.70 \times 10^{+7}$	$1.25 \times 10^{+0}$	E50	$1.25 \times 10^{+0}$	E50	$1.25 \times 10^{+0}$	E50	$1.25 \times 10^{+0}$	E50
40	Mn-56	$9.28 \times 10^{+3}$	$1.00 \times 10^{+3}$	E50	$1.00 \times 10^{+3}$	E50	$1.00 \times 10^{+3}$	E50	$1.00 \times 10^{+3}$	E50
41	Fe-52+	$2.98 \times 10^{+4}$	$1.49 \times 10^{+2}$	E50	$1.49 \times 10^{+2}$	E50	$1.49 \times 10^{+2}$	E50	$1.49 \times 10^{+2}$	E50
42	Fe-55	$8.64 \times 10^{+7}$	$5.59 \times 10^{+2}$	E50	$5.59 \times 10^{+2}$	E50	$5.64 \times 10^{+2}$	E50	$5.64 \times 10^{+2}$	E50
43	Fe-59	$3.84 \times 10^{+6}$	$3.48 \times 10^{+0}$	E50	$3.48 \times 10^{+0}$	E50	$3.48 \times 10^{+0}$	E50	$3.48 \times 10^{+0}$	E50
44	Fe-60+	$4.73 \times 10^{+13}$	2.48×10^{-1}	E50	2.48×10^{-1}	E50	2.49×10^{-1}	E50	2.49×10^{-1}	E50
45	Co-55	$6.31 \times 10^{+4}$	$1.12 \times 10^{+2}$	E50	$1.12 \times 10^{+2}$	E50	$1.12 \times 10^{+2}$	E50	$1.12 \times 10^{+2}$	E50
46	Co-56	$6.67 \times 10^{+6}$	7.55×10^{-1}	E50	7.55×10^{-1}	E50	7.55×10^{-1}	E50	7.54×10^{-1}	E50
47	Co-57	$2.35 \times 10^{+7}$	$7.11 \times 10^{+0}$	E50	$7.11 \times 10^{+0}$	E50	$7.11 \times 10^{+0}$	E50	$7.11 \times 10^{+0}$	E50
48	Co-58	$6.12 \times 10^{+6}$	$2.56 \times 10^{+0}$	E50	$2.56 \times 10^{+0}$	E50	$2.56 \times 10^{+0}$	E50	$2.56 \times 10^{+0}$	E50
49	Co-58m	$3.25 \times 10^{+4}$	$4.52 \times 10^{+2}$	E50	$4.52 \times 10^{+2}$	E50	$4.52 \times 10^{+2}$	E50	$4.52 \times 10^{+2}$	E50
50	Co-60	$1.66 \times 10^{+8}$	3.34×10^{-1}	E50	3.34×10^{-1}	E50	3.34×10^{-1}	E50	3.34×10^{-1}	E50
51	Co-60m	$6.28 \times 10^{+2}$	$7.81 \times 10^{+4}$	E50	$7.81 \times 10^{+4}$	E50	$7.81 \times 10^{+4}$	E50	$7.81 \times 10^{+4}$	E50
52	Co-61	$5.94 \times 10^{+3}$	$1.53 \times 10^{+4}$	E50	$1.53 \times 10^{+4}$	E50	$1.53 \times 10^{+4}$	E50	$1.53 \times 10^{+4}$	E50
53	Co-62m	$8.35 \times 10^{+2}$	$7.12 \times 10^{+3}$	E50	$7.12 \times 10^{+3}$	E50	$7.12 \times 10^{+3}$	E50	$7.12 \times 10^{+3}$	E50
54	Ni-59	$3.19 \times 10^{+12}$	$1.32 \times 10^{+3}$	E50	$1.32 \times 10^{+3}$	E50	$1.33 \times 10^{+3}$	E50	$1.28 \times 10^{+3}$	E50

(Continued.)

Table A1. (Continued.)

Nr.	Nuclide	Half-life (s)	SCL Reference (Bq cm^{-2})	Percentile Reference	SCL With α-skin (Bq cm^{-2})	Percentile With α-skin	SCL AMAD = 1 μm (Bq cm^{-2})	Percentile AMAD = 1 μm	SCL Public (Bq cm^{-2})	Percentile Public
55	Ni-63	$3.16 \times 10^{+9}$	$1.37 \times 10^{+3}$	E50	$1.37 \times 10^{+3}$	E50	$1.39 \times 10^{+3}$	E50	$1.23 \times 10^{+3}$	E50
56	Ni-65	$9.06 \times 10^{+3}$	$2.98 \times 10^{+3}$	E50	$2.98 \times 10^{+3}$	E50	$2.98 \times 10^{+3}$	E50	$2.98 \times 10^{+3}$	E50
57	Cu-64	$4.57 \times 10^{+4}$	$1.47 \times 10^{+3}$	E50	$1.47 \times 10^{+3}$	E50	$1.47 \times 10^{+3}$	E50	$1.47 \times 10^{+3}$	E50
58	Cu-67	$2.23 \times 10^{+5}$	$3.97 \times 10^{+2}$	E50	$3.97 \times 10^{+2}$	E50	$3.97 \times 10^{+2}$	E50	$3.97 \times 10^{+2}$	E50
59	Zn-65	$2.11 \times 10^{+7}$	$2.02 \times 10^{+0}$	E50	$2.02 \times 10^{+0}$	E50	$2.02 \times 10^{+0}$	E50	$2.02 \times 10^{+0}$	E50
60	Zn-69	$3.38 \times 10^{+3}$	$9.49 \times 10^{+4}$	Hskin99	$9.49 \times 10^{+4}$	Hskin99	$9.49 \times 10^{+4}$	Hskin99	$9.49 \times 10^{+4}$	Hskin99
61	Zn-69m+	$4.95 \times 10^{+4}$	$5.91 \times 10^{+2}$	E50	$5.91 \times 10^{+2}$	E50	$5.91 \times 10^{+2}$	E50	$5.91 \times 10^{+2}$	E50
62	Ga-67	$2.82 \times 10^{+5}$	$2.78 \times 10^{+2}$	E50	$2.78 \times 10^{+2}$	E50	$2.78 \times 10^{+2}$	E50	$2.78 \times 10^{+2}$	E50
63	Ga-68	$4.06 \times 10^{+3}$	$3.38 \times 10^{+3}$	E50	$3.38 \times 10^{+3}$	E50	$3.38 \times 10^{+3}$	E50	$3.38 \times 10^{+3}$	E50
64	Ga-72	$5.08 \times 10^{+4}$	$1.18 \times 10^{+2}$	E50	$1.18 \times 10^{+2}$	E50	$1.18 \times 10^{+2}$	E50	$1.18 \times 10^{+2}$	E50
65	Ge-68+	$2.34 \times 10^{+7}$	$1.05 \times 10^{+0}$	E50	$1.05 \times 10^{+0}$	E50	$1.05 \times 10^{+0}$	E50	$1.05 \times 10^{+0}$	E50
66	Ge-69	$1.41 \times 10^{+5}$	$1.09 \times 10^{+2}$	E50	$1.09 \times 10^{+2}$	E50	$1.09 \times 10^{+2}$	E50	$1.09 \times 10^{+2}$	E50
67	Ge-71	$9.88 \times 10^{+5}$	$3.16 \times 10^{+4}$	Hskin99	$3.16 \times 10^{+4}$	Hskin99	$3.16 \times 10^{+4}$	Hskin99	$3.16 \times 10^{+4}$	Hskin99
68	Ge-77	$4.07 \times 10^{+4}$	$3.00 \times 10^{+2}$	E50	$3.00 \times 10^{+2}$	E50	$3.00 \times 10^{+2}$	E50	$3.00 \times 10^{+2}$	E50
69	As-72	$9.36 \times 10^{+4}$	$8.23 \times 10^{+1}$	E50	$8.23 \times 10^{+1}$	E50	$8.23 \times 10^{+1}$	E50	$8.23 \times 10^{+1}$	E50
70	As-73	$6.94 \times 10^{+6}$	$1.07 \times 10^{+2}$	E50	$1.07 \times 10^{+2}$	E50	$1.06 \times 10^{+2}$	E50	$1.06 \times 10^{+2}$	E50
71	As-74	$1.54 \times 10^{+6}$	$1.16 \times 10^{+1}$	E50	$1.16 \times 10^{+1}$	E50	$1.16 \times 10^{+1}$	E50	$1.16 \times 10^{+1}$	E50
72	As-76	$9.31 \times 10^{+4}$	$3.33 \times 10^{+2}$	E50	$3.33 \times 10^{+2}$	E50	$3.33 \times 10^{+2}$	E50	$3.33 \times 10^{+2}$	E50
73	As-77	$1.40 \times 10^{+5}$	$2.47 \times 10^{+3}$	Hskin99	$2.47 \times 10^{+3}$	Hskin99	$2.47 \times 10^{+3}$	Hskin99	$2.47 \times 10^{+3}$	Hskin99
74	Se-75	$1.03 \times 10^{+7}$	$3.63 \times 10^{+0}$	E50	$3.63 \times 10^{+0}$	E50	$3.63 \times 10^{+0}$	E50	$3.63 \times 10^{+0}$	E50
75	Se-79	$9.31 \times 10^{+12}$	$4.07 \times 10^{+1}$	E50	$4.07 \times 10^{+1}$	E50	$4.07 \times 10^{+1}$	E50	$3.99 \times 10^{+1}$	E50
76	Br-75	$5.80 \times 10^{+3}$	$1.42 \times 10^{+3}$	E50	$1.42 \times 10^{+3}$	E50	$1.42 \times 10^{+3}$	E50	$1.42 \times 10^{+3}$	E50
77	Br-76	$5.83 \times 10^{+4}$	$9.80 \times 10^{+1}$	E50	$9.80 \times 10^{+1}$	E50	$9.80 \times 10^{+1}$	E50	$9.80 \times 10^{+1}$	E50
78	Br-77	$2.05 \times 10^{+5}$	$1.91 \times 10^{+2}$	E50	$1.91 \times 10^{+2}$	E50	$1.91 \times 10^{+2}$	E50	$1.91 \times 10^{+2}$	E50
79	Br-82	$1.27 \times 10^{+5}$	$4.31 \times 10^{+1}$	E50	$4.31 \times 10^{+1}$	E50	$4.31 \times 10^{+1}$	E50	$4.31 \times 10^{+1}$	E50
80	Rb-81+	$1.65 \times 10^{+4}$	$1.15 \times 10^{+3}$	E50	$1.15 \times 10^{+3}$	E50	$1.15 \times 10^{+3}$	E50	$1.15 \times 10^{+3}$	E50
81	Rb-83+	$7.45 \times 10^{+6}$	$3.64 \times 10^{+0}$	E50	$3.64 \times 10^{+0}$	E50	$3.64 \times 10^{+0}$	E50	$3.64 \times 10^{+0}$	E50
82	Rb-84	$2.83 \times 10^{+6}$	$5.34 \times 10^{+0}$	E50	$5.34 \times 10^{+0}$	E50	$5.34 \times 10^{+0}$	E50	$5.34 \times 10^{+0}$	E50
83	Rb-86	$1.61 \times 10^{+6}$	$6.41 \times 10^{+1}$	E50	$6.41 \times 10^{+1}$	E50	$6.42 \times 10^{+1}$	E50	$6.42 \times 10^{+1}$	E50
84	Rb-87	$1.55 \times 10^{+18}$	$2.20 \times 10^{+1}$	Hskin99	$2.20 \times 10^{+1}$	Hskin99	$2.20 \times 10^{+1}$	Hskin99	$2.20 \times 10^{+1}$	Hskin99
85	Sr-82+	$2.19 \times 10^{+6}$	$5.03 \times 10^{+0}$	E50	$5.03 \times 10^{+0}$	E50	$5.03 \times 10^{+0}$	E50	$5.03 \times 10^{+0}$	E50
86	Sr-85	$5.60 \times 10^{+6}$	$4.58 \times 10^{+0}$	E50	$4.58 \times 10^{+0}$	E50	$4.58 \times 10^{+0}$	E50	$4.58 \times 10^{+0}$	E50
87	Sr-85m	$4.06 \times 10^{+3}$	$4.61 \times 10^{+3}$	E50	$4.61 \times 10^{+3}$	E50	$4.61 \times 10^{+3}$	E50	$4.61 \times 10^{+3}$	E50

(Continued.)

Table A1. (Continued.)

Nr.	Nuclide	Half-life (s)	SCL Reference (Bq cm^{-2})	Percentile Reference	SCL With α-skin (Bq cm^{-2})	Percentile With α-skin	SCL AMAD = 1 μm (Bq cm^{-2})	Percentile AMAD = 1 μm	SCL Public (Bq cm^{-2})	Percentile Public
88	Sr-87m	$1.01 \times 10^{+4}$	$3.81 \times 10^{+3}$	E50	$3.81 \times 10^{+3}$	E50	$3.81 \times 10^{+3}$	E50	$3.81 \times 10^{+3}$	E50
89	Sr-89	$4.37 \times 10^{+6}$	$7.96 \times 10^{+1}$	Hskin99	$7.96 \times 10^{+1}$	Hskin99	$7.93 \times 10^{+1}$	E50	$7.92 \times 10^{+1}$	E50
90	Sr-90+	$9.09 \times 10^{+8}$	$4.45 \times 10^{+0}$	E50	$4.45 \times 10^{+0}$	E50	$4.30 \times 10^{+0}$	E50	$4.28 \times 10^{+0}$	E50
91	Sr-91+	$3.47 \times 10^{+4}$	$3.72 \times 10^{+2}$	E50	$3.72 \times 10^{+2}$	E50	$3.72 \times 10^{+2}$	E50	$3.73 \times 10^{+2}$	E50
92	Sr-92	$9.58 \times 10^{+3}$	$9.95 \times 10^{+2}$	E50	$9.95 \times 10^{+2}$	E50	$9.95 \times 10^{+2}$	E50	$9.95 \times 10^{+2}$	E50
93	Y-86	$5.31 \times 10^{+4}$	$7.95 \times 10^{+1}$	E50	$7.95 \times 10^{+1}$	E50	$7.95 \times 10^{+1}$	E50	$7.95 \times 10^{+1}$	E50
94	Y-86m	$2.88 \times 10^{+3}$	$1.37 \times 10^{+3}$	E50	$1.37 \times 10^{+3}$	E50	$1.37 \times 10^{+3}$	E50	$1.37 \times 10^{+3}$	E50
95	Y-87+	$2.87 \times 10^{+5}$	$5.38 \times 10^{+1}$	E50	$5.38 \times 10^{+1}$	E50	$5.38 \times 10^{+1}$	E50	$5.38 \times 10^{+1}$	E50
96	Y-88	$9.21 \times 10^{+6}$	7.67×10^{-1}	E50	7.67×10^{-1}	E50	7.67×10^{-1}	E50	7.67×10^{-1}	E50
97	Y-90	$2.31 \times 10^{+5}$	$1.23 \times 10^{+3}$	E50	$1.23 \times 10^{+3}$	E50	$1.23 \times 10^{+3}$	E50	$1.23 \times 10^{+3}$	E50
98	Y-90m	$1.15 \times 10^{+4}$	$1.62 \times 10^{+3}$	E50	$1.62 \times 10^{+3}$	E50	$1.62 \times 10^{+3}$	E50	$1.62 \times 10^{+3}$	E50
99	Y-91	$5.06 \times 10^{+6}$	$6.95 \times 10^{+1}$	Hskin99	$6.95 \times 10^{+1}$	Hskin99	$6.95 \times 10^{+1}$	Hskin99	$6.95 \times 10^{+1}$	Hskin99
100	Y-91m	$2.98 \times 10^{+3}$	$7.76 \times 10^{+3}$	E50	$7.76 \times 10^{+3}$	E50	$7.76 \times 10^{+3}$	E50	$7.76 \times 10^{+3}$	E50
101	Y-92	$1.27 \times 10^{+4}$	$4.08 \times 10^{+3}$	E50	$4.08 \times 10^{+3}$	E50	$4.08 \times 10^{+3}$	E50	$4.08 \times 10^{+3}$	E50
102	Y-93	$3.66 \times 10^{+4}$	$2.97 \times 10^{+3}$	E50	$2.97 \times 10^{+3}$	E50	$2.97 \times 10^{+3}$	E50	$2.97 \times 10^{+3}$	E50
103	Zr-88	$7.21 \times 10^{+6}$	9.15×10^{-1}	E50	9.15×10^{-1}	E50	9.15×10^{-1}	E50	9.14×10^{-1}	E50
104	Zr-89	$2.82 \times 10^{+5}$	$4.14 \times 10^{+1}$	E50	$4.14 \times 10^{+1}$	E50	$4.14 \times 10^{+1}$	E50	$4.14 \times 10^{+1}$	E50
105	Zr-93	$4.83 \times 10^{+13}$	$3.17 \times 10^{+1}$	E50	$3.17 \times 10^{+1}$	E50	$3.20 \times 10^{+1}$	E50	$2.74 \times 10^{+1}$	E50
106	Zr-95+	$5.53 \times 10^{+6}$	$1.82 \times 10^{+0}$	E50	$1.82 \times 10^{+0}$	E50	$1.82 \times 10^{+0}$	E50	$1.82 \times 10^{+0}$	E50
107	Zr-97+	$6.03 \times 10^{+4}$	$1.45 \times 10^{+2}$	E50	$1.45 \times 10^{+2}$	E50	$1.45 \times 10^{+2}$	E50	$1.45 \times 10^{+2}$	E50
108	Nb-93m	$5.09 \times 10^{+8}$	$3.74 \times 10^{+1}$	E50	$3.74 \times 10^{+1}$	E50	$3.73 \times 10^{+1}$	E50	$3.72 \times 10^{+1}$	E50
109	Nb-94	$6.41 \times 10^{+11}$	4.52×10^{-1}	E50	4.52×10^{-1}	E50	4.51×10^{-1}	E50	4.51×10^{-1}	E50
110	Nb-95	$3.02 \times 10^{+6}$	$6.29 \times 10^{+0}$	E50	$6.29 \times 10^{+0}$	E50	$6.29 \times 10^{+0}$	E50	$6.29 \times 10^{+0}$	E50
111	Nb-97	$4.33 \times 10^{+3}$	$4.65 \times 10^{+3}$	E50	$4.65 \times 10^{+3}$	E50	$4.65 \times 10^{+3}$	E50	$4.65 \times 10^{+3}$	E50
112	Nb-98m	$3.08 \times 10^{+3}$	$1.73 \times 10^{+3}$	E50	$1.73 \times 10^{+3}$	E50	$1.73 \times 10^{+3}$	E50	$1.73 \times 10^{+3}$	E50
113	Mo-90	$2.00 \times 10^{+4}$	$1.51 \times 10^{+2}$	E50	$1.51 \times 10^{+2}$	E50	$1.51 \times 10^{+2}$	E50	$1.51 \times 10^{+2}$	E50
114	Mo-93	$1.26 \times 10^{+11}$	$5.22 \times 10^{+0}$	E50	$5.22 \times 10^{+0}$	E50	$5.21 \times 10^{+0}$	E50	$5.11 \times 10^{+0}$	E50
115	Mo-99+	$2.37 \times 10^{+5}$	$1.78 \times 10^{+2}$	E50	$1.78 \times 10^{+2}$	E50	$1.78 \times 10^{+2}$	E50	$1.81 \times 10^{+2}$	E50
116	Mo-101+	$8.77 \times 10^{+2}$	$9.03 \times 10^{+3}$	E50	$9.03 \times 10^{+3}$	E50	$9.03 \times 10^{+3}$	E50	$9.03 \times 10^{+3}$	E50
117	Tc-94	$1.76 \times 10^{+4}$	$2.95 \times 10^{+2}$	E50	$2.95 \times 10^{+2}$	E50	$2.95 \times 10^{+2}$	E50	$2.95 \times 10^{+2}$	E50
118	Tc-94m	$3.12 \times 10^{+3}$	$2.34 \times 10^{+3}$	E50	$2.34 \times 10^{+3}$	E50	$2.34 \times 10^{+3}$	E50	$2.34 \times 10^{+3}$	E50
119	Tc-95m+	$5.27 \times 10^{+6}$	$3.39 \times 10^{+0}$	E50	$3.39 \times 10^{+0}$	E50	$3.39 \times 10^{+0}$	E50	$3.40 \times 10^{+0}$	E50

(Continued.)

Table A1. (Continued.)

Nr.	Nuclide	Half-life (s)	SCL Reference (Bq cm^{-2})	Percentile Reference	SCL With α-skin (Bq cm^{-2})	Percentile With α-skin	SCL AMAD = 1 μm (Bq cm^{-2})	Percentile AMAD = 1 μm	SCL Public (Bq cm^{-2})	Percentile Public
120	Tc-96	$3.70 \times 10^{+5}$	$1.49 \times 10^{+1}$	E50	$1.49 \times 10^{+1}$	E50	$1.49 \times 10^{+1}$	E50	$1.49 \times 10^{+1}$	E50
121	Tc-96m	$3.09 \times 10^{+3}$	$1.74 \times 10^{+3}$	E50	$1.74 \times 10^{+3}$	E50	$1.74 \times 10^{+3}$	E50	$1.74 \times 10^{+3}$	E50
122	Tc-97	$8.20 \times 10^{+13}$	$6.34 \times 10^{+0}$	E50	$6.34 \times 10^{+0}$	E50	$6.34 \times 10^{+0}$	E50	$6.33 \times 10^{+0}$	E50
123	Tc-97m	$7.78 \times 10^{+6}$	$1.98 \times 10^{+1}$	E50	$1.98 \times 10^{+1}$	E50	$1.98 \times 10^{+1}$	E50	$1.99 \times 10^{+1}$	E50
124	Tc-98	$1.33 \times 10^{+14}$	4.88×10^{-1}	E50	4.88×10^{-1}	E50	4.88×10^{-1}	E50	4.87×10^{-1}	E50
125	Tc-99	$6.66 \times 10^{+12}$	$2.40 \times 10^{+1}$	Hskin99	$2.40 \times 10^{+1}$	Hskin99	$2.40 \times 10^{+1}$	Hskin99	$2.40 \times 10^{+1}$	Hskin99
126	Tc-99m	$2.17 \times 10^{+4}$	$4.08 \times 10^{+3}$	E50	$4.08 \times 10^{+3}$	E50	$4.08 \times 10^{+3}$	E50	$4.08 \times 10^{+3}$	E50
127	Ru-97	$2.51 \times 10^{+5}$	$1.48 \times 10^{+2}$	E50	$1.48 \times 10^{+2}$	E50	$1.48 \times 10^{+2}$	E50	$1.48 \times 10^{+2}$	E50
128	Ru-103+	$3.39 \times 10^{+6}$	$7.80 \times 10^{+0}$	E50	$7.80 \times 10^{+0}$	E50	$7.80 \times 10^{+0}$	E50	$7.80 \times 10^{+0}$	E50
129	Ru-105	$1.60 \times 10^{+4}$	$9.51 \times 10^{+2}$	E50	$9.51 \times 10^{+2}$	E50	$9.51 \times 10^{+2}$	E50	$9.51 \times 10^{+2}$	E50
130	Ru-106+	$3.23 \times 10^{+7}$	$3.44 \times 10^{+0}$	E50	$3.44 \times 10^{+0}$	E50	$3.41 \times 10^{+0}$	E50	$3.41 \times 10^{+0}$	E50
131	Rh-99	$1.39 \times 10^{+6}$	$1.37 \times 10^{+1}$	E50	$1.37 \times 10^{+1}$	E50	$1.37 \times 10^{+1}$	E50	$1.37 \times 10^{+1}$	E50
132	Rh-99m	$1.69 \times 10^{+4}$	$1.08 \times 10^{+3}$	E50	$1.08 \times 10^{+3}$	E50	$1.08 \times 10^{+3}$	E50	$1.08 \times 10^{+3}$	E50
133	Rh-101	$1.04 \times 10^{+8}$	$1.72 \times 10^{+0}$	E50	$1.72 \times 10^{+0}$	E50	$1.72 \times 10^{+0}$	E50	$1.72 \times 10^{+0}$	E50
134	Rh-101m	$3.75 \times 10^{+5}$	$8.62 \times 10^{+1}$	E50	$8.62 \times 10^{+1}$	E50	$8.62 \times 10^{+1}$	E50	$8.62 \times 10^{+1}$	E50
135	Rh-102	$1.79 \times 10^{+7}$	$1.99 \times 10^{+0}$	E50	$1.99 \times 10^{+0}$	E50	$1.99 \times 10^{+0}$	E50	$1.99 \times 10^{+0}$	E50
136	Rh-102m	$1.18 \times 10^{+8}$	3.40×10^{-1}	E50	3.40×10^{-1}	E50	3.40×10^{-1}	E50	3.40×10^{-1}	E50
137	Rh-103m	$3.37 \times 10^{+3}$	$3.36 \times 10^{+5}$	E50	$3.36 \times 10^{+5}$	E50	$3.36 \times 10^{+5}$	E50	$3.36 \times 10^{+5}$	E50
138	Rh-105	$1.27 \times 10^{+5}$	$9.79 \times 10^{+2}$	E50	$9.79 \times 10^{+2}$	E50	$9.79 \times 10^{+2}$	E50	$9.79 \times 10^{+2}$	E50
139	Rh-106m	$7.86 \times 10^{+3}$	$6.44 \times 10^{+2}$	E50	$6.44 \times 10^{+2}$	E50	$6.44 \times 10^{+2}$	E50	$6.44 \times 10^{+2}$	E50
140	Pd-103+	$1.47 \times 10^{+6}$	$6.81 \times 10^{+1}$	E50	$6.81 \times 10^{+1}$	E50	$6.80 \times 10^{+1}$	E50	$6.80 \times 10^{+1}$	E50
141	Pd-107	$2.05 \times 10^{+14}$	$5.06 \times 10^{+3}$	E50	$5.06 \times 10^{+3}$	E50	$4.54 \times 10^{+3}$	E50	$4.47 \times 10^{+3}$	E50
142	Pd-109+	$4.93 \times 10^{+4}$	$2.57 \times 10^{+3}$	E50	$2.57 \times 10^{+3}$	E50	$2.57 \times 10^{+3}$	E50	$2.57 \times 10^{+3}$	E50
143	Ag-105	$3.57 \times 10^{+6}$	$6.08 \times 10^{+0}$	E50	$6.08 \times 10^{+0}$	E50	$6.08 \times 10^{+0}$	E50	$6.08 \times 10^{+0}$	E50
144	Ag-106	$1.44 \times 10^{+3}$	$1.22 \times 10^{+4}$	E50	$1.22 \times 10^{+4}$	E50	$1.22 \times 10^{+4}$	E50	$1.22 \times 10^{+4}$	E50
145	Ag-106m	$7.15 \times 10^{+5}$	$6.99 \times 10^{+0}$	E50	$6.99 \times 10^{+0}$	E50	$6.99 \times 10^{+0}$	E50	$6.99 \times 10^{+0}$	E50
146	Ag-108m+	$1.32 \times 10^{+10}$	3.98×10^{-1}	E50	3.98×10^{-1}	E50	3.98×10^{-1}	E50	3.98×10^{-1}	E50
147	Ag-110m+	$2.16 \times 10^{+7}$	4.18×10^{-1}	E50	4.18×10^{-1}	E50	4.18×10^{-1}	E50	4.18×10^{-1}	E50
148	Ag-111	$6.44 \times 10^{+5}$	$3.09 \times 10^{+2}$	E50	$3.09 \times 10^{+2}$	E50	$3.09 \times 10^{+2}$	E50	$3.09 \times 10^{+2}$	E50
149	Cd-104+	$3.46 \times 10^{+3}$	$1.87 \times 10^{+3}$	E50	$1.87 \times 10^{+3}$	E50	$1.87 \times 10^{+3}$	E50	$1.87 \times 10^{+3}$	E50
150	Cd-109+	$3.99 \times 10^{+7}$	$4.44 \times 10^{+0}$	E50	$4.44 \times 10^{+0}$	E50	$4.44 \times 10^{+0}$	E50	$4.44 \times 10^{+0}$	E50
151	Cd-113	$2.43 \times 10^{+23}$	$6.44 \times 10^{+0}$	E50	$6.44 \times 10^{+0}$	E50	$6.53 \times 10^{+0}$	E50	$6.53 \times 10^{+0}$	E50

(Continued.)

Table A1. (Continued.)

Nr.	Nuclide	Half-life (s)	SCL Reference (Bq cm^{-2})	Percentile Reference	SCL With α-skin (Bq cm^{-2})	Percentile With α-skin	SCL AMAD = 1 μm (Bq cm^{-2})	Percentile AMAD = 1 μm	SCL Public (Bq cm^{-2})	Percentile Public
152	Cd-113m+	$4.45 \times 10^{+8}$	$6.61 \times 10^{+0}$	E50	$6.61 \times 10^{+0}$	E50	$6.70 \times 10^{+0}$	E50	$6.70 \times 10^{+0}$	E50
153	Cd-115+	$1.92 \times 10^{+5}$	$1.46 \times 10^{+2}$	E50	$1.46 \times 10^{+2}$	E50	$1.46 \times 10^{+2}$	E50	$1.46 \times 10^{+2}$	E50
154	Cd-115m+	$3.85 \times 10^{+6}$	$4.70 \times 10^{+1}$	E50	$4.70 \times 10^{+1}$	E50	$4.70 \times 10^{+1}$	E50	$4.69 \times 10^{+1}$	E50
155	In-111+	$2.42 \times 10^{+5}$	$9.98 \times 10^{+1}$	E50	$9.98 \times 10^{+1}$	E50	$9.98 \times 10^{+1}$	E50	$9.98 \times 10^{+1}$	E50
156	In-113m	$5.97 \times 10^{+3}$	$7.20 \times 10^{+3}$	E50	$7.20 \times 10^{+3}$	E50	$7.20 \times 10^{+3}$	E50	$7.20 \times 10^{+3}$	E50
157	In-114m+	$4.28 \times 10^{+6}$	$1.55 \times 10^{+1}$	E50	$1.55 \times 10^{+1}$	E50	$1.56 \times 10^{+1}$	E50	$1.56 \times 10^{+1}$	E50
158	In-115m	$1.61 \times 10^{+4}$	$3.52 \times 10^{+3}$	E50	$3.52 \times 10^{+3}$	E50	$3.52 \times 10^{+3}$	E50	$3.52 \times 10^{+3}$	E50
159	Sn-113+	$9.94 \times 10^{+6}$	$3.70 \times 10^{+0}$	E50	$3.70 \times 10^{+0}$	E50	$3.70 \times 10^{+0}$	E50	$3.70 \times 10^{+0}$	E50
160	Sn-117m	$1.19 \times 10^{+6}$	$3.79 \times 10^{+1}$	E50	$3.79 \times 10^{+1}$	E50	$3.79 \times 10^{+1}$	E50	$3.79 \times 10^{+1}$	E50
161	Sn-119m	$2.53 \times 10^{+7}$	$1.04 \times 10^{+1}$	E50	$1.04 \times 10^{+1}$	E50	$1.04 \times 10^{+1}$	E50	$1.03 \times 10^{+1}$	E50
162	Sn-121	$9.73 \times 10^{+4}$	$4.83 \times 10^{+3}$	Hskin99	$4.83 \times 10^{+3}$	Hskin99	$4.83 \times 10^{+3}$	Hskin99	$4.83 \times 10^{+3}$	Hskin99
163	Sn-121m+	$1.39 \times 10^{+9}$	$1.54 \times 10^{+1}$	E50	$1.54 \times 10^{+1}$	E50	$1.54 \times 10^{+1}$	E50	$1.54 \times 10^{+1}$	E50
164	Sn-123	$1.12 \times 10^{+7}$	$3.63 \times 10^{+1}$	E50	$3.63 \times 10^{+1}$	E50	$3.61 \times 10^{+1}$	E50	$3.60 \times 10^{+1}$	E50
165	Sn-125	$8.33 \times 10^{+5}$	$3.44 \times 10^{+1}$	E50	$3.44 \times 10^{+1}$	E50	$3.44 \times 10^{+1}$	E50	$3.44 \times 10^{+1}$	E50
166	Sn-126+	$7.26 \times 10^{+12}$	3.27×10^{-1}	E50	3.27×10^{-1}	E50	3.27×10^{-1}	E50	3.27×10^{-1}	E50
167	Sb-120	$9.53 \times 10^{+2}$	$2.71 \times 10^{+4}$	E50	$2.71 \times 10^{+4}$	E50	$2.71 \times 10^{+4}$	E50	$2.71 \times 10^{+4}$	E50
168	Sb-120m	$4.98 \times 10^{+5}$	$1.16 \times 10^{+1}$	E50	$1.16 \times 10^{+1}$	E50	$1.16 \times 10^{+1}$	E50	$1.16 \times 10^{+1}$	E50
169	Sb-122	$2.35 \times 10^{+5}$	$1.19 \times 10^{+2}$	E50	$1.19 \times 10^{+2}$	E50	$1.19 \times 10^{+2}$	E50	$1.19 \times 10^{+2}$	E50
170	Sb-124	$5.20 \times 10^{+6}$	$1.70 \times 10^{+0}$	E50	$1.70 \times 10^{+0}$	E50	$1.70 \times 10^{+0}$	E50	$1.70 \times 10^{+0}$	E50
171	Sb-125+	$8.71 \times 10^{+7}$	$1.36 \times 10^{+0}$	E50	$1.36 \times 10^{+0}$	E50	$1.35 \times 10^{+0}$	E50	$1.35 \times 10^{+0}$	E50
172	Sb-126	$1.07 \times 10^{+6}$	$4.75 \times 10^{+0}$	E50	$4.75 \times 10^{+0}$	E50	$4.75 \times 10^{+0}$	E50	$4.75 \times 10^{+0}$	E50
173	Te-121	$1.66 \times 10^{+6}$	$1.24 \times 10^{+1}$	E50	$1.24 \times 10^{+1}$	E50	$1.24 \times 10^{+1}$	E50	$1.24 \times 10^{+1}$	E50
174	Te-121m	$1.33 \times 10^{+7}$	$1.53 \times 10^{+0}$	E50	$1.53 \times 10^{+0}$	E50	$1.53 \times 10^{+0}$	E50	$1.53 \times 10^{+0}$	E50
175	Te-123	$1.89 \times 10^{+22}$	$4.98 \times 10^{+1}$	E50	$4.98 \times 10^{+1}$	E50	$5.02 \times 10^{+1}$	E50	$5.02 \times 10^{+1}$	E50
176	Te-123m	$1.03 \times 10^{+7}$	$6.76 \times 10^{+0}$	E50	$6.76 \times 10^{+0}$	E50	$6.76 \times 10^{+0}$	E50	$6.75 \times 10^{+0}$	E50
177	Te-125m	$4.96 \times 10^{+6}$	$1.38 \times 10^{+1}$	E50	$1.38 \times 10^{+1}$	E50	$1.38 \times 10^{+1}$	E50	$1.38 \times 10^{+1}$	E50
178	Te-127	$3.37 \times 10^{+4}$	$1.09 \times 10^{+4}$	Hskin99	$1.09 \times 10^{+4}$	Hskin99	$1.09 \times 10^{+4}$	Hskin99	$1.09 \times 10^{+4}$	Hskin99
179	Te-127m+	$9.42 \times 10^{+6}$	$1.63 \times 10^{+1}$	E50	$1.63 \times 10^{+1}$	E50	$1.62 \times 10^{+1}$	E50	$1.62 \times 10^{+1}$	E50
180	Te-129	$4.18 \times 10^{+3}$	$2.86 \times 10^{+4}$	E50	$2.86 \times 10^{+4}$	E50	$2.86 \times 10^{+4}$	E50	$2.86 \times 10^{+4}$	E50
181	Te-129m+	$2.90 \times 10^{+6}$	$2.60 \times 10^{+1}$	E50	$2.60 \times 10^{+1}$	E50	$2.60 \times 10^{+1}$	E50	$2.59 \times 10^{+1}$	E50
182	Te-131	$1.50 \times 10^{+3}$	$8.19 \times 10^{+3}$	E50	$8.19 \times 10^{+3}$	E50	$8.20 \times 10^{+3}$	E50	$8.20 \times 10^{+3}$	E50
183	Te-131m+	$1.08 \times 10^{+5}$	$5.80 \times 10^{+1}$	E50	$5.80 \times 10^{+1}$	E50	$5.80 \times 10^{+1}$	E50	$5.80 \times 10^{+1}$	E50
184	Te-132+	$2.77 \times 10^{+5}$	$1.93 \times 10^{+1}$	E50	$1.93 \times 10^{+1}$	E50	$1.93 \times 10^{+1}$	E50	$1.93 \times 10^{+1}$	E50

(Continued.)

Table A1. (Continued.)

Nr.	Nuclide	Half-life (s)	SCL Reference (Bq cm^{-2})	Percentile Reference	SCL With α-skin (Bq cm^{-2})	Percentile With α-skin	SCL AMAD = 1 μm (Bq cm^{-2})	Percentile AMAD = 1 μm	SCL Public (Bq cm^{-2})	Percentile Public
185	Te-133	$7.50 \times 10^{+2}$	$9.40 \times 10^{+3}$	E50	$9.40 \times 10^{+3}$	E50	$9.40 \times 10^{+3}$	E50	$9.40 \times 10^{+3}$	E50
186	Te-133m+	$3.32 \times 10^{+3}$	$1.48 \times 10^{+3}$	E50	$1.48 \times 10^{+3}$	E50	$1.48 \times 10^{+3}$	E50	$1.48 \times 10^{+3}$	E50
187	Te-134	$2.51 \times 10^{+3}$	$1.61 \times 10^{+3}$	E50	$1.61 \times 10^{+3}$	E50	$1.61 \times 10^{+3}$	E50	$1.61 \times 10^{+3}$	E50
188	I-123	$4.78 \times 10^{+4}$	$9.65 \times 10^{+2}$	E50	$9.65 \times 10^{+2}$	E50	$9.66 \times 10^{+2}$	E50	$9.66 \times 10^{+2}$	E50
189	I-124	$3.61 \times 10^{+5}$	$3.09 \times 10^{+1}$	E50	$3.09 \times 10^{+1}$	E50	$3.10 \times 10^{+1}$	E50	$3.10 \times 10^{+1}$	E50
190	I-125	$5.13 \times 10^{+6}$	$8.95 \times 10^{+0}$	E50	$8.95 \times 10^{+0}$	E50	$8.96 \times 10^{+0}$	E50	$8.96 \times 10^{+0}$	E50
191	I-126	$1.12 \times 10^{+6}$	$1.72 \times 10^{+1}$	E50	$1.72 \times 10^{+1}$	E50	$1.72 \times 10^{+1}$	E50	$1.72 \times 10^{+1}$	E50
192	I-129	$4.95 \times 10^{+14}$	$1.46 \times 10^{+0}$	E50	$1.46 \times 10^{+0}$	E50	$1.47 \times 10^{+0}$	E50	$1.47 \times 10^{+0}$	E50
193	I-130	$4.45 \times 10^{+4}$	$1.43 \times 10^{+2}$	E50	$1.43 \times 10^{+2}$	E50	$1.43 \times 10^{+2}$	E50	$1.43 \times 10^{+2}$	E50
194	I-131	$6.93 \times 10^{+5}$	$3.25 \times 10^{+1}$	E50	$3.25 \times 10^{+1}$	E50	$3.26 \times 10^{+1}$	E50	$3.26 \times 10^{+1}$	E50
195	I-132	$8.26 \times 10^{+3}$	$7.60 \times 10^{+2}$	E50	$7.60 \times 10^{+2}$	E50	$7.60 \times 10^{+2}$	E50	$7.60 \times 10^{+2}$	E50
196	I-133	$7.49 \times 10^{+4}$	$2.23 \times 10^{+2}$	E50	$2.23 \times 10^{+2}$	E50	$2.23 \times 10^{+2}$	E50	$2.23 \times 10^{+2}$	E50
197	I-134	$3.15 \times 10^{+3}$	$1.78 \times 10^{+3}$	E50	$1.78 \times 10^{+3}$	E50	$1.78 \times 10^{+3}$	E50	$1.78 \times 10^{+3}$	E50
198	I-135+	$2.37 \times 10^{+4}$	$3.27 \times 10^{+2}$	E50	$3.27 \times 10^{+2}$	E50	$3.27 \times 10^{+2}$	E50	$3.27 \times 10^{+2}$	E50
199	Cs-125	$2.70 \times 10^{+3}$	$3.17 \times 10^{+3}$	E50	$3.17 \times 10^{+3}$	E50	$3.17 \times 10^{+3}$	E50	$3.17 \times 10^{+3}$	E50
200	Cs-129	$1.15 \times 10^{+5}$	$2.90 \times 10^{+2}$	E50	$2.90 \times 10^{+2}$	E50	$2.90 \times 10^{+2}$	E50	$2.90 \times 10^{+2}$	E50
201	Cs-131	$8.37 \times 10^{+5}$	$1.61 \times 10^{+2}$	E50	$1.61 \times 10^{+2}$	E50	$1.61 \times 10^{+2}$	E50	$1.61 \times 10^{+2}$	E50
202	Cs-132	$5.60 \times 10^{+5}$	$3.13 \times 10^{+1}$	E50	$3.13 \times 10^{+1}$	E50	$3.13 \times 10^{+1}$	E50	$3.13 \times 10^{+1}$	E50
203	Cs-134	$6.52 \times 10^{+7}$	4.96×10^{-1}	E50	4.96×10^{-1}	E50	4.96×10^{-1}	E50	4.95×10^{-1}	E50
204	Cs-134m	$1.05 \times 10^{+4}$	$2.26 \times 10^{+3}$	E50	$2.26 \times 10^{+3}$	E50	$2.26 \times 10^{+3}$	E50	$2.26 \times 10^{+3}$	E50
205	Cs-135	$7.26 \times 10^{+13}$	$3.85 \times 10^{+1}$	E50	$3.85 \times 10^{+1}$	E50	$3.85 \times 10^{+1}$	E50	$3.69 \times 10^{+1}$	E50
206	Cs-136	$1.14 \times 10^{+6}$	$5.97 \times 10^{+0}$	E50	$5.97 \times 10^{+0}$	E50	$5.97 \times 10^{+0}$	E50	$5.97 \times 10^{+0}$	E50
207	Cs-137+	$9.52 \times 10^{+8}$	$1.07 \times 10^{+0}$	E50	$1.07 \times 10^{+0}$	E50	$1.07 \times 10^{+0}$	E50	$1.07 \times 10^{+0}$	E50
208	Cs-138	$2.00 \times 10^{+3}$	$3.41 \times 10^{+3}$	E50	$3.41 \times 10^{+3}$	E50	$3.41 \times 10^{+3}$	E50	$3.41 \times 10^{+3}$	E50
209	Ba-131	$9.94 \times 10^{+5}$	$1.97 \times 10^{+1}$	E50	$1.97 \times 10^{+1}$	E50	$1.97 \times 10^{+1}$	E50	$1.97 \times 10^{+1}$	E50
210	Ba-133	$3.32 \times 10^{+8}$	$1.27 \times 10^{+0}$	E50	$1.27 \times 10^{+0}$	E50	$1.27 \times 10^{+0}$	E50	$1.26 \times 10^{+0}$	E50
211	Ba-133m	$1.40 \times 10^{+5}$	$5.01 \times 10^{+2}$	E50	$5.01 \times 10^{+2}$	E50	$5.01 \times 10^{+2}$	E50	$5.00 \times 10^{+2}$	E50
212	Ba-140	$1.10 \times 10^{+6}$	$5.54 \times 10^{+0}$	E50	$5.54 \times 10^{+0}$	E50	$5.54 \times 10^{+0}$	E50	$5.54 \times 10^{+0}$	E50
213	La-137	$1.89 \times 10^{+12}$	$7.04 \times 10^{+0}$	E50	$7.04 \times 10^{+0}$	E50	$7.05 \times 10^{+0}$	E50	$7.05 \times 10^{+0}$	E50
214	La-140	$1.45 \times 10^{+5}$	$4.67 \times 10^{+1}$	E50	$4.67 \times 10^{+1}$	E50	$4.67 \times 10^{+1}$	E50	$4.67 \times 10^{+1}$	E50
215	Ce-139	$1.19 \times 10^{+7}$	$5.76 \times 10^{+0}$	E50	$5.76 \times 10^{+0}$	E50	$5.76 \times 10^{+0}$	E50	$5.76 \times 10^{+0}$	E50
216	Ce-141	$2.81 \times 10^{+6}$	$3.87 \times 10^{+1}$	E50	$3.87 \times 10^{+1}$	E50	$3.87 \times 10^{+1}$	E50	$3.87 \times 10^{+1}$	E50
217	Ce-143	$1.19 \times 10^{+5}$	$2.72 \times 10^{+2}$	E50	$2.72 \times 10^{+2}$	E50	$2.72 \times 10^{+2}$	E50	$2.72 \times 10^{+2}$	E50

(Continued.)

Table A1. (Continued.)

Nr.	Nuclide	Half-life (s)	SCL Reference (Bq cm^{-2})	Percentile Reference	SCL With α-skin (Bq cm^{-2})	Percentile With α-skin	SCL AMAD = 1 μm (Bq cm^{-2})	Percentile AMAD = 1 μm	SCL Public (Bq cm^{-2})	Percentile Public
218	Ce-144+	$2.46 \times 10^{+7}$	$8.32 \times 10^{+0}$	E50	$8.32 \times 10^{+0}$	E50	$8.20 \times 10^{+0}$	E50	$8.18 \times 10^{+0}$	E50
219	Pr-142	$6.88 \times 10^{+4}$	$2.22 \times 10^{+3}$	E50	$2.22 \times 10^{+3}$	E50	$2.22 \times 10^{+3}$	E50	$2.22 \times 10^{+3}$	E50
220	Pr-143	$1.17 \times 10^{+6}$	$3.02 \times 10^{+2}$	Hskin99	$3.02 \times 10^{+2}$	Hskin99	$3.02 \times 10^{+2}$	Hskin99	$3.02 \times 10^{+2}$	Hskin99
221	Nd-147	$9.49 \times 10^{+5}$	$6.62 \times 10^{+1}$	E50	$6.62 \times 10^{+1}$	E50	$6.62 \times 10^{+1}$	E50	$6.62 \times 10^{+1}$	E50
222	Nd-149	$6.22 \times 10^{+3}$	$4.44 \times 10^{+3}$	E50	$4.44 \times 10^{+3}$	E50	$4.44 \times 10^{+3}$	E50	$4.44 \times 10^{+3}$	E50
223	Pm-143	$2.29 \times 10^{+7}$	$2.88 \times 10^{+0}$	E50	$2.88 \times 10^{+0}$	E50	$2.88 \times 10^{+0}$	E50	$2.88 \times 10^{+0}$	E50
224	Pm-144	$3.14 \times 10^{+7}$	5.90×10^{-1}	E50	5.90×10^{-1}	E50	5.89×10^{-1}	E50	5.89×10^{-1}	E50
225	Pm-145	$5.59 \times 10^{+8}$	$7.71 \times 10^{+0}$	E50	$7.71 \times 10^{+0}$	E50	$7.70 \times 10^{+0}$	E50	$7.70 \times 10^{+0}$	E50
226	Pm-147	$8.28 \times 10^{+7}$	$5.35 \times 10^{+1}$	Hskin99	$5.35 \times 10^{+1}$	Hskin99	$5.35 \times 10^{+1}$	Hskin99	$5.35 \times 10^{+1}$	Hskin99
227	Pm-148m	$3.57 \times 10^{+6}$	$1.98 \times 10^{+0}$	E50	$1.98 \times 10^{+0}$	E50	$1.98 \times 10^{+0}$	E50	$1.98 \times 10^{+0}$	E50
228	Pm-149	$1.91 \times 10^{+5}$	$1.49 \times 10^{+3}$	E50	$1.49 \times 10^{+3}$	E50	$1.49 \times 10^{+3}$	E50	$1.49 \times 10^{+3}$	E50
229	Pm-151	$1.02 \times 10^{+5}$	$3.38 \times 10^{+2}$	E50	$3.38 \times 10^{+2}$	E50	$3.38 \times 10^{+2}$	E50	$3.38 \times 10^{+2}$	E50
230	Sm-145	$2.94 \times 10^{+7}$	$5.34 \times 10^{+0}$	E50	$5.34 \times 10^{+0}$	E50	$5.34 \times 10^{+0}$	E50	$5.34 \times 10^{+0}$	E50
231	Sm-147	$3.35 \times 10^{+18}$	$1.71 \times 10^{+0}$	E50	$1.71 \times 10^{+0}$	E50	$1.35 \times 10^{+0}$	E95	$1.26 \times 10^{+0}$	E95
232	Sm-151	$2.84 \times 10^{+9}$	$1.49 \times 10^{+3}$	E50	$1.49 \times 10^{+3}$	E50	$1.35 \times 10^{+3}$	E50	$1.32 \times 10^{+3}$	E50
233	Sm-153	$1.67 \times 10^{+5}$	$5.49 \times 10^{+2}$	E50	$5.49 \times 10^{+2}$	E50	$5.49 \times 10^{+2}$	E50	$5.49 \times 10^{+2}$	E50
234	Eu-146	$3.98 \times 10^{+5}$	$1.52 \times 10^{+1}$	E50	$1.52 \times 10^{+1}$	E50	$1.52 \times 10^{+1}$	E50	$1.52 \times 10^{+1}$	E50
235	Eu-147	$2.08 \times 10^{+6}$	$1.26 \times 10^{+1}$	E50	$1.26 \times 10^{+1}$	E50	$1.26 \times 10^{+1}$	E50	$1.26 \times 10^{+1}$	E50
236	Eu-148	$4.71 \times 10^{+6}$	$1.40 \times 10^{+0}$	E50	$1.40 \times 10^{+0}$	E50	$1.40 \times 10^{+0}$	E50	$1.40 \times 10^{+0}$	E50
237	Eu-149	$8.04 \times 10^{+6}$	$1.53 \times 10^{+1}$	E50	$1.53 \times 10^{+1}$	E50	$1.53 \times 10^{+1}$	E50	$1.53 \times 10^{+1}$	E50
238	Eu-150m	$4.61 \times 10^{+4}$	$3.56 \times 10^{+3}$	E50	$3.56 \times 10^{+3}$	E50	$3.56 \times 10^{+3}$	E50	$3.56 \times 10^{+3}$	E50
239	Eu-150	$1.16 \times 10^{+9}$	4.30×10^{-1}	E50	4.30×10^{-1}	E50	4.29×10^{-1}	E50	4.29×10^{-1}	E50
240	Eu-152	$4.27 \times 10^{+8}$	6.09×10^{-1}	E50	6.09×10^{-1}	E50	6.09×10^{-1}	E50	6.08×10^{-1}	E50
241	Eu-152m	$3.35 \times 10^{+4}$	$1.27 \times 10^{+3}$	E50	$1.27 \times 10^{+3}$	E50	$1.27 \times 10^{+3}$	E50	$1.27 \times 10^{+3}$	E50
242	Eu-154	$2.71 \times 10^{+8}$	5.95×10^{-1}	E50	5.95×10^{-1}	E50	5.94×10^{-1}	E50	5.93×10^{-1}	E50
243	Eu-155	$1.50 \times 10^{+8}$	$8.06 \times 10^{+0}$	E50	$8.06 \times 10^{+0}$	E50	$8.04 \times 10^{+0}$	E50	$8.04 \times 10^{+0}$	E50
244	Eu-156	$1.31 \times 10^{+6}$	$9.74 \times 10^{+0}$	E50	$9.74 \times 10^{+0}$	E50	$9.74 \times 10^{+0}$	E50	$9.74 \times 10^{+0}$	E50
245	Gd-146+	$4.17 \times 10^{+6}$	$1.29 \times 10^{+0}$	E50	$1.29 \times 10^{+0}$	E50	$1.29 \times 10^{+0}$	E50	$1.29 \times 10^{+0}$	E50
246	Gd-148	$2.35 \times 10^{+9}$	4.28×10^{-1}	E95	4.28×10^{-1}	E95	5.11×10^{-1}	E95	4.91×10^{-1}	E95
247	Gd-153	$2.08 \times 10^{+7}$	$5.61 \times 10^{+0}$	E50	$5.61 \times 10^{+0}$	E50	$5.62 \times 10^{+0}$	E50	$5.62 \times 10^{+0}$	E50
248	Gd-159	$6.65 \times 10^{+4}$	$2.09 \times 10^{+3}$	E50	$2.09 \times 10^{+3}$	E50	$2.09 \times 10^{+3}$	E50	$2.09 \times 10^{+3}$	E50

(Continued.)

Table A1. (Continued.)

Nr.	Nuclide	Half-life (s)	SCL Reference (Bq cm^{-2})	Percentile Reference	SCL With α-skin (Bq cm^{-2})	Percentile With α-skin	SCL AMAD = 1 μm (Bq cm^{-2})	Percentile AMAD = 1 μm	SCL Public (Bq cm^{-2})	Percentile Public
249	Tb-157	$2.24 \times 10^{+9}$	$5.58 \times 10^{+1}$	E50	$5.58 \times 10^{+1}$	E50	$5.57 \times 10^{+1}$	E50	$5.56 \times 10^{+1}$	E50
250	Tb-158	$5.68 \times 10^{+9}$	8.38×10^{-1}	E50	8.38×10^{-1}	E50	8.37×10^{-1}	E50	8.36×10^{-1}	E50
251	Tb-160	$6.25 \times 10^{+6}$	$2.19 \times 10^{+0}$	E50	$2.19 \times 10^{+0}$	E50	$2.19 \times 10^{+0}$	E50	$2.19 \times 10^{+0}$	E50
252	Dy-159	$1.25 \times 10^{+7}$	$1.39 \times 10^{+1}$	E50	$1.39 \times 10^{+1}$	E50	$1.39 \times 10^{+1}$	E50	$1.39 \times 10^{+1}$	E50
253	Dy-165	$8.40 \times 10^{+3}$	$2.74 \times 10^{+4}$	E50	$2.74 \times 10^{+4}$	E50	$2.74 \times 10^{+4}$	E50	$2.74 \times 10^{+4}$	E50
254	Dy-166	$2.94 \times 10^{+5}$	$2.58 \times 10^{+2}$	E50	$2.58 \times 10^{+2}$	E50	$2.59 \times 10^{+2}$	E50	$2.59 \times 10^{+2}$	E50
255	Ho-166	$9.65 \times 10^{+4}$	$1.94 \times 10^{+3}$	E50	$1.94 \times 10^{+3}$	E50	$1.94 \times 10^{+3}$	E50	$1.94 \times 10^{+3}$	E50
256	Ho-166m	$3.79 \times 10^{+10}$	4.18×10^{-1}	E50	4.18×10^{-1}	E50	4.17×10^{-1}	E50	4.17×10^{-1}	E50
257	Er-169	$8.12 \times 10^{+5}$	$6.63 \times 10^{+2}$	Hskin99	$6.63 \times 10^{+2}$	Hskin99	$6.63 \times 10^{+2}$	Hskin99	$6.63 \times 10^{+2}$	Hskin99
258	Er-171	$2.71 \times 10^{+4}$	$1.11 \times 10^{+3}$	E50	$1.11 \times 10^{+3}$	E50	$1.11 \times 10^{+3}$	E50	$1.11 \times 10^{+3}$	E50
259	Tm-167	$7.99 \times 10^{+5}$	$7.73 \times 10^{+1}$	E50	$7.73 \times 10^{+1}$	E50	$7.73 \times 10^{+1}$	E50	$7.73 \times 10^{+1}$	E50
260	Tm-170	$1.11 \times 10^{+7}$	$3.70 \times 10^{+1}$	Hskin99	$3.70 \times 10^{+1}$	Hskin99	$3.70 \times 10^{+1}$	Hskin99	$3.70 \times 10^{+1}$	Hskin99
261	Tm-171	$6.06 \times 10^{+7}$	$1.34 \times 10^{+3}$	E50	$1.34 \times 10^{+3}$	E50	$1.28 \times 10^{+3}$	E50	$1.27 \times 10^{+3}$	E50
262	Yb-169	$2.77 \times 10^{+6}$	$1.08 \times 10^{+1}$	E50	$1.08 \times 10^{+1}$	E50	$1.08 \times 10^{+1}$	E50	$1.08 \times 10^{+1}$	E50
263	Yb-175	$3.62 \times 10^{+5}$	$5.75 \times 10^{+2}$	E50	$5.75 \times 10^{+2}$	E50	$5.75 \times 10^{+2}$	E50	$5.75 \times 10^{+2}$	E50
264	Lu-171	$7.12 \times 10^{+5}$	$2.74 \times 10^{+1}$	E50	$2.74 \times 10^{+1}$	E50	$2.74 \times 10^{+1}$	E50	$2.74 \times 10^{+1}$	E50
265	Lu-172	$5.79 \times 10^{+5}$	$1.28 \times 10^{+1}$	E50	$1.28 \times 10^{+1}$	E50	$1.28 \times 10^{+1}$	E50	$1.28 \times 10^{+1}$	E50
266	Lu-173	$4.32 \times 10^{+7}$	$3.42 \times 10^{+0}$	E50	$3.42 \times 10^{+0}$	E50	$3.42 \times 10^{+0}$	E50	$3.42 \times 10^{+0}$	E50
267	Lu-174	$1.04 \times 10^{+8}$	$5.19 \times 10^{+0}$	E50	$5.19 \times 10^{+0}$	E50	$5.19 \times 10^{+0}$	E50	$5.19 \times 10^{+0}$	E50
268	Lu-174m	$1.23 \times 10^{+7}$	$1.13 \times 10^{+1}$	E50	$1.13 \times 10^{+1}$	E50	$1.13 \times 10^{+1}$	E50	$1.13 \times 10^{+1}$	E50
269	Lu-177	$5.74 \times 10^{+5}$	$3.41 \times 10^{+2}$	E50	$3.41 \times 10^{+2}$	E50	$3.41 \times 10^{+2}$	E50	$3.41 \times 10^{+2}$	E50
270	Lu-177m+	$1.39 \times 10^{+7}$	$1.14 \times 10^{+0}$	E50	$1.14 \times 10^{+0}$	E50	$1.14 \times 10^{+0}$	E50	$1.14 \times 10^{+0}$	E50
271	Hf-172+	$5.90 \times 10^{+7}$	4.05×10^{-1}	E50	4.05×10^{-1}	E50	4.05×10^{-1}	E50	4.05×10^{-1}	E50
272	Hf-175	$6.05 \times 10^{+6}$	$6.02 \times 10^{+0}$	E50	$6.02 \times 10^{+0}$	E50	$6.02 \times 10^{+0}$	E50	$6.02 \times 10^{+0}$	E50
273	Hf-181	$3.66 \times 10^{+6}$	$6.43 \times 10^{+0}$	E50	$6.43 \times 10^{+0}$	E50	$6.43 \times 10^{+0}$	E50	$6.43 \times 10^{+0}$	E50
274	Hf-182+	$2.84 \times 10^{+14}$	4.47×10^{-1}	E50	4.47×10^{-1}	E50	4.49×10^{-1}	E50	4.49×10^{-1}	E50
275	Ta-179	$5.74 \times 10^{+7}$	$1.94 \times 10^{+1}$	E50	$1.94 \times 10^{+1}$	E50	$1.94 \times 10^{+1}$	E50	$1.94 \times 10^{+1}$	E50
276	Ta-182	$9.89 \times 10^{+6}$	$1.37 \times 10^{+0}$	E50	$1.37 \times 10^{+0}$	E50	$1.37 \times 10^{+0}$	E50	$1.37 \times 10^{+0}$	E50
277	W-178+	$1.87 \times 10^{+6}$	$4.32 \times 10^{+1}$	E50	$4.32 \times 10^{+1}$	E50	$4.32 \times 10^{+1}$	E50	$4.33 \times 10^{+1}$	E50

(Continued.)

Table A1. (Continued.)

Nr.	Nuclide	Half-life (s)	SCL Reference ($Bq\ cm^{-2}$)	Percentile Reference	SCL With α-skin ($Bq\ cm^{-2}$)	Percentile With α-skin	SCL AMAD = 1 μm ($Bq\ cm^{-2}$)	Percentile AMAD = 1 μm	SCL Public ($Bq\ cm^{-2}$)	Percentile Public
278	W-181	$1.05 \times 10^{+7}$	$2.64 \times 10^{+1}$	E50	$2.64 \times 10^{+1}$	E50	$2.64 \times 10^{+1}$	E50	$2.64 \times 10^{+1}$	E50
279	W-185	$6.49 \times 10^{+6}$	$7.43 \times 10^{+1}$	Hskin99	$7.43 \times 10^{+1}$	Hskin99	$7.43 \times 10^{+1}$	Hskin99	$7.43 \times 10^{+1}$	Hskin99
280	W-187	$8.54 \times 10^{+4}$	$3.26 \times 10^{+2}$	E50	$3.26 \times 10^{+2}$	E50	$3.26 \times 10^{+2}$	E50	$3.26 \times 10^{+2}$	E50
281	W-188+	$6.03 \times 10^{+6}$	$1.91 \times 10^{+1}$	E50	$1.91 \times 10^{+1}$	E50	$1.91 \times 10^{+1}$	E50	$1.93 \times 10^{+1}$	E50
282	Re-184	$3.28 \times 10^{+6}$	$4.85 \times 10^{+0}$	E50	$4.85 \times 10^{+0}$	E50	$4.85 \times 10^{+0}$	E50	$4.85 \times 10^{+0}$	E50
283	Re-184m	$1.46 \times 10^{+7}$	$1.24 \times 10^{+0}$	E50	$1.24 \times 10^{+0}$	E50	$1.24 \times 10^{+0}$	E50	$1.24 \times 10^{+0}$	E50
284	Re-186	$3.21 \times 10^{+5}$	$6.56 \times 10^{+2}$	E50	$6.56 \times 10^{+2}$	E50	$6.56 \times 10^{+2}$	E50	$6.56 \times 10^{+2}$	E50
285	Re-187	$1.30 \times 10^{+18}$	$4.33 \times 10^{+4}$	E50	$4.33 \times 10^{+4}$	E50	$4.30 \times 10^{+4}$	E50	$4.29 \times 10^{+4}$	E50
286	Re-188	$6.12 \times 10^{+4}$	$2.10 \times 10^{+3}$	E50	$2.10 \times 10^{+3}$	E50	$2.10 \times 10^{+3}$	E50	$2.10 \times 10^{+3}$	E50
287	Re-188m	$1.12 \times 10^{+3}$	$5.91 \times 10^{+4}$	E50	$5.91 \times 10^{+4}$	E50	$5.91 \times 10^{+4}$	E50	$5.91 \times 10^{+4}$	E50
288	Re-189+	$8.75 \times 10^{+4}$	$1.61 \times 10^{+3}$	E50	$1.61 \times 10^{+3}$	E50	$1.61 \times 10^{+3}$	E50	$1.61 \times 10^{+3}$	E50
289	Os-185	$8.09 \times 10^{+6}$	$2.76 \times 10^{+0}$	E50	$2.76 \times 10^{+0}$	E50	$2.76 \times 10^{+0}$	E50	$2.76 \times 10^{+0}$	E50
290	Os-191	$1.33 \times 10^{+6}$	$8.62 \times 10^{+1}$	E50	$8.62 \times 10^{+1}$	E50	$8.61 \times 10^{+1}$	E50	$8.61 \times 10^{+1}$	E50
291	Os-191m	$4.72 \times 10^{+4}$	$2.13 \times 10^{+3}$	E50	$2.13 \times 10^{+3}$	E50	$2.13 \times 10^{+3}$	E50	$2.13 \times 10^{+3}$	E50
292	Os-193	$1.08 \times 10^{+5}$	$1.09 \times 10^{+3}$	E50	$1.09 \times 10^{+3}$	E50	$1.09 \times 10^{+3}$	E50	$1.09 \times 10^{+3}$	E50
293	Os-194+	$1.89 \times 10^{+8}$	$4.80 \times 10^{+0}$	E50	$4.80 \times 10^{+0}$	E50	$4.71 \times 10^{+0}$	E50	$4.69 \times 10^{+0}$	E50
294	Ir-189+	$1.14 \times 10^{+6}$	$1.10 \times 10^{+2}$	E50	$1.10 \times 10^{+2}$	E50	$1.10 \times 10^{+2}$	E50	$1.10 \times 10^{+2}$	E50
295	Ir-190	$1.02 \times 10^{+6}$	$8.79 \times 10^{+0}$	E50	$8.79 \times 10^{+0}$	E50	$8.79 \times 10^{+0}$	E50	$8.79 \times 10^{+0}$	E50
296	Ir-192	$6.38 \times 10^{+6}$	$2.64 \times 10^{+0}$	E50	$2.64 \times 10^{+0}$	E50	$2.64 \times 10^{+0}$	E50	$2.64 \times 10^{+0}$	E50
297	Ir-194	$6.94 \times 10^{+4}$	$1.49 \times 10^{+3}$	E50	$1.49 \times 10^{+3}$	E50	$1.49 \times 10^{+3}$	E50	$1.49 \times 10^{+3}$	E50
298	Pt-188	$8.81 \times 10^{+5}$	$7.82 \times 10^{+0}$	E50	$7.82 \times 10^{+0}$	E50	$7.82 \times 10^{+0}$	E50	$7.82 \times 10^{+0}$	E50
299	Pt-191	$2.42 \times 10^{+5}$	$1.59 \times 10^{+2}$	E50	$1.59 \times 10^{+2}$	E50	$1.59 \times 10^{+2}$	E50	$1.59 \times 10^{+2}$	E50
300	Pt-193	$1.58 \times 10^{+9}$	$1.10 \times 10^{+2}$	E50	$1.10 \times 10^{+2}$	E50	$1.10 \times 10^{+2}$	E50	$1.10 \times 10^{+2}$	E50
301	Pt-193m	$3.74 \times 10^{+5}$	$6.97 \times 10^{+2}$	E50	$6.97 \times 10^{+2}$	E50	$6.97 \times 10^{+2}$	E50	$6.97 \times 10^{+2}$	E50
302	Pt-195m	$3.47 \times 10^{+5}$	$2.52 \times 10^{+2}$	E50	$2.52 \times 10^{+2}$	E50	$2.52 \times 10^{+2}$	E50	$2.52 \times 10^{+2}$	E50
303	Pt-197	$7.16 \times 10^{+4}$	$2.85 \times 10^{+3}$	E50	$2.85 \times 10^{+3}$	E50	$2.85 \times 10^{+3}$	E50	$2.85 \times 10^{+3}$	E50
304	Pt-197m	$5.72 \times 10^{+3}$	$1.17 \times 10^{+4}$	E50	$1.17 \times 10^{+4}$	E50	$1.17 \times 10^{+4}$	E50	$1.17 \times 10^{+4}$	E50
305	Au-193	$6.35 \times 10^{+4}$	$9.73 \times 10^{+2}$	E50	$9.73 \times 10^{+2}$	E50	$9.73 \times 10^{+2}$	E50	$9.73 \times 10^{+2}$	E50
306	Au-194	$1.37 \times 10^{+5}$	$1.04 \times 10^{+2}$	E50	$1.04 \times 10^{+2}$	E50	$1.04 \times 10^{+2}$	E50	$1.04 \times 10^{+2}$	E50

(Continued.)

Table A1. (Continued.)

Nr.	Nuclide	Half-life (s)	SCL Reference (Bq cm^{-2})	Percentile Reference	SCL With α-skin (Bq cm^{-2})	Percentile With α-skin	SCL AMAD = 1 μm (Bq cm^{-2})	Percentile AMAD = 1 μm	SCL Public (Bq cm^{-2})	Percentile Public
307	Au-195	$1.61 \times 10^{+7}$	$9.94 \times 10^{+0}$	E50	$9.94 \times 10^{+0}$	E50	$9.93 \times 10^{+0}$	E50	$9.93 \times 10^{+0}$	E50
308	Au-198	$2.33 \times 10^{+5}$	$1.28 \times 10^{+2}$	E50	$1.28 \times 10^{+2}$	E50	$1.28 \times 10^{+2}$	E50	$1.28 \times 10^{+2}$	E50
309	Au-199	$2.71 \times 10^{+5}$	$3.46 \times 10^{+2}$	E50	$3.46 \times 10^{+2}$	E50	$3.46 \times 10^{+2}$	E50	$3.46 \times 10^{+2}$	E50
310	Hg-194+	$1.39 \times 10^{+10}$	5.67×10^{-1}	E50	5.67×10^{-1}	E50	5.67×10^{-1}	E50	5.67×10^{-1}	E50
311	Hg-195m+	$1.50 \times 10^{+5}$	$1.87 \times 10^{+2}$	E50	$1.87 \times 10^{+2}$	E50	$1.87 \times 10^{+2}$	E50	$1.87 \times 10^{+2}$	E50
312	Hg-197	$2.34 \times 10^{+5}$	$5.25 \times 10^{+2}$	E50	$5.25 \times 10^{+2}$	E50	$5.25 \times 10^{+2}$	E50	$5.25 \times 10^{+2}$	E50
313	Hg-197m	$8.57 \times 10^{+4}$	$5.64 \times 10^{+2}$	E50	$5.64 \times 10^{+2}$	E50	$5.64 \times 10^{+2}$	E50	$5.64 \times 10^{+2}$	E50
314	Hg-203	$4.03 \times 10^{+6}$	$1.24 \times 10^{+1}$	E50	$1.24 \times 10^{+1}$	E50	$1.24 \times 10^{+1}$	E50	$1.24 \times 10^{+1}$	E50
315	Tl-200	$9.40 \times 10^{+4}$	$1.16 \times 10^{+2}$	E50	$1.16 \times 10^{+2}$	E50	$1.16 \times 10^{+2}$	E50	$1.16 \times 10^{+2}$	E50
316	Tl-201	$2.62 \times 10^{+5}$	$3.80 \times 10^{+2}$	E50	$3.80 \times 10^{+2}$	E50	$3.80 \times 10^{+2}$	E50	$3.80 \times 10^{+2}$	E50
317	Tl-202	$1.06 \times 10^{+6}$	$2.55 \times 10^{+1}$	E50	$2.55 \times 10^{+1}$	E50	$2.55 \times 10^{+1}$	E50	$2.55 \times 10^{+1}$	E50
318	Tl-204	$1.19 \times 10^{+8}$	$2.06 \times 10^{+1}$	Hskin99	$2.06 \times 10^{+1}$	Hskin99	$2.06 \times 10^{+1}$	Hskin99	$2.06 \times 10^{+1}$	Hskin99
319	Pb-201	$3.36 \times 10^{+4}$	$4.40 \times 10^{+2}$	E50	$4.40 \times 10^{+2}$	E50	$4.40 \times 10^{+2}$	E50	$4.40 \times 10^{+2}$	E50
320	Pb-202+	$1.66 \times 10^{+12}$	$1.22 \times 10^{+0}$	E50	$1.22 \times 10^{+0}$	E50	$1.22 \times 10^{+0}$	E50	$1.22 \times 10^{+0}$	E50
321	Pb-203	$1.87 \times 10^{+5}$	$1.96 \times 10^{+2}$	E50	$1.96 \times 10^{+2}$	E50	$1.96 \times 10^{+2}$	E50	$1.96 \times 10^{+2}$	E50
322	Pb-205	$4.83 \times 10^{+14}$	$9.13 \times 10^{+1}$	E50	$9.13 \times 10^{+1}$	E50	$9.14 \times 10^{+1}$	E50	$9.06 \times 10^{+1}$	E50
323	Pb-210+	$7.01 \times 10^{+8}$	2.24×10^{-1}	E50	2.24×10^{-1}	E50	2.21×10^{-1}	E50	1.08×10^{-1}	E50
324	Pb-212+	$3.83 \times 10^{+4}$	$2.73 \times 10^{+2}$	E50	$1.23 \times 10^{+1}$	Hskin99	$2.73 \times 10^{+2}$	E50	$2.68 \times 10^{+2}$	E50
325	Bi-205	$1.32 \times 10^{+6}$	$7.06 \times 10^{+0}$	E50	$7.06 \times 10^{+0}$	E50	$7.06 \times 10^{+0}$	E50	$7.06 \times 10^{+0}$	E50
326	Bi-206	$5.39 \times 10^{+5}$	$8.19 \times 10^{+0}$	E50	$8.19 \times 10^{+0}$	E50	$8.19 \times 10^{+0}$	E50	$8.19 \times 10^{+0}$	E50
327	Bi-207	$1.04 \times 10^{+9}$	4.74×10^{-1}	E50	4.74×10^{-1}	E50	4.74×10^{-1}	E50	4.74×10^{-1}	E50
328	Bi-210+	$4.33 \times 10^{+5}$	$2.03 \times 10^{+1}$	E50	$2.03 \times 10^{+1}$	E50	$1.93 \times 10^{+1}$	E50	$4.60 \times 10^{+0}$	E50
329	Bi-210m+	$9.59 \times 10^{+13}$	$1.38 \times 10^{+0}$	E50	$1.38 \times 10^{+0}$	E50	$1.29 \times 10^{+0}$	E50	$1.26 \times 10^{+0}$	E50
330	Bi-212+	$3.63 \times 10^{+3}$	$3.62 \times 10^{+3}$	E50	$1.30 \times 10^{+2}$	Hskin99	$3.62 \times 10^{+3}$	E50	$3.62 \times 10^{+3}$	E50
331	Po-203	$2.20 \times 10^{+3}$	$1.54 \times 10^{+3}$	E50	$1.54 \times 10^{+3}$	E50	$1.54 \times 10^{+3}$	E50	$1.54 \times 10^{+3}$	E50
332	Po-205	$5.98 \times 10^{+3}$	$7.68 \times 10^{+2}$	E50	$7.68 \times 10^{+2}$	E50	$7.68 \times 10^{+2}$	E50	$7.68 \times 10^{+2}$	E50
333	Po-207	$2.09 \times 10^{+4}$	$5.17 \times 10^{+2}$	E50	$5.17 \times 10^{+2}$	E50	$5.17 \times 10^{+2}$	E50	$5.17 \times 10^{+2}$	E50
334	Po-209	$3.22 \times 10^{+9}$	6.17×10^{-1}	E50	6.17×10^{-1}	E50	5.87×10^{-1}	E50	1.28×10^{-1}	E50
335	Po-210	$1.20 \times 10^{+7}$	$1.33 \times 10^{+0}$	E50	$1.33 \times 10^{+0}$	E50	$1.26 \times 10^{+0}$	E50	2.96×10^{-1}	E50
336	At-211+	$2.60 \times 10^{+4}$	$2.97 \times 10^{+3}$	E50	$5.76 \times 10^{+1}$	Hskin99	$2.99 \times 10^{+3}$	E50	$2.97 \times 10^{+3}$	E50
337	Ra-223+	$9.88 \times 10^{+5}$	$8.88 \times 10^{+0}$	E50	8.41×10^{-1}	Hskin99	$8.45 \times 10^{+0}$	E50	$7.91 \times 10^{+0}$	E50
338	Ra-224+	$3.16 \times 10^{+5}$	$2.04 \times 10^{+1}$	E50	$1.30 \times 10^{+0}$	Hskin99	$2.00 \times 10^{+1}$	E50	$1.95 \times 10^{+1}$	E50
339	Ra-225	$1.29 \times 10^{+6}$	$5.44 \times 10^{+0}$	E50	2.55×10^{-1}	Hskin99	$5.10 \times 10^{+0}$	E50	$4.72 \times 10^{+0}$	E50

(Continued.)

Table A1. (Continued.)

Nr.	Nuclide	Half-life (s)	SCL Reference (Bq cm^{-2})	Percentile Reference	SCL With α-skin (Bq cm^{-2})	Percentile With α-skin	SCL AMAD = 1 μm (Bq cm^{-2})	Percentile AMAD = 1 μm	SCL Public (Bq cm^{-2})	Percentile Public
340	Ra-226+	$5.05 \times 10^{+10}$	1.17×10^{-1}	E50	3.36×10^{-2}	Hskin99	1.15×10^{-1}	E50	7.19×10^{-2}	E50
341	Ra-227	$2.53 \times 10^{+3}$	$4.09 \times 10^{+3}$	E50	$3.11 \times 10^{+3}$	E50	$4.36 \times 10^{+3}$	E50	$4.32 \times 10^{+3}$	E50
342	Ra-228+	$1.81 \times 10^{+8}$	1.32×10^{-1}	E50	3.61×10^{-2}	Hskin99	1.24×10^{-1}	E50	1.10×10^{-1}	E50
343	Ac-224+	$1.00 \times 10^{+4}$	$5.74 \times 10^{+2}$	E50	$3.85 \times 10^{+1}$	Hskin99	$5.65 \times 10^{+2}$	E50	$5.53 \times 10^{+2}$	E50
344	Ac-225+	$8.64 \times 10^{+5}$	$1.76 \times 10^{+1}$	E50	3.78×10^{-1}	Hskin99	$1.64 \times 10^{+1}$	E50	$1.59 \times 10^{+1}$	E50
345	Ac-227+	$6.87 \times 10^{+8}$	2.01×10^{-2}	E95	1.91×10^{-2}	E50	2.31×10^{-2}	E95	2.26×10^{-2}	E95
346	Ac-228	$2.21 \times 10^{+4}$	$2.65 \times 10^{+2}$	E50	$6.06 \times 10^{+1}$	Hskin99	$2.43 \times 10^{+2}$	E50	$2.37 \times 10^{+2}$	E50
347	Th-226+	$1.83 \times 10^{+3}$	$3.05 \times 10^{+4}$	E50	$3.24 \times 10^{+2}$	Hskin99	$3.05 \times 10^{+4}$	E50	$1.67 \times 10^{+4}$	E50
348	Th-227	$1.61 \times 10^{+6}$	$3.80 \times 10^{+0}$	E50	5.20×10^{-1}	Hskin99	$3.54 \times 10^{+0}$	E50	$3.39 \times 10^{+0}$	E50
349	Th-228+	$6.03 \times 10^{+7}$	2.68×10^{-1}	E50	2.50×10^{-2}	Hskin99	2.39×10^{-1}	E50	2.31×10^{-1}	E50
350	Th-229+	$2.32 \times 10^{+11}$	1.20×10^{-1}	E50	1.63×10^{-2}	Hskin99	1.02×10^{-1}	E50	4.91×10^{-2}	E95
351	Th-230	$2.38 \times 10^{+12}$	3.36×10^{-1}	E50	2.59×10^{-1}	E50	2.84×10^{-1}	E50	1.25×10^{-1}	E95
352	Th-231	$9.19 \times 10^{+4}$	$1.01 \times 10^{+3}$	E50	$1.01 \times 10^{+3}$	E50	$1.01 \times 10^{+3}$	E50	$1.01 \times 10^{+3}$	E50
353	Th-232+	$4.43 \times 10^{+17}$	7.92×10^{-2}	E50	2.09×10^{-2}	Hskin99	7.15×10^{-2}	E50	5.54×10^{-2}	E50
354	Th-234+	$2.08 \times 10^{+6}$	$6.52 \times 10^{+1}$	E50	$6.52 \times 10^{+1}$	E50	$6.50 \times 10^{+1}$	E50	$6.50 \times 10^{+1}$	E50
355	Pa-230+	$1.50 \times 10^{+6}$	$9.74 \times 10^{+0}$	E50	$4.24 \times 10^{+0}$	E50	$9.46 \times 10^{+0}$	E50	$9.17 \times 10^{+0}$	E50
356	Pa-231	$1.03 \times 10^{+12}$	1.78×10^{-2}	E95	1.67×10^{-2}	E50	1.89×10^{-2}	E95	1.84×10^{-2}	E95
357	Pa-233	$2.33 \times 10^{+6}$	$1.81 \times 10^{+1}$	E50	$1.81 \times 10^{+1}$	E50	$1.81 \times 10^{+1}$	E50	$1.81 \times 10^{+1}$	E50
358	U-230+	$1.80 \times 10^{+6}$	$5.81 \times 10^{+0}$	E50	3.46×10^{-1}	Hskin99	$5.23 \times 10^{+0}$	E50	$4.37 \times 10^{+0}$	E50
359	U-231	$3.63 \times 10^{+5}$	$1.50 \times 10^{+2}$	E50	$1.49 \times 10^{+2}$	E50	$1.50 \times 10^{+2}$	E50	$1.50 \times 10^{+2}$	E50
360	U-232+	$2.17 \times 10^{+9}$	1.39×10^{-1}	E50	2.32×10^{-2}	Hskin99	1.24×10^{-1}	E50	1.21×10^{-1}	E50
361	U-233	$5.02 \times 10^{+12}$	$1.40 \times 10^{+0}$	E50	8.81×10^{-1}	E50	$1.22 \times 10^{+0}$	E95	$1.01 \times 10^{+0}$	E95
362	U-234	$7.75 \times 10^{+12}$	$1.56 \times 10^{+0}$	E50	$1.56 \times 10^{+0}$	E50	$1.40 \times 10^{+0}$	E95	$1.27 \times 10^{+0}$	E95
363	U-235+	$2.22 \times 10^{+16}$	7.85×10^{-1}	E50	7.71×10^{-1}	E50	7.45×10^{-1}	E50	7.22×10^{-1}	E50
364	U-236	$7.39 \times 10^{+14}$	$1.68 \times 10^{+0}$	E50	$1.68 \times 10^{+0}$	E50	$1.50 \times 10^{+0}$	E50	$1.38 \times 10^{+0}$	E95
365	U-237	$5.83 \times 10^{+5}$	$8.18 \times 10^{+1}$	E50	$8.18 \times 10^{+1}$	E50	$8.17 \times 10^{+1}$	E50	$8.18 \times 10^{+1}$	E50
366	U-238+	$1.41 \times 10^{+17}$	$1.42 \times 10^{+0}$	E50	$1.42 \times 10^{+0}$	E50	$1.29 \times 10^{+0}$	E50	$1.23 \times 10^{+0}$	E50

(Continued.)

Table A1. (Continued.)

Nr.	Nuclide	Half-life (s)	SCL Reference (Bq cm^{-2})	Percentile Reference	SCL With α-skin (Bq cm^{-2})	Percentile With α-skin	SCL AMAD = 1 μm (Bq cm^{-2})	Percentile AMAD = 1 μm	SCL Public (Bq cm^{-2})	Percentile Public
367	U-239	$1.41 \times 10^{+3}$	$2.20 \times 10^{+4}$	E50	$2.20 \times 10^{+4}$	E50	$2.20 \times 10^{+4}$	E50	$2.20 \times 10^{+4}$	E50
368	U-240+	$5.08 \times 10^{+4}$	$5.80 \times 10^{+2}$	E50	$5.80 \times 10^{+2}$	E50	$5.80 \times 10^{+2}$	E50	$5.78 \times 10^{+2}$	E50
369	Np-235+	$3.42 \times 10^{+7}$	$1.91 \times 10^{+1}$	E50	$1.91 \times 10^{+1}$	E50	$1.91 \times 10^{+1}$	E50	$1.91 \times 10^{+1}$	E50
370	Np-236m	$8.10 \times 10^{+4}$	$5.28 \times 10^{+2}$	E50	$3.97 \times 10^{+2}$	E50	$4.76 \times 10^{+2}$	E50	$3.55 \times 10^{+2}$	E50
371	Np-236+	$4.86 \times 10^{+12}$	6.24×10^{-1}	E50	2.50×10^{-1}	E50	5.71×10^{-1}	E50	4.77×10^{-1}	E50
372	Np-237+	$6.77 \times 10^{+13}$	4.64×10^{-1}	E50	4.64×10^{-1}	E50	4.14×10^{-1}	E50	2.48×10^{-1}	E95
373	Np-239	$2.04 \times 10^{+5}$	$2.06 \times 10^{+2}$	E50	$2.06 \times 10^{+2}$	E50	$2.06 \times 10^{+2}$	E50	$2.06 \times 10^{+2}$	E50
374	Np-240	$3.71 \times 10^{+3}$	$3.06 \times 10^{+3}$	E50	$3.06 \times 10^{+3}$	E50	$3.05 \times 10^{+3}$	E50	$3.05 \times 10^{+3}$	E50
375	Pu-234	$3.17 \times 10^{+4}$	$3.43 \times 10^{+2}$	E50	$1.97 \times 10^{+2}$	E50	$3.38 \times 10^{+2}$	E50	$3.32 \times 10^{+2}$	E50
376	Pu-235	$1.52 \times 10^{+3}$	$4.42 \times 10^{+4}$	E50	$4.42 \times 10^{+4}$	E50	$4.42 \times 10^{+4}$	E50	$4.42 \times 10^{+4}$	E50
377	Pu-236	$9.02 \times 10^{+7}$	7.46×10^{-1}	E50	3.85×10^{-1}	E50	6.31×10^{-1}	E95	3.22×10^{-1}	E95
378	Pu-237	$3.91 \times 10^{+6}$	$3.04 \times 10^{+1}$	E50	$3.04 \times 10^{+1}$	E50	$3.03 \times 10^{+1}$	E50	$3.03 \times 10^{+1}$	E50
379	Pu-238	$2.77 \times 10^{+9}$	3.54×10^{-1}	E50	3.54×10^{-1}	E50	2.81×10^{-1}	E95	1.16×10^{-1}	E95
380	Pu-239+	$7.61 \times 10^{+11}$	3.30×10^{-1}	E50	3.30×10^{-1}	E50	2.56×10^{-1}	E95	1.06×10^{-1}	E95
381	Pu-240	$2.07 \times 10^{+11}$	3.28×10^{-1}	E50	3.28×10^{-1}	E50	2.56×10^{-1}	E95	1.06×10^{-1}	E95
382	Pu-241+	$4.53 \times 10^{+8}$	$7.49 \times 10^{+0}$	E50	$7.49 \times 10^{+0}$	E50	$6.03 \times 10^{+0}$	E95	$2.49 \times 10^{+0}$	E95
383	Pu-242	$1.18 \times 10^{+13}$	3.41×10^{-1}	E50	3.41×10^{-1}	E50	2.73×10^{-1}	E95	1.16×10^{-1}	E95
384	Pu-243	$1.78 \times 10^{+4}$	$1.04 \times 10^{+4}$	E50	$1.04 \times 10^{+4}$	E50	$1.04 \times 10^{+4}$	E50	$1.03 \times 10^{+4}$	E50
385	Pu-244+	$2.52 \times 10^{+15}$	2.69×10^{-1}	E50	2.69×10^{-1}	E50	2.30×10^{-1}	E50	1.13×10^{-1}	E95
386	Am-238	$5.88 \times 10^{+3}$	$2.37 \times 10^{+3}$	E50	$2.37 \times 10^{+3}$	E50	$2.34 \times 10^{+3}$	E50	$2.23 \times 10^{+3}$	E50
387	Am-241	$1.36 \times 10^{+10}$	3.78×10^{-1}	E50	3.78×10^{-1}	E50	3.08×10^{-1}	E95	1.32×10^{-1}	E95
388	Am-242	$5.77 \times 10^{+4}$	$6.90 \times 10^{+2}$	E50	$6.83 \times 10^{+2}$	E50	$6.17 \times 10^{+2}$	E50	$5.36 \times 10^{+2}$	E50
389	Am-242m+	$4.45 \times 10^{+9}$	2.71×10^{-1}	E50	2.71×10^{-1}	E50	2.23×10^{-1}	E95	9.44×10^{-2}	E95
390	Am-243+	$2.33 \times 10^{+11}$	3.12×10^{-1}	E50	3.12×10^{-1}	E50	2.68×10^{-1}	E50	1.31×10^{-1}	E95
391	Cm-240	$2.33 \times 10^{+6}$	$1.14 \times 10^{+1}$	E50	$6.51 \times 10^{+0}$	E50	$9.85 \times 10^{+0}$	E50	$6.37 \times 10^{+0}$	E95
392	Cm-241	$2.83 \times 10^{+6}$	$7.26 \times 10^{+0}$	E50	$7.26 \times 10^{+0}$	E50	$7.22 \times 10^{+0}$	E50	$7.09 \times 10^{+0}$	E50
393	Cm-242	$1.41 \times 10^{+7}$	$5.36 \times 10^{+0}$	E95	$5.35 \times 10^{+0}$	E95	$4.17 \times 10^{+0}$	E95	$3.17 \times 10^{+0}$	E95
394	Cm-243	$9.18 \times 10^{+8}$	4.50×10^{-1}	E50	4.50×10^{-1}	E50	3.84×10^{-1}	E50	1.84×10^{-1}	E95
395	Cm-244	$5.71 \times 10^{+8}$	6.53×10^{-1}	E50	6.53×10^{-1}	E50	4.91×10^{-1}	E95	2.26×10^{-1}	E95
396	Cm-245	$2.68 \times 10^{+11}$	3.07×10^{-1}	E50	3.07×10^{-1}	E50	2.56×10^{-1}	E50	1.12×10^{-1}	E95
397	Cm-246	$1.50 \times 10^{+11}$	3.90×10^{-1}	E50	3.90×10^{-1}	E50	3.01×10^{-1}	E95	1.30×10^{-1}	E95
398	Cm-247+	$4.92 \times 10^{+14}$	3.28×10^{-1}	E50	3.28×10^{-1}	E50	2.83×10^{-1}	E50	1.38×10^{-1}	E95
399	Cm-248	$1.10 \times 10^{+13}$	7.28×10^{-2}	E50	7.28×10^{-2}	E50	6.38×10^{-2}	E50	3.46×10^{-2}	E95

(Continued.)

Table A1. (Continued.)

Nr.	Nuclide	Half-life (s)	SCL Reference (Bq cm^{-2})	Percentile Reference	SCL With α-skin (Bq cm^{-2})	Percentile With α-skin	SCL AMAD = 1 μm (Bq cm^{-2})	Percentile AMAD = 1 μm	SCL Public (Bq cm^{-2})	Percentile Public
400	Bk-247	$4.35 \times 10^{+10}$	2.17×10^{-1}	E50	2.17×10^{-1}	E50	1.82×10^{-1}	E50	1.72×10^{-1}	E95
401	Bk-249+	$2.85 \times 10^{+7}$	$4.32 \times 10^{+1}$	E50	$4.32 \times 10^{+1}$	E50	$3.64 \times 10^{+1}$	E50	$3.53 \times 10^{+1}$	E50
402	Cf-246	$1.29 \times 10^{+5}$	$2.90 \times 10^{+2}$	E50	$2.68 \times 10^{+1}$	Hskin99	$2.53 \times 10^{+2}$	E50	$2.14 \times 10^{+2}$	E95
403	Cf-248	$2.89 \times 10^{+7}$	$2.26 \times 10^{+0}$	E95	$1.80 \times 10^{+0}$	E50	$1.70 \times 10^{+0}$	E95	$1.36 \times 10^{+0}$	E95
404	Cf-249	$1.11 \times 10^{+10}$	2.04×10^{-1}	E50	2.03×10^{-1}	E50	1.71×10^{-1}	E50	1.66×10^{-1}	E50
405	Cf-250	$4.13 \times 10^{+8}$	4.99×10^{-1}	E50	4.99×10^{-1}	E50	3.85×10^{-1}	E95	3.63×10^{-1}	E95
406	Cf-251	$2.84 \times 10^{+10}$	2.11×10^{-1}	E50	2.11×10^{-1}	E50	1.76×10^{-1}	E50	1.69×10^{-1}	E95
407	Cf-252	$8.35 \times 10^{+7}$	4.87×10^{-1}	E50	4.84×10^{-1}	E50	4.43×10^{-1}	E50	4.28×10^{-1}	E50
408	Cf-253+	$1.54 \times 10^{+6}$	$3.06 \times 10^{+1}$	E50	$3.50 \times 10^{+0}$	Hskin99	$2.77 \times 10^{+1}$	E50	$2.66 \times 10^{+1}$	E50
409	Cf-254	$5.23 \times 10^{+6}$	9.68×10^{-3}	E50	9.68×10^{-3}	E50	9.61×10^{-3}	E50	9.59×10^{-3}	E50
410	Es-253	$1.77 \times 10^{+6}$	$4.46 \times 10^{+1}$	E50	$3.07 \times 10^{+0}$	Hskin99	$3.73 \times 10^{+1}$	E95	$3.47 \times 10^{+1}$	E95
411	Es-254+	$2.38 \times 10^{+7}$	6.32×10^{-1}	E50	4.65×10^{-1}	E50	5.93×10^{-1}	E50	5.83×10^{-1}	E50
412	Es-254m+	$1.41 \times 10^{+5}$	$9.08 \times 10^{+1}$	E50	$9.07 \times 10^{+0}$	Hskin99	$8.70 \times 10^{+1}$	E50	$8.62 \times 10^{+1}$	E50
413	Fm-254	$1.17 \times 10^{+4}$	$7.02 \times 10^{+3}$	E50	$1.07 \times 10^{+2}$	Hskin99	$6.10 \times 10^{+3}$	E50	$5.92 \times 10^{+3}$	E50

Table A2. List of progeny radionuclides that are *fully* accounted for in the surface-specific clearance level of the parent radionuclide in table A.1. These progeny radionuclides should not be taken into account when applying the 'sum of weights' rule for (decisions on) clearance (see section 2.4 for details).

Parent radionuclide	Progeny radionuclides										
	1	2	3	4	5	6	7	8	9	10	11
Mg-28	Al-28										
Sc-44m	Sc-44										
Ti-44	Sc-44										
Fe-52	Mn-52m										
Fe-60	Co-60m	Co-60									
Zn-69m	Zn-69										
Ge-68	Ga-68										
Rb-81	Kr-81m										
Rb-83	Kr-83m										
Sr-82	Rb-82										
Sr-90	Y-90										
Sr-91	Y-91m										
Y-87	Sr-87m										
Zr-95	Nb-95m										
Zr-97	Nb-97										
Mo-99	Tc-99m										
Mo-101	Tc-101										
Tc-95m	Tc-95										
Ru-103	Rh-103m										
Ru-106	Rh-106										
Pd-103	Rh-103m										
Pd-109	Ag-109m										
Ag-108m	Ag-108										
Ag-110m	Ag-110										
Cd-104	Ag-104m										
Cd-109	Ag-109m										
Cd-113m	In-113m										
Cd-115	In-115m										
Cd-115m	In-115m										
In-111	Cd-111m										
In-114m	In-114										
Sn-113	In-113m										
Sn-121m	Sn-121										

(Continued.)

Table A2. (Continued.)

Parent radionuclide	Progeny radionuclides										
	1	2	3	4	5	6	7	8	9	10	11
Sn-126	Sb-126m	Sb-126									
Sb-125	Te-125m										
Te-127m	Te-127										
Te-129m	Te-129										
Te-131m	Te-131										
Te-132	I-132										
Te-133m	Te-133										
I-135	Xe-135m										
Cs-137	Ba-137m										
Ce-144	Pr-144	Pr-144m									
Gd-146	Eu-146										
Lu-177m	Lu-177										
Hf-172	Lu-172m	Lu-172									
Hf-182	Ta-182										
W-178	Ta-178										
W-188	Re-188										
Re-189	Os-189m										
Os-194	Ir-194										
Ir-189	Os-189m										
Hg-194	Au-194										
Hg-195m	Hg-195										
Pb-202	Tl-202										
Pb-210	Hg-206	Bi-210	Tl-206	Po-210							
Pb-212	Bi-212	Tl-208	Po-212								
Bi-210m	Tl-206										
Bi-210	Tl-206										
Bi-212	Tl-208	Po-212									
At-211	Po-211										
Ra-223	Pb-211	Bi-211	Tl-207	Po-211	Po-215	Rn-219					
Ra-224	Rn-220	Pb-212	Bi-212	Tl-208	Po-212	Po-216					
Ra-226	Rn-222	Po-218	Pb-214	Bi-214	Tl-210	Po-214	At-218	Rn-218			

(Continued.)

Table A2. (Continued.)

Parent radionuclide	Progeny radionuclides										
	1	2	3	4	5	6	7	8	9	10	11
Ra-228	Ac-228										
Ac-224	Fr-220										
Ac-225	Fr-221	Bi-213	Tl-209	Pb-209	Po-213	At-217	Rn-217				
Ac-227	Fr-223	Th-227	Ra-223	At-219	Pb-211	Bi-211	Tl-207	Bi-215	Po-211	Po-215	Rn-219
Th-226	Ra-222	Po-214	Rn-218								
Th-228	Ra-224	Rn-220	Pb-212	Bi-212	Tl-208	Po-212	Po-216				
Th-229	Ra-225	Ac-225	Fr-221	Bi-213	Tl-209	Pb-209	Po-213	At-217			
Th-232	Ra-228	Ac-228	Th-228	Ra-224	Rn-220	Pb-212	Bi-212	Tl-208	Po-212	Po-216	
Th-234	Pa-234m	Pa-234									
Pa-230	Ac-226	Fr-222									
U-230	Th-226	Ra-222	Po-214	Rn-218							
U-232	Th-228	Ra-224	Rn-220	Pb-212	Bi-212	Tl-208	Po-212	Po-216			
U-235	Th-231										
U-238	Th-234	Pa-234m	Pa-234								
U-240	Np-240m	Np-240									
Np-235	U-235m										
Np-236	Pa-232	Pu-236									
Np-237	Pa-233										
Pu-239	U-235m										
Pu-241	U-237										
Pu-244	U-240	Np-240m	Np-240								
Am-242m	Np-238	Am-242	Cm-242								
Am-243	Np-239										
Cm-247	Pu-243										
Bk-249	Am-245										
Cf-253	Cm-249										
Es-254	Bk-250	Fm-254									
Es-254m	Bk-250	Fm-254									

Appendix B. Summary of equations in the SUDOQU methodology

This appendix briefly describes and summarises the equations of the SUDOQU methodology used for the calculations in this report. A more detailed description of the methodology can be found in van Dillen and van Dijk (2018).

An object with a well-defined solid surface is contaminated with radionuclide i over a surface area A_{cont} (cm^2) and is used in an *indoor environment* for a total duration of $\Delta T_{\text{use}} = f_{\text{use}} \Delta T_{\text{tot}}$ (h) within a scenario-integration time ΔT_{tot} (8760 h, i.e. one year). Here, the fraction f_{use} (dimensionless fraction between 0 and 1) is called the so-called duty factor.

The indoor environment is a room of area A_{floor} (cm^2) and height H (cm) ventilated at an air-exchange rate λ_v (h^{-1}), i.e. with a volumetric ventilation rate $\kappa_v = \lambda_v V$ ($\text{cm}^3\ \text{h}^{-1}$), where $V = A_{\text{floor}} H$ (cm^3) is the volume of the room. Airborne activity due to resuspension (see below) from the object's surface is not only removed by ventilation, but also by deposition at a velocity of $v_{d,i}$ (cm h^{-1}), leading to a deposition loss rate of $\lambda_{d,i} = v_{d,i}/H$ (h^{-1}).

At the start of object use, at $t = 0$, the total surface-contamination level for radionuclide i is given by $C_{0,i}$ (Bq cm^{-2}), comprising of a (fully) removable component $f_{\text{rem},i} C_{0,i}$ (that can be removed by resuspension and wipe-off) and a fixed component $(1 - f_{\text{rem},i}) C_{0,i}$. Here, $f_{\text{rem}.i}$ is called the (initial) removable fraction, a dimensionless quantity with values between 0 and 1. The surface-contamination level is assumed to be and remain homogeneous/uniform over the area of contamination A_{cont}.

During object use, resuspension occurs at an average rate $\bar{\xi}_{\text{use},i}$ (h^{-1}), which defines the fraction of *removable* activity that becomes airborne per unit time. At the same time, removable activity is wiped off the object's surface, also leading to a decrease of the removable surface-contamination level. The average wipe-off loss rate during use is given by

$$\bar{\lambda}_{\text{wo,use},i} = \bar{f}_{\text{oth},i} \bar{\phi}_{\text{use}} \frac{A_{\text{hands}}}{A_{\text{cont}}}, \tag{B.1}$$

where $\bar{f}_{\text{oth},i}$ is the average transfer efficiency (ratio of the surface-contamination level of the hands after a single wipe-off event to the removable surface-contamination level of the object prior to this event: $C_{\text{surf,hands},i}/C_{\text{surf,rem},i}$), $\bar{\phi}_{\text{use}}$ (h^{-1}) is the average frequency or rate of wipe-off events and A_{hands} (cm^2) is the skin area of the hands contaminated during the contamination-transfer process from using and thus touching the object.

Following this description, the time-dependence of the removable, fixed and total surface-contamination levels (Bq cm^{-2}) are described by

$$C_{\text{surf,rem},i}(t) = \frac{f_{\text{rem},i} C_{0,i}}{\lambda_i^*} \left((\lambda_{1,i} - d_i) \exp[-\lambda_{1,i} t] + (d_i - \lambda_{2,i}) \exp[-\lambda_{2,i} t] \right), \tag{B.2}$$

$$C_{\text{surf,fix},i}(t) = (1 - f_{\text{rem},i}) C_{0,i} \exp[-\lambda_{r,i} \delta t], \tag{B.3}$$

and

$$C_{\text{surf,tot},i}(t) = C_{\text{surf,rem},i}(t) + C_{\text{surf,fix},i}(t), \tag{B.4}$$

respectively, with $\lambda_{r,i}$ (h^{-1}) the physical decay constant of radionuclide i. Parameter δ is a switch for enabling (value of 1) or disabling (value of 0) physical decay and other contamination removal processes. In equations (B.2–B.4), the following constants are defined:

$$a_i = \lambda_{\text{surf},i} \delta,\ b_i = \lambda_{d,i} H \delta,\ c_i = \frac{f_{\text{use}} \bar{\xi}_{\text{use},i} A_{\text{cont}}}{V}, \text{ and } d_i = \lambda_v + (\lambda_{r,i} + \lambda_{d,i}) \delta, \tag{B.5}$$

(h^{-1}, cm h^{-1}, $\text{cm}^{-1}\ \text{h}^{-1}$ and h^{-1}, respectively) with the surface loss-rate constant $\lambda_{\text{surf},i}$ (h^{-1}) defined as

$$\lambda_{\text{surf},i} = \lambda_{r,i} + f_{\text{use}} \left(\bar{\xi}_{\text{use},i} + \bar{\lambda}_{\text{wo,use},i} \right). \tag{B.6}$$

Furthermore, the characteristic loss-rate constants $\lambda_{1,i}$ and $\lambda_{2,i}$ are given by

$$\lambda_{1,i} = \frac{1}{2} \left((a_i + d_i) + \lambda_i^* \right) \quad \text{and} \quad \lambda_{2,i} = \frac{1}{2} \left((a_i + d_i) - \lambda_i^* \right), \tag{B.7}$$

with

$$\lambda_i^* = \lambda_{1,i} - \lambda_{2,i} \equiv \sqrt{4 b_i c_i + (a_i - d_i)^2}. \tag{B.8}$$

In SUDOQU, fixed and removable components of the surface-contamination level are treated separately, without interaction between them. This means that, with time, fixed contamination does not become removable nor vice versa.

Using these constants, the air-activity concentration (Bq m^{-3}) from removable surface contamination reads

$$C_{\mathrm{air},i}(t) = f_{\mathrm{rem},i}\frac{c_i C_{0,i}}{\lambda_i^*}\left(\exp\left[-\lambda_{2,i}t\right] - \exp\left[-\lambda_{1,i}t\right]\right)\cdot 10^6, \tag{B.9}$$

where factor 10^6 converts cm^{-3} to m^{-3}. Here, $C_{\mathrm{air},i}(t)$ is not the air concentration during actual product use at time t, but is the continuously-experienced air-activity concentration as if object use and exposure are spread out over the entire duration ΔT_{tot} of the scenario.

The time-integrated counterparts of equations (B.2–B4, B9) are given by:

$$\mathrm{TISC}_{\mathrm{use,rem},i}(t) \equiv f_{\mathrm{use}}\cdot\int_0^t C_{\mathrm{surf,rem},i}(t')\mathrm{d}t'$$
$$= f_{\mathrm{use}} f_{\mathrm{rem},i}\frac{C_{0,i}\cdot t}{\lambda_i^*}\left(\left(\lambda_{1,i}-d_i\right)\Psi\left(\lambda_{1,i}t\right) + \left(d_i-\lambda_{2,i}\right)\Psi\left(\lambda_{2,i}t\right)\right), \tag{B.10}$$

$$\mathrm{TISC}_{\mathrm{use,fix},i}(t) \equiv f_{\mathrm{use}}\cdot\int_0^t C_{\mathrm{surf,fix},i}(t')\mathrm{d}t' = f_{\mathrm{use}}\left(1-f_{\mathrm{rem},i}\right)C_{0,i}\Psi\left(\lambda_{r,i}\delta t\right)\cdot t, \tag{B.11}$$

$$\mathrm{TISC}_{\mathrm{use,tot},i}(t) = \mathrm{TISC}_{\mathrm{use,rem},i}(t) + \mathrm{TISC}_{\mathrm{use,fix},i}(t), \tag{B.12}$$

(all in Bq h cm^{-2}) for surface contamination and

$$\mathrm{TIAC}_{\mathrm{use},i}(t) \equiv \int_0^t C_{\mathrm{air},i}(t')\mathrm{d}t' = f_{\mathrm{rem},i}\frac{c_i C_{0,i}\cdot t}{\lambda_i^*}\left(\Psi\left(\lambda_{2,i}t\right) - \Psi\left(\lambda_{1,i}t\right)\right)\cdot 10^6 \tag{B.13}$$

(Bq h m^{-3}) for air contamination, with dimensionless removal function Ψ defined by $\Psi(x) = (1-\exp[-x])/x$ for $x > 0$ and $\Psi(0) = 1$. These time-integrated contamination levels are input for subsequent calculations of individual effective-dose contributions (all in μSv) from various exposure pathways and of the local skin-equivalent dose from transfer of contamination and direct contact with the object (also in μSv).

B.1. Exposure to external radiation from the object's contaminated surface

The effective dose from external gamma (and neutron) radiation from the contamination residing on the surface of the object is given by

$$E_{\mathrm{ext},i}(t) = g(\mathbf{D};L)\,h_p(10)_i f_{\mathrm{conv},i} f_{\mathrm{att},i}\mathrm{TISC}_{\mathrm{use,tot},i}(t)\cdot 10^{10}, \tag{B.14}$$

where $h_p(10)_i$ is the radionuclide's personal dose-equivalent-rate constant (Sv h^{-1} m^2 Bq^{-1}), $f_{\mathrm{conv},i}$ is the conversion factor from personal dose equivalent to effective dose (depending on exposure geometry), $f_{\mathrm{att},i}$ is the attenuation factor (in the case of a shielding material between source and receptor) and $g(\mathbf{D};L)$ is a dimensionless, geometrical factor depending on the dimensions $\mathbf{D}$ of the object and its distance L (cm) to the receptor. For a disc-shaped contamination of radius R (cm) we use

$$g_{\mathrm{disc}}(R;L) = \pi\ln\left[1+\left(\frac{R}{L}\right)^2\right] = \pi\ln\left[1+\frac{A_{\mathrm{cont}}}{\pi L^2}\right], \tag{B.15}$$

where $A_{\mathrm{cont}} = \pi R^2$.

B.2. Internal exposure from inhalation of resuspended activity

The committed effective dose resulting from the inhalation of activity that has become airborne by resuspension is given by

$$E_{\mathrm{inh},i}(t) = \mathrm{DC}_{\mathrm{inh},i} f_{\mathrm{resp},i}\mathrm{cor}_{\mathrm{air},i} I\cdot\mathrm{TIAC}_{\mathrm{use},i}(t)\cdot 10^6, \tag{B.16}$$

where $\mathrm{DC}_{\mathrm{inh},i}$ (Sv Bq^{-1}) is the effective inhalation dose coefficient, $f_{\mathrm{resp},i}$ is the respirable fraction of airborne activity, $\mathrm{cor}_{\mathrm{air},i}$ is a dimensionless correction factor taking account of inhomogeneities of the room's air concentration and I is the individual's breathing rate (m^3 h^{-1}).

B.3. Internal exposure from inadvertent, secondary ingestion of activity (hands-to-mouth)

The committed effective dose resulting from the inadvertent, secondary ingestion of activity transferred to the hands reads

$$E_{\mathrm{ing},i}(t) = \mathrm{DC}_{\mathrm{ing},i} \bar{f}_{\mathrm{oth},i} F_{\mathrm{htm},i} f_{\mathrm{ing}} m_{\mathrm{hands},i} A_{\mathrm{hands}} \Phi_{\mathrm{ing}} \cdot \mathrm{TISC}_{\mathrm{use,rem},i}(t) \cdot 10^{6} \tag{B.17}$$

where $\mathrm{DC}_{\mathrm{ing},i}$ (Sv Bq^{-1}) is the effective ingestion dose coefficient, f_{ing} is the fraction of contaminated area of the hands from which ingestion of activity occurs with a hands-to-mouth transfer factor of $F_{\mathrm{htm},i}$ (both dimensionless and per ingestion event), $m_{\mathrm{hands},i}$ is the effective time-multiplication factor of skin contamination of the hands and Φ_{ing}(h^{-1}) is the rate of secondary ingestion events.

B.4. External exposure of the skin from transfer of activity

The effective dose due to skin contamination and exposure of the hands is evaluated as follows

$$E_{\mathrm{skin,hands},i}(t) = \mathrm{DC}_{\mathrm{skin},i} \bar{f}_{\mathrm{oth},i} m_{\mathrm{hands},i} w_{\mathrm{skin}} \frac{A_{\mathrm{hands}}}{A_{\mathrm{skin,total}}} \cdot \mathrm{TISC}_{\mathrm{use,rem},i}(t) \cdot 3.6 \cdot 10^{9}, \tag{B.18}$$

where $\mathrm{DC}_{\mathrm{skin},i}$ is the local skin-equivalent dose-rate coefficient (Sv s^{-1} cm^2 Bq^{-1}), w_{skin} is the tissue-weighting factor of the skin and $A_{\mathrm{skin,total}}$ (cm^2) is the total area of the skin. As discussed in section 5.2 and in van Dillen and van Dijk (2018), we assumed this value to represent the total UVR-exposed skin area of 3000 cm^2. Skin contamination of the face is evaluated similarly by

$$E_{\mathrm{skin,face},i}(t) = \mathrm{DC}_{\mathrm{skin},i} \bar{f}_{\mathrm{htf},i} \bar{f}_{\mathrm{oth},i} m_{\mathrm{face},i} w_{\mathrm{skin}} \frac{A_{\mathrm{face}}}{A_{\mathrm{skin,total}}} \cdot \mathrm{TISC}_{\mathrm{use,rem},i}(t) \cdot 3.6 \cdot 10^{9}. \tag{B.19}$$

Here, $\bar{f}_{\mathrm{htf},i}$ is the average transfer efficiency of activity from the hands to the face, $m_{\mathrm{face},i}$ is the effective time-multiplication factor of skin contamination and exposure of the face and A_{face} (cm^2) is the contaminated skin area of the face.

B.5. External exposure of the skin due to direct contact with the object

Direct contact of the skin with the object can also lead to external exposure of the skin. The corresponding effective dose contribution is evaluated as

$$E_{\mathrm{skin,contact},i}(t) = \mathrm{DC}_{\mathrm{skin},i} m_{\mathrm{skin,contact}} w_{\mathrm{skin}} \frac{A_{\mathrm{skin,contact}}}{A_{\mathrm{skin,total}}} \cdot \mathrm{TISC}_{\mathrm{use,tot},i}(t) \cdot 3.6 \cdot 10^{9}, \tag{B.20}$$

with $m_{\mathrm{skin,contact}}$ the time-multiplication factor for direct-skin-contact exposure ($\leqslant 1$) and $A_{\mathrm{skin,contact}}$ (cm^2) the corresponding skin area.

B.6. Total annual doses

The total *annual* effective dose at $t = \Delta T_{\mathrm{tot}}$ (one year) is evaluated as

$$E_{\mathrm{tot},i}(\Delta T_{\mathrm{tot}}) = \sum_{\mathrm{pathways}} E_{\mathrm{pathway},i}(\Delta T_{\mathrm{tot}}), \tag{B.21}$$

where the sum extends over the aforementioned pathways comprising six contributions, i.e. equations (B.14, B.16–B.20). In the probabilistic study, equation (B.21) is used to generate the annual effective dose distribution.

Since the highest skin-contamination levels are expected to be located on the hands, and since direct contact is also assumed to occur primarily with the hands (or parts of the wrists), the local skin-equivalent dose incurred by an individual in a year is estimated to be

$$H_{\mathrm{skin,tot},i}(\Delta T_{\mathrm{tot}}) = \mathrm{DC}_{\mathrm{skin},i} \cdot \left(\bar{f}_{\mathrm{oth},i} m_{\mathrm{hands},i} \mathrm{TISC}_{\mathrm{use,rem},i}(\Delta T_{\mathrm{tot}}) + m_{\mathrm{skin,contact}} \mathrm{TISC}_{\mathrm{use,tot},i}(\Delta T_{\mathrm{tot}})\right) \cdot 3.6 \cdot 10^{9}, \tag{B.22}$$

where we regard that part of the skin that is both contaminated by transfer of contamination and in direct contact with the object. Equation (B.22) is a conservative estimate in the sense that both contributions in this overlapping skin region (i.e. any 1 cm^2 in this region) are added independently. In the probabilistic study, equation (B.22) is used to generate the local skin-equivalent dose distribution.

Note that the local skin-equivalent dose-rate coefficient $\mathrm{DC}_{\mathrm{skin},i}$ in equation (B.22) as well as in equations (B.18) through (B.20) may depend on the skin site on the body. See section 2.3.4 for more details and for assumptions related to the calculations in this paper.

ORCID iD

Teun van Dillen https://orcid.org/0000-0002-8754-0071

References

Charles M W 2007 Radon exposure of the skin: I. Biological effects *J. Radiol. Prot.* **27** 231–52

Dimitroulopoulou C 2012 Ventilation in European dwellings: a review *Build. Environ.* **47** 109–25

Eatough J P 1997 Alpha-particle dosimetry for the basal layer of the skin and the radon progeny 218-Po and 214-Po *Phys. Med. Biol.* **42** 1899–911

EC 1993 Principles and methods for establishing concentrations and quantities (exemption values) below which reporting is not required in the European Directive *Radiation Protection* 65 (Luxembourg: Commission of the European Communities) (available at: https://ec.europa.eu/energy/sites/ener/files/documents/065.pdf)

EC 1999 Basis for the definition of surface contamination clearance levels for the recycling or reuse of metals arising from the dismantling of nuclear installations, final report *European Commission, Radiation Protection 101* (Luxembourg: Office for official publications of the European Communities) (available at: https://ec.europa.eu/energy/sites/ener/files/documents/101.pdf)

EC 2000 Practical use of the concepts of clearance and exemption—part I: guidance on general clearance levels for practices *European Commission, Radiation Protection 122-I* (Luxembourg: Office for official publications of the European Communities) (available at: https://ec.europa.eu/energy/sites/ener/files/documents/122_part1.pdf)

EC 2014 European Council Directive 2013/59/EURATOM of 5 December 2013 laying down basic safety standards for protection against the dangers arising from exposure to ionising radiation, and repealing directives 89/618/Euratom, 90/641/Euratom, 96/29/Euratom, 97/43/Euratom and 2003/122/Euratom *OJ L 13, 17.1.2014* (L 13/1) (Luxembourg: Official Journal of the European Union) (available at: https://eur-lex.europa.eu/eli/dir/2013/59/oj)

Fairbairn A 1961 The derivation of maximum permissible levels of radioactive surface contamination of transport containers and vehicles, notes on certain aspects of the regulations for the transport of radioactive materials *Safety Series No. 7* (Vienna: International Atomic Energy Agency) p 79

Geiger H and Nuttal J M 1911 The ranges of the α particles from various radioactive substances and a relation between range and period of transformation *Phil. Mag.* **22** 613–21

Hattori T 2008 Reconsideration of the minimum dose constraint for public exposures in radiological protection *Radiat. Prot. Dosim.* **131** 340–5

IAEA 2004 Application of the concepts of exclusion, exemption and clearance *Safety Standards Series No. RS-G-1.7* (Vienna: International Atomic Energy Agency)

IAEA 2005a Radiological aspects of non-fixed contamination of packages and conveyances *IAEA-TECDOC-1449* (Vienna: International Atomic Energy Agency)

IAEA 2005b Derivation of activity concentration values for exclusion, exemption and clearance *Safety Reports Series No. 44* (Vienna: International Atomic Energy Agency)

IAEA 2012 Monitoring for compliance with exemption and clearance levels *Safety Reports Series No. 67* (Vienna: International Atomic Energy Agency)

IAEA 2018 Regulations for the safe transport of radioactive material *Safety Standards Series No. SSR-6 (Rev.1)* (Vienna: International Atomic Energy Agency)

ICRP 1992 The biological basis for dose limitation in the skin. ICRP publication 59 *Ann. ICRP* **22**

ICRP 1994 Human respiratory tract model for radiological protection. ICRP publication 66 *Ann. ICRP* **24**

ICRP 1995 Age-dependent doses to the members of the public from intake of radionuclides—part 5 compilation of ingestion and inhalation coefficients. ICRP publication 72 *Ann. ICRP* **26**

ICRP 2006 Assessing dose of the representative person for the purpose of the radiation protection of the public. ICRP publication 101a *Ann. ICRP* **36**

ICRP 2008 Nuclear decay data for dosimetric calculations. ICRP publication 107 *Ann. ICRP* **38**

ICRP 2010 Conversion coefficients for radiological protection quantities for external radiation exposures. ICRP publication 116 *Ann. ICRP* **40**

ICRP 2012 Compendium of dose coefficients based on ICRP publication 60. ICRP publication 119 *Ann. ICRP* **41**

ICRP 2015 Occupational intakes of radionuclides: part 1. ICRP publication 130 *Ann. ICRP* **44**

JAERI 2002 Dose coefficients for radionuclides produced in high energy proton accelerator facilities: coefficients for radionuclides not listed in ICRP publications *JAERI-Data/Code 2002-013* (Naka-gun: Japan Atomic Energy Research Institute)

Kamboj S, Yu C and Rabovsky J 2011 Potential dose distributions at proposed surface radioactivity clearance levels resulting from occupational scenarios *ANL/EVS/TM/11-3* (Argonne, IL: Argonne National Laboratory) (available at: http://resrad.evs.anl.gov/docs/Surface_clearance_criteria_for_workers.pdf)

NRPB 1997 Assessment of skin doses *Documents of the NRPB* vol 8 (Chilton: National Radiological Protection Board)

Ogino H and Hattori T 2009 Verification of validity of isotope-specific exemption levels for surface contamination using Monte Carlo calculation *Jpn. J. Health Phys.* **44** 400–7

Otto T 2016 Personal dose-equivalent conversion coefficients for 1252 radionuclides *Radiat. Prot. Dosim.* **168** 1–70

Russo F, Mommaert C and van Dillen T 2018a Application of the SUDOQU methodology: preliminary results for clearance of objects from the controlled area of a nuclear facility *Bel V Report* (Brussels: Bel V) (available at: www.belv.be/images/pdf/SUDOQU_report.pdf)

Russo F, Mommaert C and van Dillen T 2018b Clearance of surface-contaminated objects from the controlled area of a nuclear facility: application of the SUDOQU methodology *Atw* **63** 29–32

SSK 2017 Berechnungsgrundlage für die Ermittlung von Körperdosen bei äußerer Strahlenexposition *Veröffentlichungen der Strahlenschutzkommission, Band 43* (Berlin: Schnelle Verlag) German Commission on Radiological Protection (in German) (available at: www.ssk.de)

van Dillen T 2015 SUDOQU: a new dose model to derive criteria for surface contamination of non-food (consumer) goods, containers and conveyances *Radiat. Prot. Dosim.* **164** 160–4 van Dillen T and van Dijk A 2018 SUDOQU, a new dose-assessment methodology for radiological surface contamination *J. Radiol. Prot.* **38** 1147–203

van Dillen T, van Dijk A, Kloosterman A, Russo F and Mommaert C 2020 Accounting for ingrowth of radioactive progeny in dose assessments: generic weighting factors for dose coefficients *J. Radiol. Prot.* **40** 83–118

Yu C *et al* 2003 *User's Manual for RESRAD-BUILD Version 3 ANL/EAD/03-1* (Argonne, IL: Argonne National Laboratory) (available at: http://resrad.evs.anl.gov/docs/ANL-EAD-03-1.pdf)